



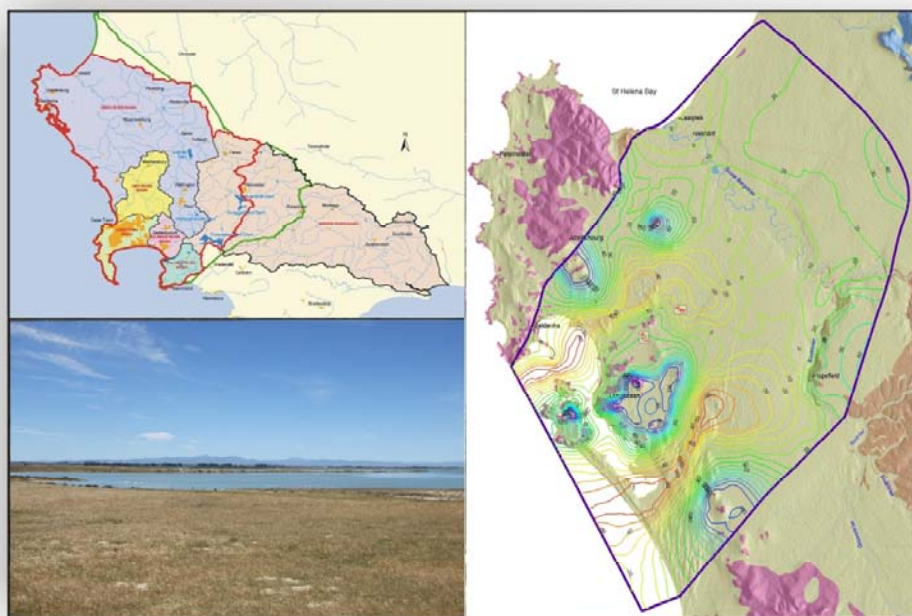
Ref No: P WMA19/000/00/0408

Department of Water Affairs and Forestry

Directorate: National Water Resource Planning

The Assessment of Water Availability in the Berg Catchment
(WMA 19) by means of Water Resource Related Models

GROUNDWATER MODEL REPORT VOL. 6 LANGEBAAN ROAD AND ELANDSFONTEIN AQUIFER SYSTEM MODEL



Final

August 2008

Submitted by
Umvoto Africa (Pty) Ltd
in Association with
Ninham Shand (Pty) Ltd



NINHAM SHAND
CONSULTING SERVICES

UMVOTO



DEPARTMENT OF
WATER AFFAIRS AND FORESTRY

DEPARTMENT OF WATER AFFAIRS AND FORESTRY

**THE ASSESSMENT OF WATER AVAILABILITY IN THE BERG
CATCHMENT (WMA 19) BY MEANS OF WATER RESOURCE
RELATED MODELS**

**GROUNDWATER MODEL REPORT VOLUME 6
LANGEBAAN ROAD AND ELANDSFONTEIN AQUIFER
SYSTEM MODEL**

Final

August 2008

Department of Water Affairs and Forestry
Directorate National Water Resource Planning

THE ASSESSMENT OF WATER AVAILABILITY IN THE BERG CATCHMENT (WMA 19) BY MEANS
OF WATER RESOURCE RELATED MODELS

GROUNDWATER MODEL REPORT VOLUME 6
LANGEBAAN ROAD AQUIFER SYSTEM AND ELANDSFONTEIN
AQUIFER SYSTEM MODEL

APPROVAL

TITLE : The Assessment of Water Availability in the Berg Catchment
(WMA 19) by Means of Water Resource Related Models :
Groundwater Model Report Volume 6
Langebaan Road and Elandsfontein Aquifer System Model

DWAF REPORT NO. : P WMA 19/000/00/0408

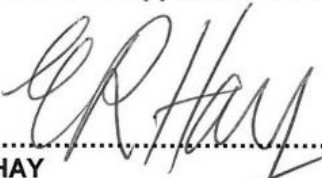
CONSULTANTS : Umvoto Africa in association with Ninham Shand

AUTHORS : Helen Seyler, Rowena Hay, Chris Hartnady, Leon
Groenewald

REPORT STATUS : Final

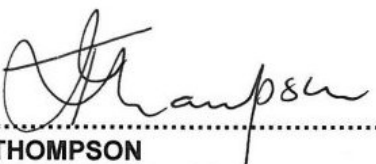
DATE : August 2008

STUDY TEAM: Approved for Umvoto and Ninham Shand


.....
E.R HAY


.....
A. Görgens

DEPARTMENT OF WATER AFFAIRS AND FORESTRY
Directorate National Water Resource Planning
Approved for Department of Water Affairs and Forestry


.....
I THOMPSON
CE : NWRP (South)


.....
J A VAN ROOYEN
Director : NWRP

REFERENCE

This report is to be referred to in bibliographies as :

Department of Water Affairs and Forestry, South Africa. 2008. *The Assessment of Water Availability in the Berg Catchment (WMA 19) by Means of Water Resource Related Models : Groundwater Model Report Volume 6 – Langebaan Road and Elandsfontein Aquifer System Model*. Prepared by Umvoto Africa (Pty) Ltd in association with Ninham Shand (Pty) Ltd on behalf of the Directorate : National Water Resource Planning. DWAF Report No. P WMA 19/000/00/0408

REPORT No	REPORT TITLE	VOLUME No.	VOLUME TITLE
1	Final Summary Report		
2	Rainfall Data Preparation and MAP Surface		
3	The Assessment of Flow Gauging Stations		
4	Land Use and Water Requirements	Vol 1	Data in Support of Catchment Modelling
		Vol 2	Invasive Alien Plant Mapping
		Vol 3	Water Use and Water Requirements
5	Update of Catchment Hydrology	Vol 1	Berg River
		Vol 2	Upper Breede River
		Vol 3	Peripheral Rivers
6	Water Quality	Vol 1	A Literature Review of Water Quality Related Studies in the Berg WMA, 1994 - 2006
		Vol 2	Updating of the ACRU Salinity Model for the Berg River
		Vol 3	Update Monthly FLOSAL Model to WQT
7	(Report No Not Used)		
8	System Analysis Status Report		
9	Groundwater Model	Vol 1	Overview of Methodology and Results
		Vol 2	Data Availability and Evaluation
		Vol 3	Regional Conceptual Model
		Vol 4	Regional Water Balance Model
		Vol 5	Cape Flats Aquifer Model
		Vol 6	Langebaan Road and Elandsfontein Aquifer System Model
		Vol 7	TMG Aquifer, Piketberg Model
		Vol 8	TMG Aquifer, Witzenberg – Nuy Model
		Vol 9	Breede River Alluvium Aquifer Model
10	Berg and Mhlathuze Assessment Studies (Refer to Report No.1)		
11	Applicability of the Sami Groundwater Model to the Berg WAAS Area		

**THE ASSESSMENT OF WATER AVAILABILITY IN THE BERG CATCHMENT (WMA 19) BY MEANS
OF WATER RESOURCE RELATED MODELS**

**GROUNDWATER MODEL REPORT VOLUME 6
LANGEBAAN ROAD AND ELANDSFONTEIN AQUIFER SYSTEM
MODEL**

EXECUTIVE SUMMARY

INTRODUCTION

The Berg Water Availability Assessment Study (WAAS) forms part of five studies commissioned nationally by DWAF to support, *inter alia*, allocable water quantification as a prerequisite for compulsory licensing. The main objectives of the Study are to (DWAF, 2005a):

- Reconfigure the existing Water Resources Yield Model (WRYM) configurations at a spatial resolution suitable for allocable water quantification to support compulsory licensing.
- Use reconfigured existing models or newly configured models for allocable water quantification for both surface water and groundwater, where applicable.

The Study comprises two phases: Phase 1 (Inception) and Phase 2 (Model configurations for assessment of current water availability and selected augmentation options). Phase 2 comprises several distinct components that can be grouped into:

- Surface water hydrology
- Groundwater hydrology
- Surface water quality
- Water resources analysis
- Reconciliation options analysis
- Study management and review.

Based on the hydrogeological analysis and the requirements for modelling as well as the overarching strategic management intent established for the Berg Catchment, a number of models are considered for evaluating the groundwater availability on a regional scale.

After finalizing all tasks, a combined modelling report will be prepared, comprising separate volumes for each task. Each report documents model development and model scenarios, as well as recommendations for implementation and model upgrade.

These volumes are:

Volume 1: Summary Groundwater Availability Assessment (due at end of project)

Volume 2: Data Availability and Evaluation

Volume 3: Regional Conceptual Model

Volume 4: Regional Water Balance Model

Volume 5: Cape Flats Aquifer Model

Volume 6: Langebaan Road and Elandsfontein Aquifer System Model

Volume 7: Table Mountain Group Aquifers – Piketberg area

Volume 8: Table Mountain Group Aquifers – Witzenberg - Nuy area

Volume 9: Breede River Alluvium Model

This report is Volume 6 in the project series. Volumes 2 and 3 can be read as a background to this report as the available data has informed the regional conceptual model, and the regional conceptual model has informed the delineation of individual model domains, data selection for model input and calibration.

THE LANGEBAAN ROAD AND ELANDSFONTEIN STUDY AREA

Wave-cut terraces overlain by aeolian dunes dominate the topography of the Langebaan area, with sand covered plains, fixed dunes and surface limestone ridges forming the visible landscape. Intrusive granitic plutons are responsible for raised highlands and koppies, which reach up to heights of 450 mamsl.

The perennial Berg River is the most significant river in the region, and is located along the northeastern boundary of the study area (see **Figure 2-1**). The Berg River drains northwestwards into the Atlantic Ocean near Velddrif, with its lower courses subjected to tidal influence (Timmerman, 1985b).

Langebaan and its environs have a Mediterranean climate, with evaporation exceeding rainfall, and most of the rainfall occurring between the months of May to August (**Table 2-1**). Average annual rainfall for the study area ranges between < 100 mm to ~ 500 mm, with most of the region having an annual rainfall of less than 280 mm.

Focussing on geological features salient to the hydrogeology, the Langebaan region is dominated by semi- to unconsolidated Cenozoic sediments that unconformably overlie basement rocks. The oldest Cenozoic deposits, the fluvial lower Elandsfontyn gravels, occur within the deeper basement areas of the palaeochannels. (Note: the Elandsfontyn gravel unit is not to be confused with the Elandsfontein Aquifer System, which is named after a farm in the area.) The lower Elandsfontyn gravel deposits were subsequently covered with clays and peats. Overlying the Elandsfontyn gravels, the aeolian sands of the Bredasdorp Group form the palaeo- and currently active dunes.

The palaeotopography reflects the palaeoclimatological interpretation that a marine transgression dammed up Proto-Berg Rivers, which previously exited to the southwest coastline. Two clear palaeochannel systems are evident in the basement. Previous workers have published basement elevation maps of the area which show these palaeochannels as enclosed basins rather than continuous channels. The interpretation suggested here is that the palaeochannels are continuous to the southwest coast.

Each of these palaeochannels comprise (semi-) separate aquifer systems. The southern palaeochannel in the area encompasses the Elandsfontein Aquifer system (EAS) and the northern palaeochannel, the Langebaan Road Aquifer System (LRAS). The sedimentary succession can be separated into 3 significant hydrogeological units:

- the basal gravels of the Elandsfontyn, forming the lower aquifer unit, LAU,
- the clay layer of the upper Elandsfontyn, which acts to (semi) confine the basal aquifer,
- the variably consolidated sands and calcretes, with interbedded peat clay of the Bredasdorp, the upper unconfined aquifer unit, UAU.

These 3 units are present in each aquifer system. The basal unit is separate between systems, and the UAU is continuous. Flow in the LAU is controlled by topography of the basement, flowing southwest towards the coast. Flow in the UAU is more controlled by surface topography and flows from a recharge high in the south, semi radially, towards the Berg River northeast, towards the LRAS to the north, and into the EAS to the southwest. The LAU is recharged in areas where the head difference between upper and lower aquifer is large enough to drive vertical recharge downwards (via leakage through clay if clay layer is present).

There is a direct interaction between the UAU and the Berg River. The regional gradient is towards the Berg River and hence on average the Berg River gains from groundwater. However during winder flood events, this gradient is likely to reverse and flood waters recharge the aquifer.

CONCEPTUAL MODEL

The conceptual model assumes that:

- It is assumed that the palaeotopography is representative of ancient fluvial systems and continuous palaeochannels are inferred.
- The geology can be interpreted as 3 distinct hydrostratigraphical units:
 1. The upper unconfined aquifer unit comprising the Bredasdorp formation sediments and Varswater sediments if present;
 2. The confining layer (Upper Elandsfontyn clay)
 3. The lower (semi-) confined aquifer unit (Elandsfontyn sediments)
- The aquifer is underlain by impermeable basement.
- The UAU is recharged directly from rainfall.
- The LAU is recharged in via leakage through the clay unit.
- The UAU discharges to the Berg River, to the coastline at Saldanha Bay and the coastline at Langebaan Lagoon and south of the lagoon.
- The Berg River acts as a recharge source to the aquifer during flood events.
- Flow in the LAU is basement controlled and occurs along the axes of the palaeochannels.
- The LAU discharges to the coastline at Saldanha Lay and the coastline at Langebaan Lagoon and south of the lagoon.
- The Berg River is in direct hydraulic connectivity with the UAU only.

NUMERICAL MODEL

A fully 3-dimensional finite element model is developed of an ~2000km² area with ~7135 triangular prismatic elements. The elements are 500–1200 m in length. The landward boundaries of the numerical model lie along topographical divides or across observed groundwater contours, and are no-flow boundary conditions. The ocean acts as a constant head in the southeast and northwest. The model is 5-layered.

The following data sets were used to construct the bedrock topography:

- Borehole depths from the NGDB data set, using records of shale and granite as indications of basement rocks.
- Offshore basement data of De la Cruz (1978).

- Spot heights on bedrock outcrops as shown in the 1:250 000 geological maps.

The recharge data used in the model is generated through a modified version of the Breede River Basin Study (BRBS) method (DWAf, 2002). Recharge over the modelled area is ~122 Mm³/a.

Water-use Authorisation and Management System data was used for abstractions. The total abstraction over the modelled area is 3.6 Mm³/a.

As per the model assumptions that the rivers act as a sink to the aquifer and the river, stages were set below the groundwater level. As an initial estimate of the modelled groundwater levels the topography and the measured water level distribution was used and river stages were input relative to this water level distribution, between 1-3 m below it.

A calibration standard of modelled water levels within 10% average error to observed point data is set. The model is calibrated to this standard with the use of groundwater fluxes and groundwater as compared to topography as an additional guide.

The numerical model was considered calibrated with the following parameter set; the model basal layer within the palaeochannels calibrated with $K_x=K_y$ of ~10 m/d. a discontinuous low K layer overlies the basal later, at $K_x=K_y$ of 0.01 m/d. The upper layer dominantly has a K of 10 m/d, with some area in the south at ~1 m/d. The model calibrated with vertical K an order of magnitude less than horizontal K.

MODEL RESULTS

The results show the ocean as a dominant sink to the aquifer, and that on average (i.e. the steady-state model) the Berg River behaves as a sink. The modelled groundwater fluxes are shown in **Table E.1**. There is an imbalance of 100 m³/d between the flux in and out of the model.

Table E.1 Modelled Groundwater Fluxes

Flux into Model (m ³ /d)	Flux out of Model (m ³ /d)	
Recharge	Ocean	Rivers
59,800	-32,800	-27,100

The effect of abstraction is shown in **Table E.2**.

Table E.2 The effect of Abstraction

	Flux into Model (m ³ /d)		Flux out of Model (m ³ /d)			Balance (m ³ /d)
	Recharge	Rivers	Ocean	Rivers	Abstraction	
Abstraction (i.e. standard model case)	59 800	0	-29 500	-21200	-10 100	-1000
Zero Abstraction	59 800	0	-32 800	-27 00	0	-100
Difference caused by abstraction	-	-	Decrease of 10%	Decrease of 22%	-	Increase of 900%

The seasonal variation of the aquifer was simulated in transient modelling. The best fit was achieved using a specific yield of 2%. Scenario testing on the transient model suggests that there is a resource available for additional abstraction in the EAS, and that it is possible to abstract small quantities without affecting the water levels at potentially sensitive receptors such as the Langebaan Lagoon. An ASR scenario suggests that it is possible to site injection boreholes within the cone of depression and raise water levels, reversing some of the depression.

RECCOMENDATIONS

The following recommendations are made:

Summary Recommendation 1: Hydrocensus data collected across the Langebaan area: water levels and borehole use, accurate GPS of X,Y,Z coordinates

Summary Recommendation 2: Make surface water data available to all disciplines by allowing it to be converted to a universal datum. All gauging stations are required to be surveyed at the point at which the measurements are taken.

Summary Recommendation 3: Additional modelling at a smaller scale in order to understand the hydraulic nature of the aquifers and replicate differing flow directions at different depths. In the vicinity of the Berg River this will generate a better understanding of the nature of the SW-GW interaction.

Summary Recommendation 4: Additional modelling at a smaller wellfield scale in order to manage the current situation of abstraction from storage.

Summary Recommendation 5: Smaller- scale model to be constructed for the purpose of optimisation of abstraction volume and rate, and positions, for additional potential wellfields and licensing thereof.

Summary Recommendation 6: Smaller scale- model to be constructed for the purpose of optimisation of ASR injection volume and rate, and borehole positions.

**THE ASSESSMENT OF WATER AVAILABILITY IN THE BERG CATCHMENT (WMA 19) BY MEANS
OF WATER RESOURCE RELATED MODELS**

**GROUNDWATER MODEL REPORT VOLUME 4
LANGEBAAN ROAD AND ELANDSFONTEIN AQUIFER SYSTEM
MODEL**

TABLE OF CONTENTS

	Page No
1. INTRODUCTION	1
1.1 THE WAAS PROJECT	1
1.1.1 Project background	1
1.1.2 Study area delineation.....	1
1.1.3 Project components.....	3
1.1.4 Terms of Reference for groundwater.....	3
1.2 LANGEBAAN ROAD AND ELANDSFONTEIN AQUIFER SYSTEM REPORT	5
1.2.1 Background to the Langebaan Road and Elandsfontein Aquifer system report and report purpose	5
1.2.2 Summary of Langebaan Road and Elandsfontein Aquifer Conceptual Model.....	7
1.2.3 Structure of this volume of the report.....	8
2. GENERAL DESCRIPTION OF STUDY AREA.....	11
2.1 TOPOGRAPHY & DRAINAGE	11
2.2 HYDROLOGY AND HYDROCLIMATOLOGY.....	14
2.3 GEOLOGY	17
2.3.1 Stratigraphy	17
2.3.2 Palaeo-topography	23
2.3.3 Summary of hydrostratigraphy	26
2.4 HYDROGEOLOGY.....	29
2.4.1 The flow regime.....	29
2.4.2 SW-GW interaction.....	34
2.4.3 Recharge.....	36
2.4.4 Groundwater use.....	39
2.5 WATER QUALITY	42
2.6 LANDUSE	44
3. CONCEPTUAL MODEL.....	47
3.1 CONCEPTUAL MODEL OF GROUNDWATER FLOW SYSTEM	47
3.2 TRANSLATION INTO NUMERICAL MODEL	48
4. MODEL INPUT DATA.....	54
4.1 REQUIRED PARAMTERS	54
4.2 THE MODEL MESH	54
4.3 TOPOGRAPHY	55

4.4	BEDROCK.....	55
4.5	INTERNAL AQUIFER GEOMETRY.....	56
4.6	AQUIFER HYDRAULIC PROPERTIES	57
4.6.1	Hydraulic conductivity, K	57
4.6.2	Storage properties.....	58
4.6.3	Porosity	58
4.7	RECHARGE	58
4.8	ABSTRACTIONS.....	59
4.9	RIVERS.....	60
4.9.1	Positions and river stages	60
4.9.2	Hydraulic connectivity.....	61
4.10	INPUT PARAMETER SUMMARY	61
5.	NUMERICAL MODEL: STEADY-STATE MODELLING	63
5.1	CALIBRATION PROCEDURE.....	63
5.2	CALIBRATION STANDARD	63
5.3	CALIBRATION DATA: STEADY-STATE WATER LEVELS	64
5.4	PARAMETER CALIBRATION	67
5.4.1	River transfer rate.....	67
5.4.2	Hydraulic conductivity (K).....	68
5.5	RESULTS.....	75
5.5.1	The flow regime.....	75
5.5.2	Discussion.....	77
5.5.3	Parameter calibration summary.....	77
5.6	SURFACE WATER- GROUNDWATER INTERACTIONS	78
5.7	THE IMPACT OF CURRENT ABSTRACTION	78
5.8	MODEL CONFIDENCE	83
6.	TRANSIENT MODEL	84
6.1	TRANSIENT MODEL ASSUMPTIONS.....	84
6.2	REQUIRED INPUT DATA	84
6.3	RIVER STAGES	85
6.4	RECHARGE DATA.....	85
6.5	STORAGE DATA	86
6.6	CALIBRATION DATA AND STANDARD	87
6.7	MODEL RESULTS	94
6.7.1	Parameter Calibration: Storage	94
6.7.2	Modelled water level variations	95
6.7.3	Mass balance	96
6.7.4	Groundwater – surface water interaction.....	99
7.	SCENARIO TESTING	100
7.1	SCENARIO 1: SENSITIVITY TO RAINFALL	100

7.2	SCENARIO 2: UTILISATION OF THE LRAS/ EAS TO AUGMENT THE WATER SUPPLY TO THE WEST COAST MUNICIPALITY	104
7.2.1	Scenario 2.1 The West Coast Wellfield	104
7.2.2	Scenario 2.2 Alternative Wellfield	105
7.3	YIELD ESTIMATION	108
7.4	SCENARIO 3 RIVER FLOOD EVENTS	108
7.5	SCENARIO 4 AQUIFER STORAGE RECOVERY SCHEME	112
8.	CONCLUSIONS AND RECOMMENDATIONS	117
8.1	SUMMARY OF INTERPRETATIONS	117
8.2	GROUNDWATER LEVEL DATA	118
8.3	SURFACE WATER DATA	118
8.4	HYDRAULIC NATURE OF THE AQUIFER AND GROUNDWATER-SURFACE WATER INTERACTIONS	118
8.5	MANAGEMENT OF CURRENT ABSTRACTION	119
8.6	OPTIMISATION OF ADDITIONAL ABSTRACTION	119
8.7	OPTIMISATION OF ASR SCHEME	119
9.	REFERENCES	120

LIST OF TABLES

Table 2-1	Available hydrological data at catchment scale (Berg WAAS Volume 2)	14
Table 2-2	Baseflow and groundwater contribution to baseflow and per catchment, after GRDM database. (Berg WAAS Volume 3)	15
Table 2-3	Stratigraphy of the Wider Study Area	17
Table 2-4	Stratigraphy of the Cenozoic (65 Ma to present) sediments between Saldanha and the Berg River (after Rogers, 1980, and Timmerman, 1985b)	19
Table 2-5	Hydrostratigraphy (Timmerman, 1985b)	27
Table 2-6	Recharge estimations in the Study Domain from previous studies and standard methods	37
Table 2-7	GW use per catchment after GRAII	39
Table 3-1	Description of model boundaries	48
Table 4-1	Summary of required input parameters	54
Table 4-2	Model Layering	56
Table 4-3	Hydraulic conductivity estimates for the Langebaan area from Timmerman (1985b.)	57
Table 4-4	Abstraction input data	59
Table 4-5	Input parameter summary	62
Table 5-1	Transfer rate calibration (magnitude)	68
Table 5-2	Results of key indicators for various hydraulic conductivity scenarios, including results for final model scenario	73
Table 5-3	The Effect of current abstraction on modelled fluxes	82
Table 6-1	Transient model input parameters	85
Table 6-2	Typical values for specific yield (Driscoll, 1986)	87
Table 6-3	Observed annual water level variations at observation points	91
Table 6-4	Results for calibration of Sy	94
Table 6-5	Monthly fluxes	97
Table 7-1	Mass balance for increased recharge	101
Table 7-2	Mass balance for decreased recharge	102
Table 7-3	Observed water level decline in LAU since 2000	105
Table 7-4	Scenario 2.2 Additional wellfield mass balance	106
Table 7-5	Mass balance under river flood event	110

Table 7-6	Mass balance under Aquifer Storage and Recovery scheme.....	114
-----------	---	-----

LIST OF FIGURES

Figure 1-1	Study area locality.....	2
Figure 1-2	Locality map.....	9
Figure 1-3	Conceptual model (from Volume 3 of this report, DWAF, 2007b).....	10
Figure 2-1	Topography and drainage.....	12
Figure 2-2	Typically flat topography around the Groot-Berg River: view of the floodplain to the north of the Berg River, Piketberg Mountains in the distance.....	13
Figure 2-3	Monthly rainfall data for the Langebaan Area.....	15
Figure 2-4	Rainfall (MAP).....	16
Figure 2-5	Regional geology.....	21
Figure 2-6	Geological cross-sections of the Cenozoic units.....	22
Figure 2-7	Palaeotopography.....	25
Figure 2-8	Geological summary.....	28
Figure 2-9	Water Levels.....	32
Figure 2-10	Artesian Borehole in groundwater fed pool: Evidence of 2 water tables.....	33
Figure 2-11	Schematic diagram displaying hydraulically connected gaining and losing rivers (Winter et al 1998).....	35
Figure 2-12	Recharge as based on DWAF BRBS method (DWAF, 2002).....	38
Figure 2-13	Groundwater Use- WARMS.....	41
Figure 2-14	Durov diagram; all data.....	42
Figure 2-15	Spatial variability of groundwater quality (Woodford et al, 2007).....	43
Figure 2-16	Durov diagram; upper and lower aquifer separated.....	44
Figure 2-17	Landuse.....	45
Figure 3-1	Translation into numerical model.....	51
Figure 3-2	Boundary conditions and the model mesh: the Upper Model Surface.....	52
Figure 3-3	Boundary conditions and the model mesh: the Lower Model Surface.....	53
Figure 5-1	Calibration data points: Upper Aquifer.....	66
Figure 5-2	Calibration data points: Lower Aquifer.....	67
Figure 5-3	Model hydraulic conductivity distribution for Layers 1&2 – the Upper Aquifer Unit (Kx is shown).....	70
Figure 5-4	Model hydraulic conductivity distribution for Layer 3 – the confining unit (Kx is shown).....	71
Figure 5-5	Observed and modelled groundwater surface, upper and lower aquifer.....	76
Figure 5-6	Scatter plot of modelled verses observed groundwater levels: Upper Aquifer.....	77
Figure 5-7	Scatter plot of Modelled verses Observed groundwater levels: Lower Aquifer.....	77
Figure 5-8	The effect of abstraction at the West Coast Wellfield on water levels.....	80
Figure 5-9	Modelled water level surface with no abstraction (shown for Upper Aquifer).....	82
Figure 6-1	Monthly rainfall and recharge.....	86
Figure 6-2	UAU observation points.....	88
Figure 6-3	LAU observation points.....	89
Figure 6-4	Observed water level variations at borehole from observation point T1.8, in the UAU.....	90
Figure 6-5	Distribution of annual variation in water levels, UAU.....	92
Figure 6-6	Distribution of annual variation in water levels, LAU.....	93
Figure 6-7	Correlation between observed and modelled annual fluctuations specific yield (Sy is 0.02).....	95
Figure 6-8	Modelled water levels.....	96
Figure 6-9	Monthly fluxes.....	98
Figure 7-1	Water level variation under increased and decreased recharge, at T1.5.....	103
Figure 7-2	Water levels under scenario 2.2 additional wellfield.....	107
Figure 7-3	Modelled water level for ASR scheme (small scale).....	115
Figure 7-4	Modelled water level for ASR scheme (larger scale).....	116

ABBREVIATIONS

ASR	Aquifer storage and recovery
BP	Before present
BRHS	Breede River Hydrological Study
CDSM	Department of Land Affairs - Chief Directorate Surveys and Mapping
CMA	Catchment Management Agency
CRD	Cumulative Rainfall Departure
CSIR	Council for Scientific and Industrial Research
DEM	Digital Elevation Model
DWAF	Department of Water Affairs and Forestry
EAS	Elandsfontein Aquifer System
EC	electrical conductivity
E-W	east west
FE	Finite Element
GIS	Geographical Information System
GRA	Groundwater Resources Assessment
GRDM	Groundwater Resource Directed Measures – Software
IWR	Integrated Water Resources
IWRM	Integrated Water Resources Management
K	Hydraulic conductivity [L/T]
km	kilometre
LAU	Lower Aquifer Unit
LRAS	Langebaan Road Aquifer System
m	metre
N-S	north-south
Ma	Millions of years ago
MAE	Mean annual evaporation
MAP	Mean annual precipitation
Mamsl	Metres above mean sea level
MAR	Mean annual runoff
NGDB	National Groundwater Database
NWRS	National Water Resources Strategy
NWA	National Water Act
op.cit.	work previously cited
PhD	Doctor of Philosophy
RDM	Resource Directed Measures
RMS	Root mean square
RQO	Resource Quality Objectives
S	Storage parameter [dimensionless]
SAWS	South African Weather Service
SFRA	streamflow reduction activities
STCC	short term characteristic curve

SVF	Saturated Volume Fluctuations
T	Transmissivity [L^2/T]
TDS	Total dissolved solids
TMG	Table Mountain Group
TMGA	Table Mountain Group Aquifer
TOR	Terms of Reference
UAU	Upper Aquifer Unit
WAA	Water Availability Assessment
WAAS	WAA Study
WARMS	Water-use Authorisation and Management System
WCSA	Western Cape System Analysis
WCWSS	Western Cape Water Supply System
WECSA	Western Cape Situation Assessment
WMA	Water Management Area
WRC	Water Research Commission
WRPM	Water Resources Planning Model
WRYM	Water Resources Yield Model
WR	Water Resources

1. INTRODUCTION

1.1 THE WAAS PROJECT

1.1.1 Project background

The Berg River Catchment in the Berg Management Area (WMA) forms the heart of the Western Cape Water Supply System (WCWSS), whose supply area constitutes the economic hub of the Western Cape and serves a primary export industry based on agricultural produce. The WCWSS serves the City of Cape Town, both urban water users and irrigators along the Berg, Eerste, Lourens, Steenbras and Palmiet Rivers, domestic and industrial users on the West Coast, as well as irrigators and urban users in the Riviersonderend catchment of the Breede WMA.

The Department of Water Affairs and Forestry (DWAF) have initiated two major water resource management and planning undertakings in the environment of the WCWSS:

- a) Compulsory licensing in terms of the National Water Act (NWA) - Act 36 of 1998 - is due to be piloted in the Berg WMA, in response to concerns that growing water user demands, as well as stream flow salinity increases, might place parts of the WCWSS in a water-stress condition during the foreseeable future.
- b) A Reconciliation Strategy Study has been completed, which reviewed the future water requirements and the options for meeting these demands. The Study identified the most favourable augmentation options and recommended a programme of feasibility studies and other investigations to improve the operation and planning of the system, and to ensure that the necessary infrastructure or other interventions are implemented timeously so as to reconcile the supplies with the future demands.

This Berg Water Availability Assessment Study (WAAS) forms part of five studies commissioned nationally by DWAF to support, *inter alia*, allocable water quantification as a prerequisite for compulsory licensing. The objectives of the Study are to (DWAF, 2005):

- Reconfigure the existing Water Resources Yield Model (WRYM) configurations at a spatial resolution suitable for allocable water quantification to support compulsory licensing.
- Use reconfigured existing models or newly configured models for allocable water quantification for both surface water and groundwater, where applicable.
- Incorporate changes in concepts, models and approaches, as derived from pilot studies initiated by DWAF elsewhere, if these become available in time.
- Support the Reconciliation Study with model-based assessment of water resource augmentation options.

Ninham Shand (Pty) Ltd is the Lead Consultant for the Berg WAAS and is responsible for the surface water components of the Study, as well as study management, while Umvoto Africa (Pty) Ltd is responsible for the groundwater components. Both Consulting Firms contribute either conceptually or directly to certain shared tasks.

1.1.2 Study area delineation

The study area shown in **Figure 1-1** comprises the following drainage systems and bulk water infrastructure:

- The complete Berg River catchment from its source in the Groot Drakenstein Mountains to its estuary at Laaiplek on the Atlantic West Coast.

- The Cape Town Basin, which includes the Eerste, Lourens and Sir Lowry's Pass rivers – all of which drain into False Bay.
- The Diep River, which flows westerly from its source in the Riebeeck Kasteel Mountains to its mouth in the northern suburbs of Cape Town.
- The complete Palmiet and Steenbras catchments in the south of the Study Area, which flow in a southwesterly direction to the south of False Bay.
- The Breede River, which flows easterly to the Indian Ocean and of which the Upper and Middle Breede and the Upper Riviersonderend catchments are focus areas for this Study.

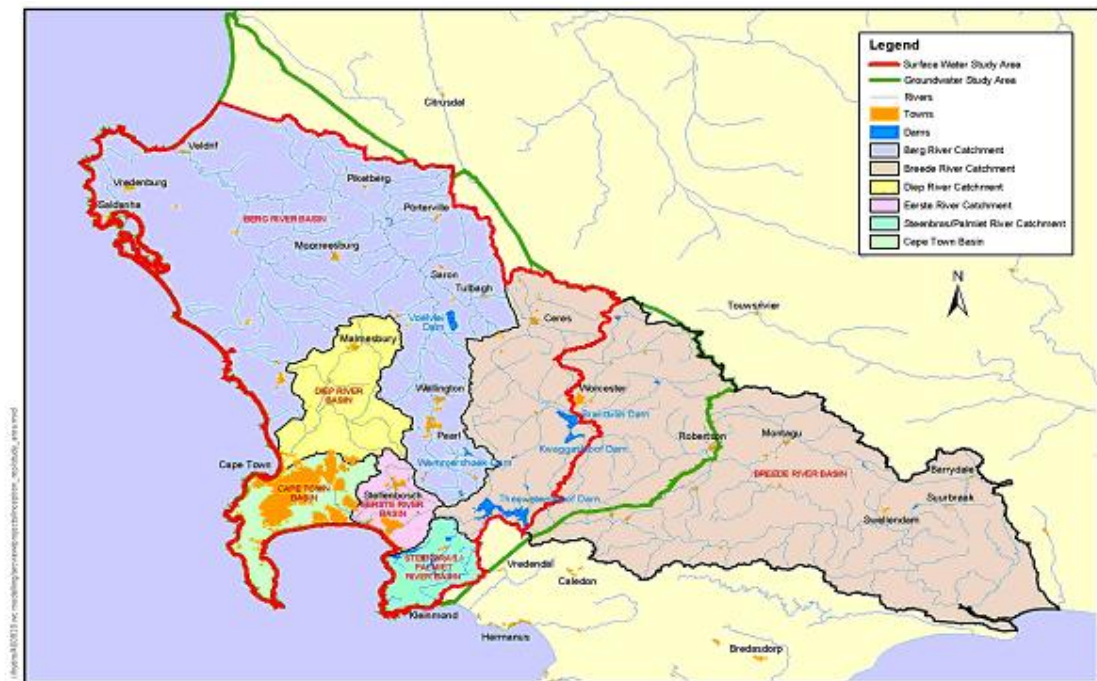


Figure 1-1 Study area locality

The Western Cape Water Supply System (WCWSS) is an integrated system of reservoirs, linked via a complex network of tunnels, pump stations and pipelines that stores and reticulates the runoff from rivers for use in the greater Cape Town Metropolitan area. Surface water inter-basin transfers take place between the Berg, Riviersonderend and Eerste catchments, while water from the existing Steenbras Scheme is supplied from the Lower Steenbras water treatment works into the Cape Town Water Undertaking network. The Palmiet Scheme is a dual hydroelectric pumped-storage and water transfer scheme (to the Steenbras pumped-storage scheme), of which the water transfer component has not yet been fully implemented.

The study domain for the groundwater component extends beyond the boundary of the Berg WMA and includes the upper part of the Breede WMA as well as southern portions of the Olifants/Doorn WMA. This extended area between Tulbagh-Ceres, Kleinmond and Robertson approximately coincides with the “syntaxis” zone of N-S and E-W cross- or interference folding in the Cape Fold Belt. The high mountain exposures of the Table Mountain Group (TMG) in the anticlinal folds, the confined TMG fractured-rock aquifers in the synclinal folds and the hydroteacts are the main structural elements forming natural boundaries of groundwater flow. These structures would therefore build the conceptual basis of any sound groundwater models in the TMG terrain of the Berg WMA.

1.1.3 Project components

The Study comprises two phases: Phase 1 (Inception) and Phase 2 (Model configurations for assessment of current water availability and selected augmentation options). Phase 2 comprises several distinct components that can be grouped into:

- Surface water hydrology
- Groundwater hydrology
- Surface water quality
- Water resources analysis
- Reconciliation options analysis
- Study management and review.

1.1.4 Terms of Reference for groundwater

In 2001 it was estimated that a minimum of 30 Mm³/a of water was available to augment supply to the WCWSS from the confined Peninsula Aquifer alone (City of Cape Town, 2001). More recent evaluations of both the confined Peninsula and the Skurweberg aquifers suggest that between 20 and 400 Mm³/a can be abstracted from the TMG within the Breede River basin area of the WCWSS domain (City of Cape Town, 2004a) if these aquifers are drawn down by 1 and 20 m respectively.

DWAF, as the custodian of the water resources in South Africa, has several tools available under the National Water Act for ensuring that the goals of Integrated Water Resources Management are met within the boundaries of the WMAs, of which compulsory licensing is one. The aim of compulsory licensing is to equitably and sustainably distribute the available supply of water (i.e. current yield, not potential yield) within the catchment between all potential users, without compromising future needs or foreclosing on certain water resource development options.

Allocation of future surface water involves a 2-dimensional analysis of the hydrology and current use. Similarly the impact of future groundwater use on current users and therefore the sustainable utilisation of water in aquifer storage by both user groups can only be assessed if the potential yield rather than the current yield is analysed with appropriate spatial and time series detail. This is primarily a 3D problem in the study domain.

In order to achieve this, the regulatory authority needs to have knowledge of the following:

- total amount of water available within the catchment;
- temporal and spatial distribution of water availability;
- current and future water requirements;
- impact of water abstraction at any point and time on the environment and other users;
- scenario for optimal development of the aquifer and
- scenario for best possible aquifer development and management given the *status quo*.

The contrast between the two scenarios will indicate the extent to which *ad hoc* aquifer development and management impacts on the resource from a Source Directed (SDM) and a Water Quality (RQD) directed perspective.

The Promotion of Administrative Justice Act (PAJA) - Act 3 of 2000 – suggests that it is necessary that any water resource modelling undertaken to support administrative or regulatory

decisions be based on all available data and uses the most appropriate models and methodologies available (and/or notes the limitations and uncertainties thereof). Water resource quantification or allocation models need to be configured, sequenced or linked in such a way that different scenarios may be assessed for aligning water supply and demand to best meet the Reserve and the Resource Quality Objectives (RQOs) in a given catchment (DWAf, 2003). Where limited data is available, it is good practise to establish an agreed-upon set of scenarios, which reflect a range of values for model input parameters. As improved data becomes available the range in value of model input variables or scenario testing is narrowed down.

The manner in which surface and groundwater model usage should be integrated will likely vary between catchments. Sound modelling outcomes would depend, not only on the impact of groundwater abstraction on baseflow and on the ecology, but also on the temporal relationship/operating rules for groundwater storage and surface water storage and the impact of surface water storage and reduced stream flows on groundwater levels and on the ecology.

Based on the hydrogeological analysis and the requirements for modelling as well as the overarching strategic management intent established for the Berg Catchment, the following models are considered the minimum requirement to address the Terms of Reference and to evaluate the groundwater availability on a regional scale:

- Task 7a: GIS database for groundwater component
- Task 7b: Digitising geological maps
- Task 12: Regional model development
 - Conceptual model for study domain
 - GIS-based water balance model for study domain
- Task 13: Configuration of a numerical model for the Cape Flats Aquifer
 - Quantification of surface water – groundwater interaction
 - Calibration of recharge estimation and water balance
 - Scenario for augmentation of bulk water supply to the City of Cape Town (in support of Western Cape Reconciliation Study)
 - Scenario for flood management (in support of Western Cape Reconciliation Study)
- Task 14: Review and update conceptual model for West Coast aquifers
 - Review of conceptual model
 - Quantification of surface water – groundwater interaction
 - Review and revision of recharge estimation and water balance
- Task 14a: Configuration of a numerical groundwater model for Langebaan Road Aquifer
 - Refinement of surface water – groundwater interaction
 - Refinement of recharge and yield estimation
 - Scenario for artificial recharge schemes (in support of Western Cape Reconciliation Study)
- Task 15: Water balance and storage model for TMG Aquifer
 - Recharge estimation and water balance on regional scale
- Task 15a: Configuration of a numerical TMG groundwater model for Worcester
 - Quantification of surface water – groundwater interaction
 - Refinement of recharge and yield estimation

- Scenario for Aquifer Storage Recovery (ASR) schemes (in support of Western Cape Reconciliation Study)
- Task 15b: Configuration of a numerical TMG groundwater model for Tulbagh – Ceres
 - Quantification of surface water – groundwater interaction
 - Refinement of recharge and yield estimation
- Task 15c: Configuration of a numerical TMG groundwater model for the Hex River Mountains
 - Quantification of surface water – groundwater interaction
 - Refinement of recharge and yield estimation
 - Scenario for Aquifer Storage Recovery (ASR) schemes (in support of Western Cape Reconciliation Study)
- Task 15d: Configuration of a numerical TMG groundwater model for Piketberg
 - Quantification of surface water – groundwater interaction
 - Refinement of recharge and yield estimation

After finalizing all tasks, a combined modelling report will be prepared, comprising separate volumes for each task. Each report documents model development and model scenarios, as well as recommendations for implementation and model upgrade. Volume 2 and 3 below are to be read in conjunction with each other as the available data has informed the conceptual model and the conceptual model has informed the selection of data for model input and calibration.

The complete set of volumes are:

Volume 1: Summary Groundwater Availability Assessment (due at end of project)

Volume 2: Data Availability and Evaluation

Volume 3: Regional Conceptual Model

Volume 4: Regional Water Balance Model

Volume 5: Cape Flats Aquifer Model

Volume 6: Langebaan Road and Elandsfontein Aquifer Systems Model

Volume 7: Table Mountain Group Aquifers – Piketberg area

Volume 8: Table Mountain Group Aquifers - Witzenberg-Nuy Valley area

Volume 9: Breede River Alluvium Model

This report is Volume 6 in the project series. Volumes 2 and 3 form a basis to this report as the available data has informed the regional conceptual model upon which conceptual modelling at the smaller scale of the Langebaan Road and Elandsfontein Aquifer Systems is based and refined, and the conceptual model has informed the selection of data for model input and calibration.

1.2 LANGEBAAN ROAD AND ELANDSFONTEIN AQUIFER SYSTEM REPORT

1.2.1 Background to the Langebaan Road and Elandsfontein Aquifer system report and report purpose

The ultimate purpose of the present Water Availability Assessment and groundwater modeling study is to provide a sound quantitative basis for resource assessment into the future. A regional conceptual model and GIS water balance model has been developed in order to further

the understanding of the hydrogeology of the TMG system (Volume 4 of this report, DWAF 2007c). In addition to the regional scale model, smaller scale modelling is undertaken in selected areas, to characterise and quantify the available water resource with greater confidence at a smaller spatial scale for specific aquifers (DWAF 2005). The conceptual understanding on the regional scale can be iteratively reviewed based on the insight gained from the smaller scale modelling and, in due course, on the basis of monitoring data and analysis. This report forms the second within the volume series of reporting on these smaller model domains.

There is scientific and economic motivation to model the Langebaan area in detail. The West Coast Aquifers were recently investigated as part of the DWAF project, “Pre-Feasibility Study of Potential Water Resources for the area served by the West Coast District Municipality”. The associated assessment of the groundwater potential (Woodford et al., 2003) is critically reviewed as part of this present investigation. The present conceptual model for the Langebaan Road and Elandsfontein Aquifer Systems (Woodford et al., 2003, Fig. 15) is based upon a pattern of bed-rock elevation (op. cit., Fig. 16) that is not readily explained by any obvious geomorphological process. It also overlooks the potential for lateral recharge via up-gradient connections to surface water sources in the lower Berg and Sout-Groen river channels.

The actual extent and 3D geometry of the aquifer therefore requires critical re-examination, since it is likely to be larger than currently thought, and the lateral recharge relationships along the eastern boundary are probably more complex than previously considered. The impact of these revisions on resource planning or optimisation using Artificial Recharge and Storage Recovery will be significant, especially since it is known that the mean annual recharge of the West Coast Aquifers is low relative to their typical storativity.

Presented here is a conceptual model and subsequent numerical model that characterises the groundwater resource, providing a quantitative basis for resource assessment into the future. More precisely, this report documents (DWAF, 2005):

- Configuration of a numerical model for Langebaan Aquifers based on a revised conceptual model
- Delineation of aquifer boundaries
- Identification of key data gaps and uncertainties in quaternary-scale resource evaluation
- Evaluate lateral and vertical inflow/recharge and discharge into ocean and on-land open water bodies
- Calibration of:
 - Vertical and lateral recharge
 - Natural aquifer discharge into rivers and ocean
 - Storage capacity
 - Yield estimation
- Rainfall dependency of groundwater-surface water interaction, recharge and yield
- One scenario for utilising the aquifer to augment the water supply to the West Coast District Municipality
- Identification and quantification of impact of aquifer abstraction on stream flow
- Evaluate impact of preferred abstraction scenario on existing wetlands, open water bodies and areas of natural/indigenous/protected vegetation

- Evaluate potential for saline intrusion under the preferred abstraction scenario
- Scenario testing for flood events of the Berg River
- One scenario for Aquifer Storage Recovery schemes, using surplus winter floodwater.

A locality map showing the study area is shown in **Figure 1-2**. The boundary shown is the study area boundary; the relevant area under question in the study, and that area considered in the development of the conceptual model in Volume 3 of this report (DWAF 2007b). To avoid using the Berg River as a boundary to the numerical model, the numerical model boundary is extended to the north of the Berg River. The area north of the Berg River is included briefly in descriptions of the study area, however the focus and area of interest remains the area south of the river, shown in **Figure 1-2**.

1.2.2 Summary of Langebaan Road and Elandsfontein Aquifer Conceptual Model

The outline of the conceptual model for the smaller-scale model domains is given in Volume 3 of this report (DWAF, 2007b). It is summarised below as an introduction to developing the conceptual model through detailed analysis of relevant features in chapters 2 and 3 of this report (See **Figure 1-3**).

In the current scheme (Woodford et al., 2003), the two larger Sandveld aquifer systems situated in palaeo-drainage channels south of the Berg River are designated as (1) the “Langebaan Road Aquifer System” (op. cit., p.38-43; henceforward LRAS) and the “Elandsfontein Aquifer System” (op. cit., p. 43-46; henceforward EAS).

The piezometric map drawn from water level data points (non-strata specific) reveals that the water levels relative to mean annual sea level are higher in the areas immediately adjacent to the intrusive Granite plutons as well as the Malmesbury outcrop basins to the east. The water levels become lower toward the coast. The piezometric map also indicates the existence of a channel of lower water levels traversing the Langebaan-Elandsfontein area northeast to southwest from the Berg River to Saldanha Bay at the entrance of the Langebaan Lagoon. This low in water levels is located in the region of the Langebaan Road Aquifer palaeochannel of the “proto-Berg” River (Hendey, 1982).

The Langebaan Road Aquifer is located between the lower Berg River and Saldanha Bay. The geomorphological origins of Saldanha Bay are related to deep fluvial incision of bedrock by a “proto-Berg” river during Miocene or pre-Miocene times, as revealed by marine geological and geophysical investigations in Saldanha Bay (De la Cruz, 1978; and references cited therein, which – surprisingly - seem never to have been properly correlated with onland depth-to-bedrock investigations.). “The fact that the bedrock is deep close to the north-eastern coast of the Bay suggests that it continues at a considerable depth under the adjacent onland dunes in the region” (op. cit., p. 27). Rogers (1982, Fig. 3.21), however, inferred a bedrock depth of only -20 m to 0 m elevation along the Saldanha Bay coastline, and drew a palaeodrainage divide at <+20 m elevation roughly midway between the coastline and Langebaan Road.

In our view, the LRAS palaeochannel displays greater axial continuity and a consistent westerly slope. Particularly in the west between Lynch Point (Club Mykonos) and the Saldanha Steel site, its bedrock base is inferred to be substantially greater in depth than indicated on existing maps (cf. Woodford et al., 2003, Fig. 16). Furthermore, the deeper (semi-) confined part of the LRAS, which is located along the axis of the “proto-Berg” palaeochannel, is not limited on the

west by a bedrock ridge. Its westerly extension toward and beneath the Spreeuwal dunefield (Witzand Formation) may therefore be much larger than presently conceived.

The Elandsfontein Aquifer System is wholly contained within the southern palaeochannel, which evidently contained the Miocene palaeodrainage of the Sout and Groen River systems. Timmerman (1988) records that groundwater in the Elandsfontein catchment area is recharged at the foot of the granitic hills near Darling, and flows northwards to Elandsfontein before turning westwards towards Langebaan Lagoon. There is a localised discharge zone on the western part of Elandsfontein (*op. cit.*, p. 92), formed by flow concentration where permeable strata were deposited in the Elandsfontein palaeochannel. It is separated from the discharge zone east of Langebaan Lagoon by a local water-table divide (See **Figure 1-3**). (Note: in **Figure 1-3** the Elandsfontein Aquifer system is referred to as Geelbek.)

The 3D geometry, facies continuity and hydraulic properties of variably sorted, aquifer sandstones and gravels in the fluvial Sandveld depositional system differs substantially from the finer, well-sorted calcareous sands in the overlying Bredasdorp depositional system, with the latter being much less favourable from a hydrogeological perspective.

1.2.3 Structure of this volume of the report

This Volume of the report is structured into a number of sections with several sub-sections each.

Chapter 1 describes the background to the project, determines the terms of reference for the groundwater component and gives the purpose of this specific report.

Chapter 2 provides a detailed information base for the Langebaan area, based on literature review and data, describing relevant physical features such as topography and geology.

Chapter 3 provides a conceptual model for the groundwater flow regime as based on the data and information in chapter 2. The translation to the numerical model and assumptions made therein are described.

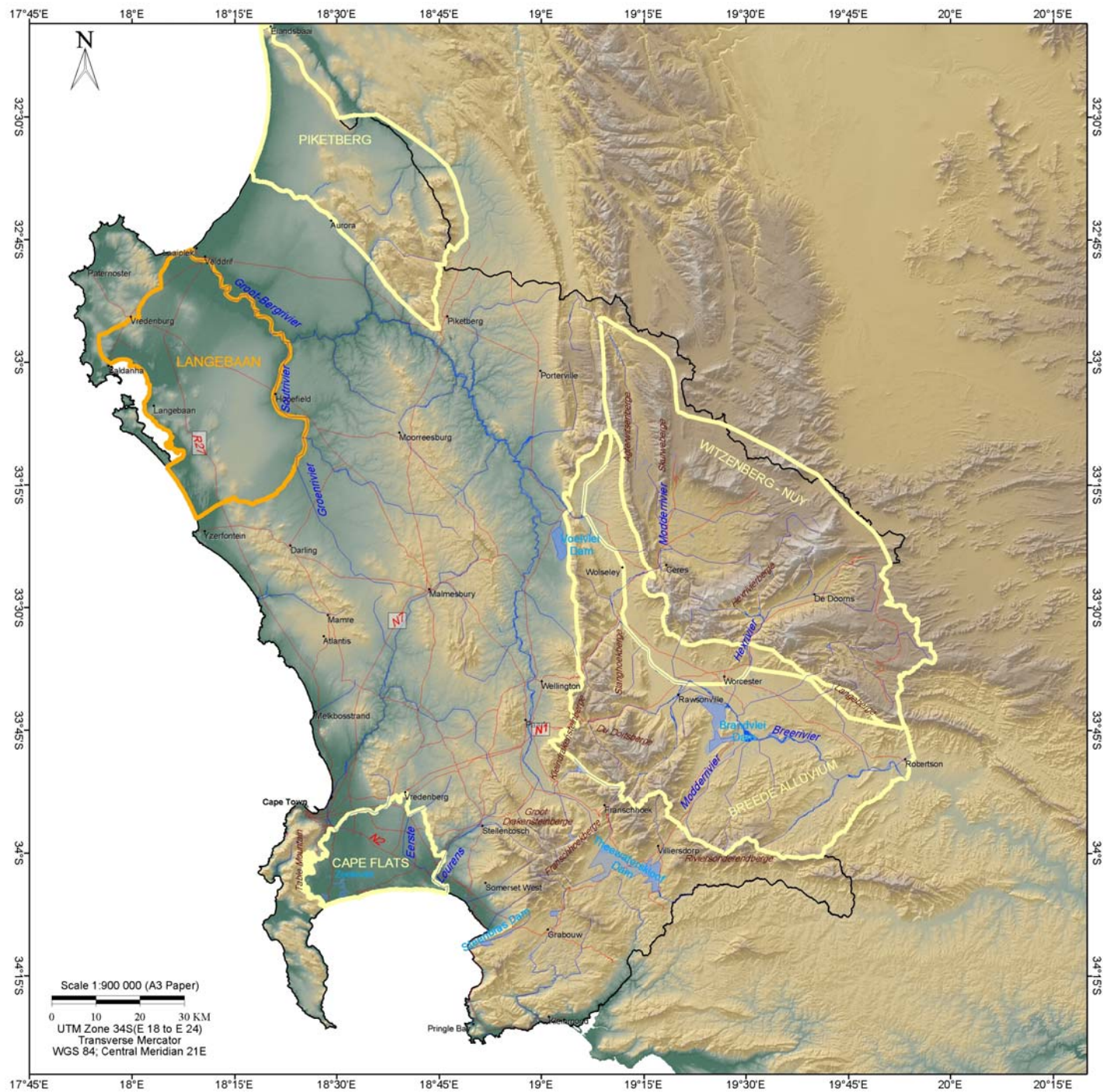
Chapter 4 details available relevant data for the Langebaan area, and describes data input to the numerical model.

Chapter 5 presents the numerical model results. The steady-state model parameter calibration and results are described.

Chapter 6 presents results from calibration of transient modelling.

Chapter 7 details results from using the numerical model scenario testing.

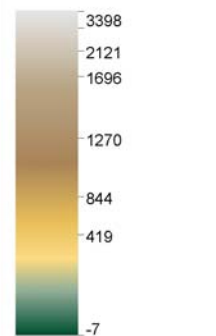
Chapter 8 states the conclusions drawn from the modelling and details recommendations.



LEGEND

- Towns
- Major Rivers
- Roads
- Dams
- Groundwater Study Area
- Langebaan Study Domain
- Other BERG WAAS Study Domains

Elevation (mamsl)



PROJECT NAME

BERG WATER AVAILABILITY
ASSESSMENT STUDY

CLIENT



DEPARTMENT OF WATER
AFFAIRS AND FORESTRY

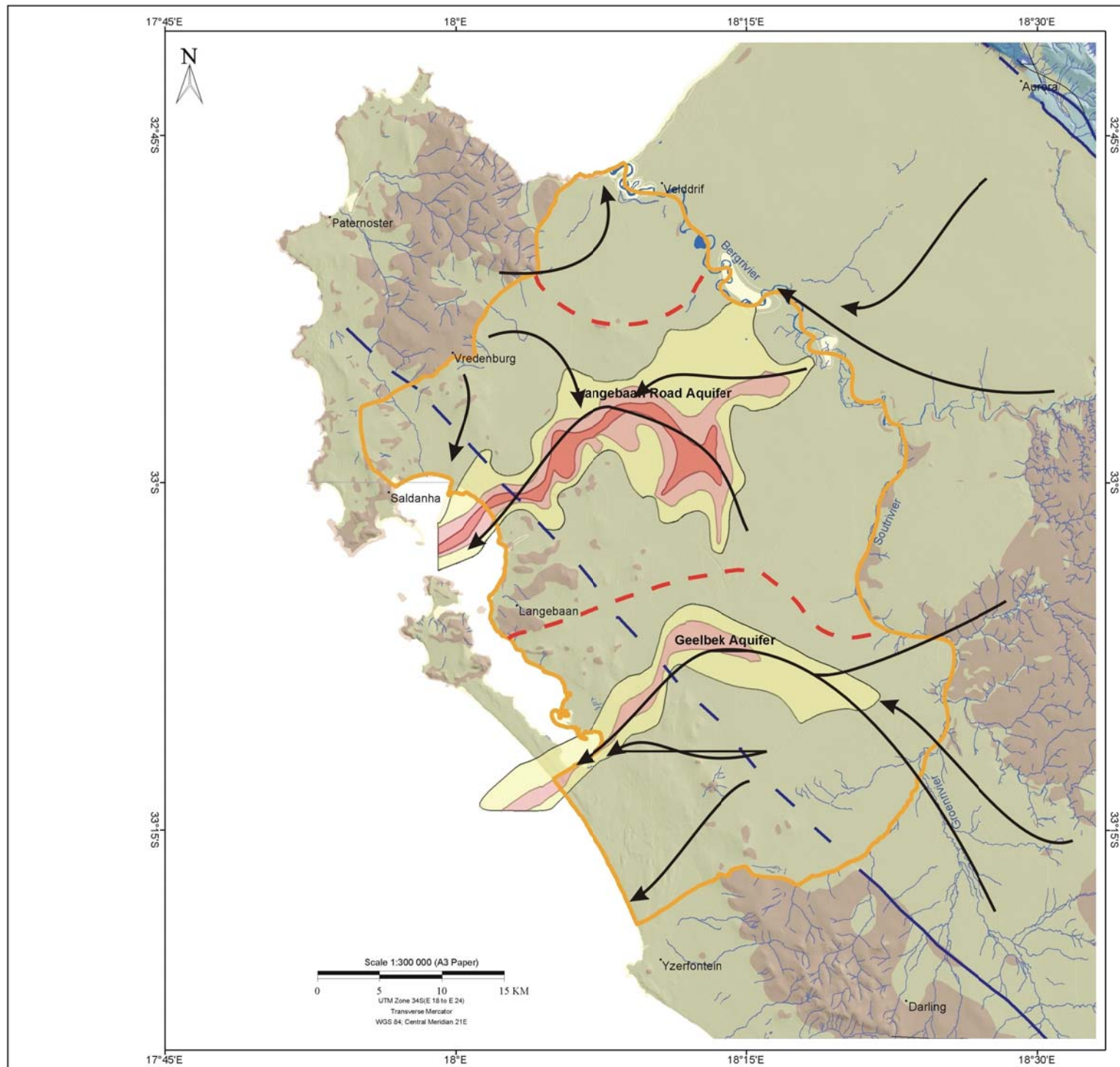
CONSULTANT

UMVOTO

TITLE

LOCALITY MAP

FIGURE 1.2



LEGEND

- Towns
- Rivers
- Faults
- Hydrotects
- Langebaan Model Domain
- Model Sub-domain

Bedrock Elevation (mamsl)

- <-40
- 20_-40
- 0_-20

(For geology legend, refer to figure 5.1)

→ Flow paths

PROJECT NAME

BERG WATER AVAILABILITY
ASSESSMENT STUDY

CLIENT



DEPARTMENT OF WATER
AFFAIRS & FORESTRY

CONSULTANT

UMVOTO

TITLE

CONCEPTUAL MODEL OF
GROUNDWATER FLOW IN THE
LANGEBAAAN ROAD-

FIGURE 1.3

2. GENERAL DESCRIPTION OF STUDY AREA

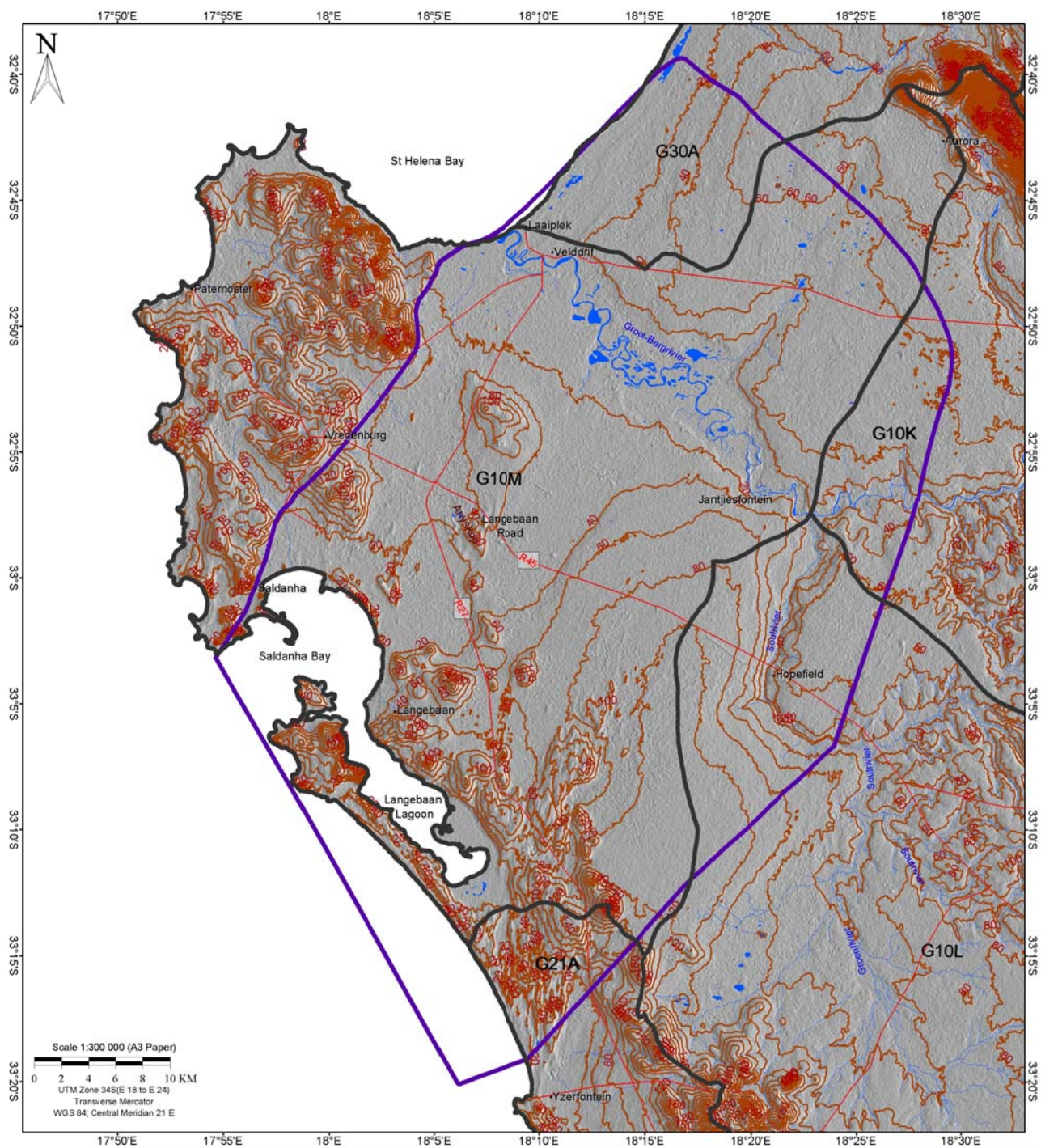
2.1 TOPOGRAPHY & DRAINAGE

Wave-cut terraces overlain by aeolian dunes dominate the topography of the Langebaan area, with sand-covered plains (see **Figure 2-1**), fixed dunes and surface limestone ridges forming the visible landscape. The lower relief plains and dunes generally reach heights of 0 mamsl along the coast to 100 mamsl in the south (see **Figure 2-1**). Intrusive granitic plutons are responsible for raised highlands and koppies, which reach up to heights of 450 mamsl in the regions surrounding Vredenburg and Darling. The Vredenburg highlands and Darling koppies in turn form the northwestern and southeastern boundaries of the study area respectively.

The perennial Berg River is the most significant river in the region, and is located along the northeastern boundary of the study area (see **Figure 2-1**). The Berg River drains northwestwards into the Atlantic Ocean near Velddrif, with its lower courses subjected to tidal influence (Timmerman, 1985b). The non-perennial Sout and Groen Rivers form the eastern and southeastern boundaries of the study area, and drain northwards into the Berg River (see **Figure 2-1**). The rivers themselves are sourced in the higher relief areas to the south and the east of the study area, and are supplemented by water shedding off low permeability Malmesbury Group outcrops.

The study area covers parts of the following Quaternary catchments (**Figure 2.1**):

- G10M
- G10L
- G21A
- G30A
- G10K



LEGEND

- Towns
- Contours
- Roads
- Rivers
- G21A Quaternary Catchments
- Model Domain

PROJECT NAME

BERG WATER AVAILABILITY
ASSESSMENT STUDY

CLIENT



DEPARTMENT OF WATER
AFFAIRS & FORESTRY

CONSULTANT

UMVOTO

TITLE

TOPOGRAPHY

FIGURE 2.1



Figure 2-2 Typically flat topography around the Groot-Berg River: view of the floodplain to the north of the Berg River, Piketberg Mountains in the distance.

2.2 HYDROLOGY AND HYDROCLIMATOLOGY

The WR90 provides certain hydrological and climatological parameters averaged at the catchment scale (Midgley et al, 1994), however the WR90 data shows no flow gauging stations exist within the Langebaan study area. Langebaan and its environs have a Mediterranean climate, with evaporation exceeding rainfall, and most of the rainfall occurring between the months of May to August (**Table 2-1**). Average annual rainfall for the study area ranges between < 100 mm to ~ 500 mm, with most of the region having an annual rainfall of less than 280 mm. The highest rainfall occurs in the southern portion of the study area between Yzerfontein and Langebaan, and the lowest rainfall occurs in the northwest in the granite highlands surrounding Vredenburg (**Figure 2-4**).

Monthly rainfall data for the study domain (which is shown in **Figure 2-3**) is generated by the re-calculation of mean monthly-modelled values, as given by agrohydrology data sets. The rainfall data are then summed to the annual modelled rainfall, as used in Volume 4 of this series (DWAF, 2007c). Rainfall data for the period 1927-2003 from a station near Hopefield (040604W), which is situated where rainfall appears typical for the area, is shown for comparison (“rainfall station mean”) (see **Figure 2-3**). The data shows a higher average than the Berg WAAS modelled rainfall. It is likely that the average across the model domain is reduced significantly by the very low rainfall occurring in the west of the study area, i.e. around the north of Saldanha Bay.

Table 2-1 Available hydrological data at catchment scale (Berg WAAS Volume 2)

Quaternary Catchment	Area	MAP <i>Berg WAAS</i>	MAR <i>WR90</i>	Run-off Efficiency <i>WR90</i>
	km ²	mm	mm	
G10L	1 754.55	305	29	0.07
G10M	2 004.68	225	9	0.03
G21A	523.29	345	32	0.08
G30A	761.28	309	6	0.02
G10K	1 175.89	318	21	0.05

Data on groundwater contribution to baseflow is at catchment scale, and there are numerous limitations with the data (**Table 2-2**). For example, an ephemeral stream which is groundwater fed at certain times of the year would have a baseflow recorded as zero (for a full discussion of the GRAII baseflow and groundwater contribution to baseflow see Volume 2 of this report series, DWAF 2007a). These data hence provide little information on the specific hydrological behaviour of the rivers traversing the Langebaan area.

Data from a DWAF flow gauging station at Jantjiesfontein show typical annual fluctuations of 1.6 m between summer and winter levels (see section 2.2). The data also show peak river flows are up to 2 m above the annual average stage (data supplied by Frans Mouski, DWAF).

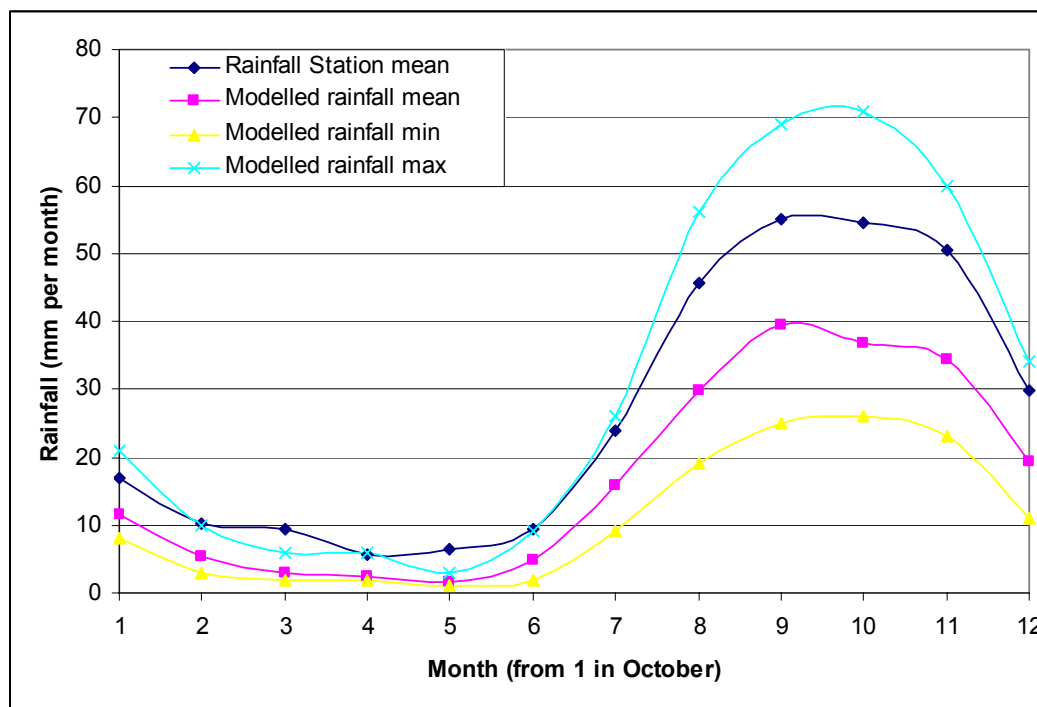
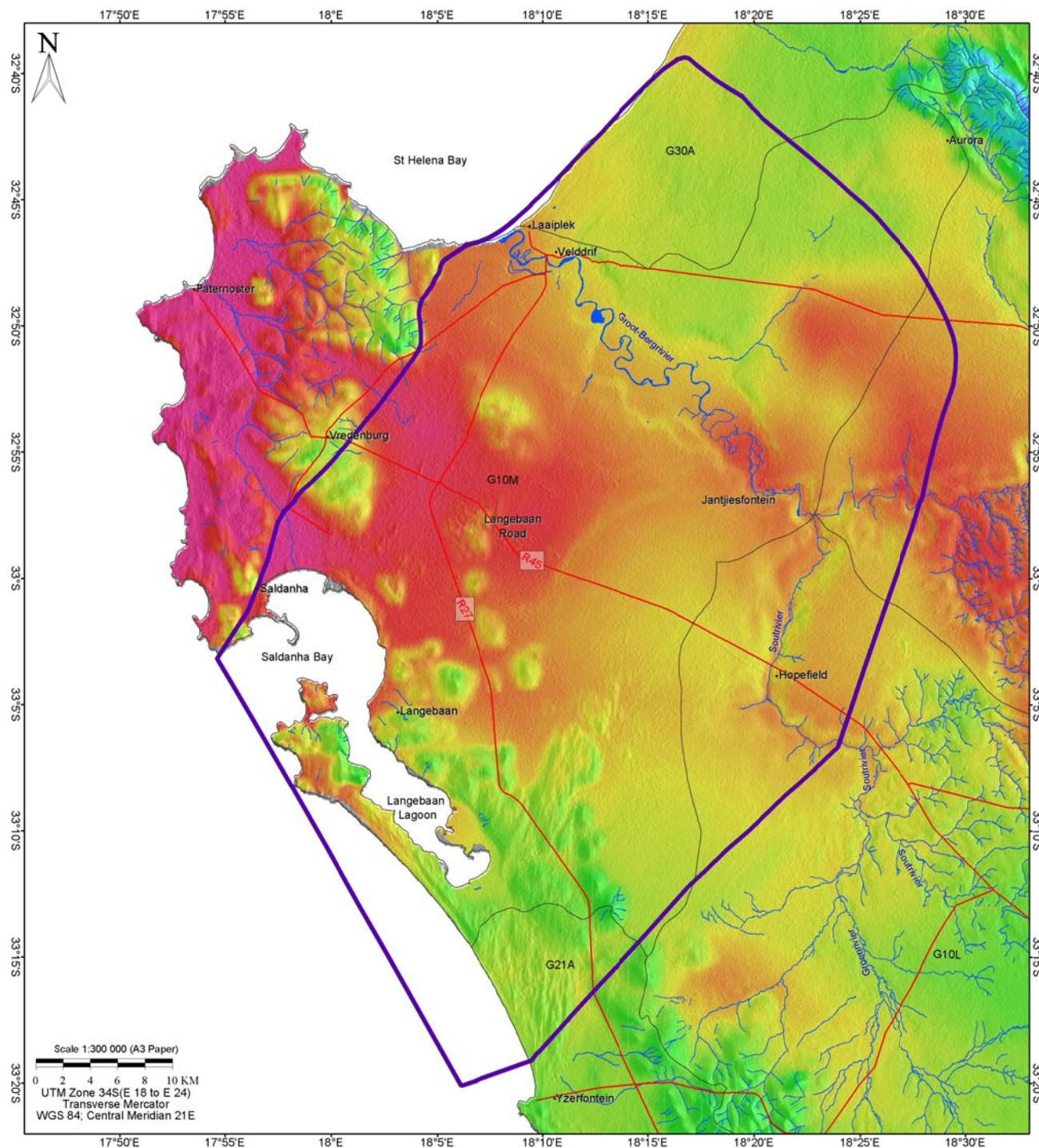


Figure 2-3 Monthly rainfall data for the Langebaan Area

Table 2-2 Baseflow and groundwater contribution to baseflow and per catchment, after GRDM database. (Berg WAAS Volume 3)

Quaternary catchment	Base Flow GRDM	Base Flow HUGHES	Base Flow PITMAN	Base Flow SCHULZE	GW Contribution to Base Flow GW_BFLOW
	mm	mm	mm	mm	mm
G10L	0.0	2.83	0.00	0.00	0.00
G10M	0.0	0.56	0.00	0.00	0.00
G21A	0.0	2.28	0.00	0.00	0.58
G30A	0.0	0.07	0.00	0.00	0.00
G10K	0.0	2.14	0.00	0.00	0.00



LEGEND

- Towns
- Roads
- Rivers
- G21A Quaternary Catchments
- Model Domain

MEAN ANNUAL RAINFALL(mm/a)

- 100 - 140
- 140 - 180
- 180 - 220
- 220 - 260
- 260 - 300
- 300 - 400
- 400 - 500
- 500 - 600
- 600 - 800
- 800 - 1000

PROJECT NAME

BERG WATER AVAILABILITY
ASSESSMENT STUDY

CLIENT



DEPARTMENT OF WATER
AFFAIRS & FORESTRY

CONSULTANT

UMVOTO

TITLE

MEAN ANNUAL PRECIPITATION
(DWAF, 2007)

FIGURE 2.4

2.3 GEOLOGY

2.3.1 Stratigraphy

The Langebaan region is dominated by semi- to unconsolidated Cenozoic (65 Ma to present) sediments, which unconformably overlie the metamorphosed shales of the Malmesbury Group and granites of the Cape Granite Suite. Rocks of the Cape and Karoo Supergroup are distinctly absent. The full stratigraphic sequence for the greater study area is shown in **Table 2-3** below with the units present in the study domain highlighted in blue.

Table 2-3 Stratigraphy of the Wider Study Area

Age range (Ma)	Supergroup	Group	Formation
0 – 2.5		Bredasdorp	Witzand
			Langebaan
			Velddrif
			Springsfontyn
2.5 - 25		Sandveld	Varswater
			Saldanha
			Elandsfontyn
~~~~~ Major unconformity ~~~~~			
65 - 144		Uitenhage	Enon
		False Bav Suite	(dolerite swarm)
~~~~~ Major unconformity ~~~~~			
248 - 290	Karoo	Ecca	
		Dwyka	
290 - 354	Cape	Witteberg	(various)
354 - 417		Bokkeveld	(various)
		Table Mountain	Rietvlei
Skurweberg			
Goudini			
Cedarberg			
Pakhuis			
Peninsula			
443 - 495			Graafwater
		Piekenierskloof	
~~~~~ Major unconformity ~~~~~			
495 - 545	(Saldanian)	Klinheuwel	
545 – >750		Cape Granite Suite	
		Malmesbury	

In the most recent South African stratigraphic updates, Cenozoic sediments west of Kaap Hangklip are now entirely classified as the Sandveld Group, while those east of Kaap Hangklip are termed the Bredasdorp Group (Johnson et al, 2006). In this report however, the original divided group names (i.e. Sandveld and Bredasdorp Groups occur on either side of Kaap Hangklip) are retained for ease of comparison with previous literature on the area. Emphasis in this report is on the geological elements that have influenced modelling decisions, and the reader is referred to Volume 3 of this series for detailed geological descriptions of all stratigraphic units if required (DWAF, 2007b).

The basement rocks of the study area are composed of metasediments of the Malmesbury Group and granites of the Cape Granite Suite. The deeply weathered shales of the Malmesbury Group underlie the younger sediments in the northeast, while the Vredenburg and Darling Plutons of the Cape Granite Suite underlie younger sediments in the southwest (**Figure 2-5**). The Berg River flows approximately parallel to and just east of the regional contact between the Malmesbury Group and Cape Granite Suite.

The Vredenburg Pluton dominates the topography, distinctive geomorphology and coastline of the area from Langebaan up to St Helena Bay. Vredenburg lies at the southern edge of the most exposed sections of the pluton and falls just west of the model domain. The Swartberg forms the northernmost outcrop of the Darling Pluton, which also extends beyond the model domain. Both these areas are characterised by low-lying, granitic hills.

The Sandveld and Bredasdorp Groups unconformably overlie the basement. The geology of the Sandveld and Bredasdorp Groups in the area has been described in detail by various workers including Timmerman, 1988; Rogers, 1980, and more recently by Rogers, 2006. It is only briefly summarised here however, with an emphasis on factors relevant to their hydrogeology, such as aerial extent and hydraulic nature. The various formations in each of these two Groups are summarised in **Table 2-4** below.

The fluvial Elandsfontyn Formation (not to be confused with the Elandsfontein Aquifer system) occurs within the deeper basement areas of the palaeochannels, and is overlain by the phosphatic marine deposits of the Varswater Formation. The sands of the Bredasdorp Group form the palaeo- and currently active dunes.

**Table 2-4 Stratigraphy of the Cenozoic (65 Ma to present) sediments between Saldanha and the Berg River (after Rogers, 1980, and Timmerman, 1985b)**

Group	Formation	ORIGIN	DESCRIPTION
Bredasdorp  <i>Summary: Clean sand, calcareous sands, and calcrete.</i>	Witzand	Aeolian	Semi consolidated calcareous dune sand
	Langebaan Limestone	Aeolian	Consolidated calcareous dune sand. The Aeolian deposit accumulated during the last glacial lowering of sea level when vast tracks of un-vegetated sand lay exposed on the emerging sea floor.
	Velddrif	Marine	Beach sand. Associated with the last interglacial sea level rise with 6-7 m above present level.
	Springfontyn	Aeolian	Clean quartzitic sands, a decalcified dune sand. Dominates in the coastal zone.
Sandveld  <i>Summary: Basal gravel overlain by clay, overlain by various sands with peat /clay layers.</i>	Varswater		Various subdivisions are proposed in literature (for a summary see Rogers, 1980). Deposits include a coarse basal beach gravel member, peat layers, clay beds, rounded fine to medium quartzes sand member and palatal phosphate rich deposits. Varswater sediments do not extend further than 15 km inland of Saldanha Bay (reaching ~halfway to the Berg River) (Timmerman, 1985b).
	Elandsfontyn	Fluvial	Coarse fluvial sands and gravels, deposited in a number of palaeochannels filling depressions. The deposits were subsequently covered by clays and peat.

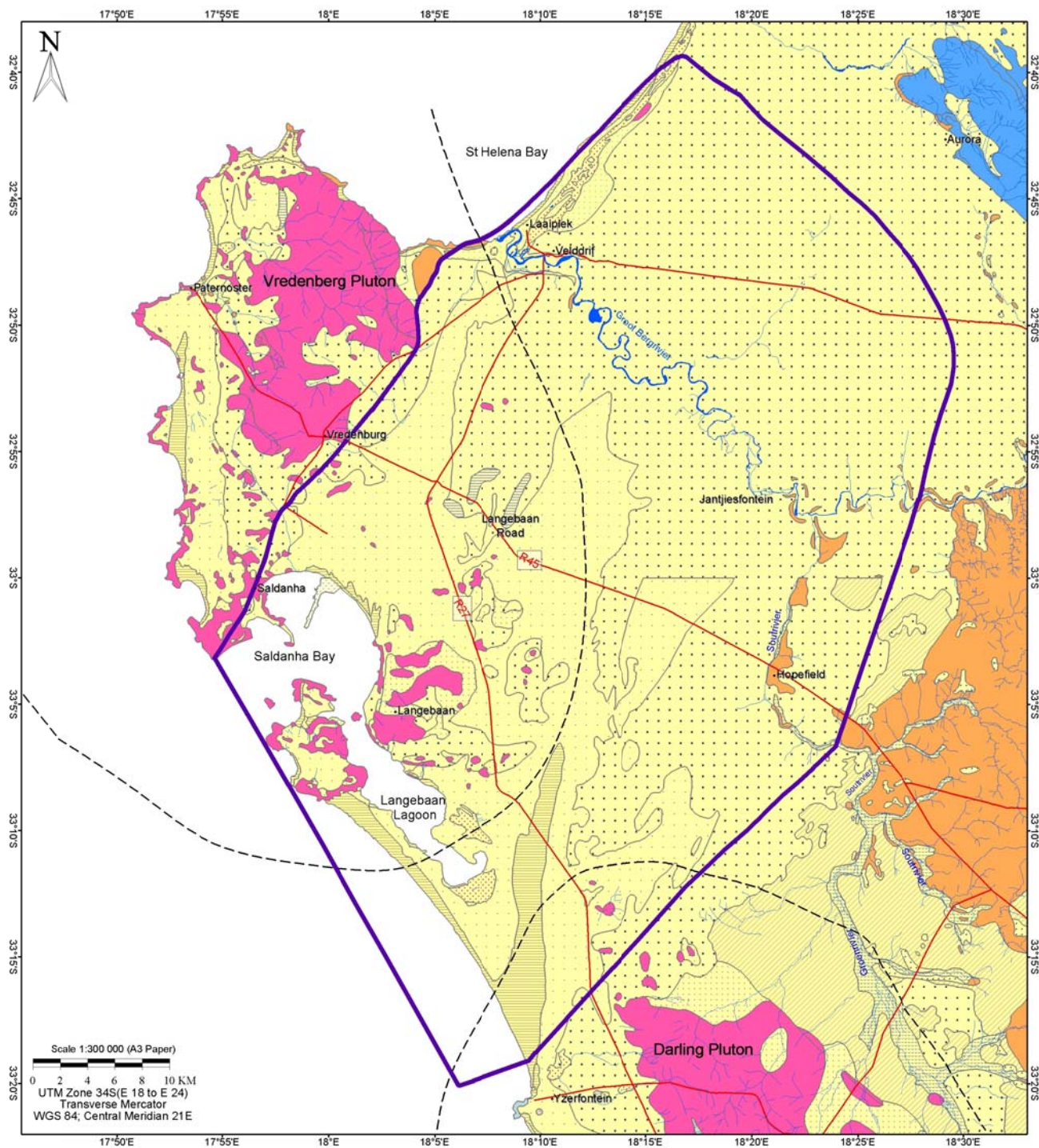
The Bredasdorp Group formations all outcrop at surface in the area, however no exposure of the Elandsfontein Formation, natural or artificial, has been recognised (Rogers, 1980).

Sediment in the study area has an average thickness of ~ 70 m, reaching a maximum thickness of >100 m at Anyskop (Woodford et al, 2003). The Elandsfontyn Formation gravels can reach a maximum thickness of 60m, with their overlying clays reaching a maximum thickness of 50 m (Woodford et al 2003). The basal gravels are restricted exclusively to palaeochannels however, and reach a maximum stratigraphic height of 5 mamsl. The sand unit is not continuous beneath the Berg River, nor is it continuous between the two palaeochannels (Timmerman, 1988). The uppermost clay unit of the Elandsfontyn Formation is aerially extensive, covering all areas south of the Berg River where the lower sands and gravels are deposited (Timmerman, 1988) and absent beneath the Berg River (Timmerman, 1988).

North of the Berg River the basal Elandsfontyn Formation is absent in a 3-4 km wide zone along the coastline, but attains a thickness of 40 m thick inland (Timmerman 1985a, fig 17). The Varswater Formation only exists to a limited extent. The Bredasdorp Group sediments vary from 0-10 m thick, reaching a maximum 25-30 m thick, and are finer grained and muddier than south of the Berg River (Timmerman, 1985b).

The Cenozoic (65 Ma to present) sedimentary succession in **Table 2-4** can be explained by changing palaeoclimate. During the Middle Miocene, between about 15.6 and 12.5 million years ago, one of the largest shifts in global climate produced dramatic global cooling and the reorganisation of ocean-circulation patterns. This dramatic and permanent shift set the stage for modern oceanic and atmospheric circulation, and ushered in the bipolar ice ages that have dominated climate records for the last 2.5 million years.

During the Neogene (25 – 2 Ma) marine transgression, the granite-dominated topography was flooded, forming a set of islands surrounded by shallow seawater. A proto-Berg River in the area would no longer have discharged into the sea via the Geelbek Gap (a well-defined 10 km wide gap in granite outcrops at Geelbek that is mapped at < 20 mamsl), which now acted as an inlet for the Neogene sea. Work done by Hendey (1974) indicated that the mouth of the proto-Berg river then shifted northwards to the northeast corner of the Varswater Quarry. The basal gravels deposited by the proto-Berg River were therefore overlain by phosphate rich marine sediments. During the Pliocene (5 – 2 Ma) the Berg River mouth continued to shift northwards as seen in evolutionary changes within fauna. Thus a change from dominant, fluvial erosive conditions along the coastal plain to aggradational, aeolian processes occurred. These aeolian processes were dominated by the dune-migration of fine carbonate-rich sands, which led to the Pliocene-Pleistocene (5 Ma – 10 000 years BP) development of aeolian landforms along the coastal plain of the Western Cape. This in turn produced significant changes in the surface hydrology of the river systems by damming and diverting their lower courses (Volume 3 of this report, DWAF, 2007c). The dominant palaeo-wind direction is evident in the present surface geology, as the palaeodunes of the Langebaan and Witzand Formation both generally trend north-south.



## LEGEND

- Towns
- Approximate Plutons Extent
- Roads
- Rivers
- ▭ Model Domain

## LITHOLOGY

- Alluvium
- Loam and sandy loam
- Brackish, calcareous soil
- Gravelly clay/loam soil
- Witzand
- Springfontyn
- Velddrif
- Langebaan
- Varswater
- Ferricrete, Silcrete
- Table Mountain Group
- Cape Granite Suite
- Malmesbury Group

## PROJECT NAME

BERG WATER AVAILABILITY  
ASSESSMENT STUDY

## CLIENT



DEPARTMENT OF WATER  
AFFAIRS & FORESTRY

## CONSULTANT

UMVOTO

## TITLE

## REGIONAL GEOLOGY

FIGURE 2.5



### 2.3.2 Palaeo-topography

It is accepted in the literature that the basement in the study area is incised by distinct palaeochannels that can be correlated with palaeo-courses of the Kuilders, Berg and Groen rivers (Timmerman 1985b, Hay & Hartnady 1995, Woodford et al, 2003). However, many of the previously documented basement elevation maps of the area show these palaeochannels as enclosed basins rather than continuous channels.

According to Rogers (1980), the bedrock topography is a result of fluvial and marine processes. A weakly-defined palaeochannel exists to the north east of Saldanha Bay (the northern palaeochannel). Bedrock depth is at -20 mamsl around the coast and the channel trends NE at depths of between -20 to 0 mamsl, linking Saldanha with St Helena Bay. However, lower bedrock depths exist to the east of this palaeochannel (less than -20 mamsl), suggesting an isolated basin that is not connected to the coastline. A southern palaeochannel exists between the Yzerfontein-Langebaan Peninsula coastline, trending inland via the Geelbek Gap.

Various descriptions of the basement topography have been generated by Timmerman (1988). Depths are recorded in the northern palaeochannel of -55 mamsl in the vicinity of Saldanha, to -25 mamsl near the Berg River, with its widest point just north of Langebaan Road (Timmerman, 1988). The southern channel slopes from -40 mamsl at Langebaan Lagoon to +10 mamsl near Hopefield.

The above workers, and in addition Woodford et al, (2003), overlooked the available offshore drilling results, which have never been correlated with onland bedrock elevations (De La Cruz, 1978). De la Cruz (1978) conducted marine geophysical investigations in Saldanha Bay. The data shows that there is an elongated depression in the bedrock extending through the central part of Saldanha Bay. The depression enters the Outer Bay from the continental shelf roughly midway between Malgas Island and Jutten Island, at a maximum depth of ~ -75 mamsl. The depression then extends in an easterly direction, passing through Marcus Island and Elandpunt at a depth of -60 mamsl. From here it extends in a SW/NE direction so that, along the northeastern shore of the Inner Bay, the bedrock is at -70 mamsl (Hay and Hartnady, 1995). The questionable nature of the closed contours in previous worker's basement elevation interpretations is discussed fully by Hay and Hartnady (1995). Through consideration of palaeofluvial processes, it is sensible from a scientific point of view to assume that the basement elevation reflects a gradual westward declination along the axis of the proto-Berg palaeochannel, from elevations of around 0 to -20 mamsl below the present Berg River, downstream to -60 mamsl beneath the shoreline at Saldanha Bay (Hay and Hartnady, 1995, and Volume 3 of this report, DWAF, 2007c). By the same geological process consideration, the southern palaeochannel is also interpreted as a continuous channel.

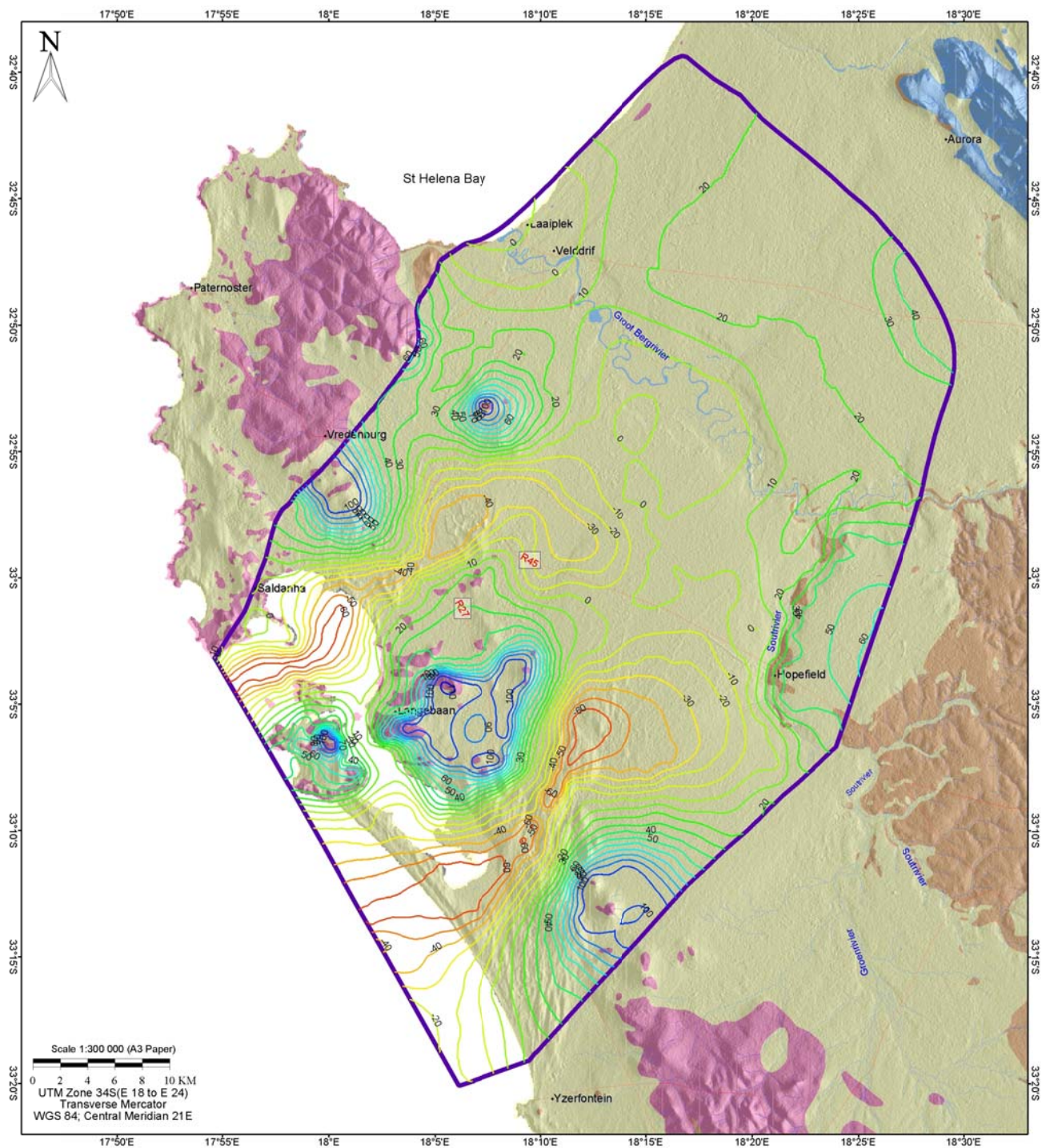
This interpretation of continuous palaeochannels has been used to generate the basement topography used in the modelling. The data set is based on points from the NGDB database-filtered for only those boreholes that were reliably recorded as reaching bedrock, and using bedrock outcrops as constraints. Automatic contouring of this data generated some closed contours along the axis of the palaeochannel. Closed contours were caused by the interpolation technique through which a point along the palaeochannel axis is affected by points on its flanks, rather than interpolating a gradually decreasing depth along axis. These contours were manually adjusted along the axis of the palaeochannel to create a gradual and smoother decrease in elevation towards the coast. The basement topography is shown in **Figure 2-7**. The interpolation technique used by the GIS software to produce this figure re-introduced

closed contours that are open in the model input file, for example the –40 mamsl contour along the LRAS palaeochannel and the -60, -50, and -40 contour in the EAS (**Figure 2-7**). This is a factor of the display method only and the basement elevation in the model decreases along the palaeochannel axis.

There is a sparsity of borehole data around the Berg River, and the northern reaches of the LRAS palaeochannel. Therefore the basement elevation beneath the Berg River is less certain. The basement map of Timmerman (1988) shows the –20 mamsl contour extending from the LRAS palaeochannel beneath the Berg River. But this is not supported by borehole data. He presents 2 cross sections that traverse the Berg. These show that the basement at the Berg is indeed between 0 to 20 mamsl, but that the basement decreases to the southwest; i.e. that there is a basement high between the low under the Berg (connected to lows northeast of the river) and the LRAS. Contouring based on the NGDB data suggests the basement under the Berg River is ~0 mamsl (**Figure 2-7**).

According to Timmerman (1988) there might have been a connection in the basement between the two paleochannels during the Miocene period when the pre-Miocene surface reached its deepest cut. But this is not supported by borehole data that shows that the basement rises between the two channels to a minimum of 0 mamsl (**Figure 2-7**). Although there are uncertainties with the NGDB data, the interpretation of a 0 mamsl basement rise is based on a number of records. Also, it makes geologic sense that the palaeochannels are separated as any connection would have prevented the development of two deeply incised channels.

North of the Berg River the palaeotopography does not show deeply incised channels. Close to the St Helena Bay coast and along the Berg River the bedrock is between –20 and 0 mamsl. Bedrock elevation increases inland and to the northeast, reaching 40 mamsl (Timmerman, 1985a; figure 9).



## LEGEND

- Towns
  - Roads
  - Rivers
  - ▭ Model Domain
- BEDROCK (mamsl)**
- 60 - -50
  - 50 - -40
  - 40 - -30
  - 30 - -20
  - 20 - -10
  - 10 - 0
  - 0 - 10
  - 10 - 20
  - 20 - 30
  - 30 - 40
  - 40 - 50
  - 50 - 60
  - 60 - 70
  - 70 - 80
  - 80 - 90
  - 90 - 100
  - 100 - 110

## PROJECT NAME

BERG WATER AVAILABILITY  
ASSESSMENT STUDY

## CLIENT



DEPARTMENT OF WATER  
AFFAIRS & FORESTRY

## CONSULTANT

UMVOTO

## TITLE

PALAEOTOPOGRAPHY

FIGURE 2.7

### 2.3.3 Summary of hydrostratigraphy

The significant aquifer systems are:

- Langebaan Road Aquifer system (LRAS) situated in the northern palaeochannel
- Elandsfontein Aquifer System (EAS) situated in the southern palaeochannel
- Adamboerskraal Aquifer system (AAS) situated north of the Berg River (Timmerman 1985b, and Woodford et al, 2003). This system is not modelled explicitly, but only as part of the wider regional flow.

The significant units for the hydrogeology, which are present in each of the 3 aquifer systems above, are:

- the basal gravels of the Elandsfontyn, forming the lower aquifer unit, LAU,
- the clay layer of the upper Elandsfontyn, which acts to (semi) confine the basal aquifer,
- the variably consolidated sands and calcretes, with interbedded peat clay of the Bredasdorp, the upper unconfined aquifer unit, UAU.

The hydrostratigraphy as suggested by Timmerman (1985b) is shown in **Table 2-5**. The basal sand and gravels of the Elandsfontyn formation (LAU) are the most important aquifer, most significantly in the area of Langebaan Road where it is thick (up to 60 m) and has larger aerial extent. The aquifer is restricted to palaeochannels and it is this restriction that defines the separate LRAS and EAS. Timmerman (1988) suggests that the lower Elandsfontyn unit is not continuous all the way to the mouth of the palaeochannel, presenting an isopach map which shows the unit to pinch out ~5 km inland from the coast (Timmerman 1988, map 3.6). However NGDB boreholes within 4 km of the coast intersected the basal clay and gravel of the Elandsfontyn. If the palaeochannels are considered as continuous fluvial channels rather than isolated depressions, it is geological sense that the basal gravel would be continuous. The implication of offshore palaeochannels is that the volume of groundwater is increased but offshore groundwater is not usable due to the risk of seawater intrusion. This risk is actually reduced by the fact that there is (semi-) artesian pressure from basal aquifers which extend off shore.

The basal aquifers within the LRAS and EAS are considered not connected. There are questions over a possible connection in the basement topography between the systems, discussed above in section 2.3.2 above, and also discussed in Woodford et al (2003). Representatives of DWAF also advocate that there is the potential for a connection (Henk v Kleef, pers comm. 2007) and an unpublished report for DWAF, by Stettler et al (2007) has been suggested to support the case (received from Eddy van Wyk, November 2007). However the area covered by Stettler et al (2007) does not extend beyond the reaches of the LRAS palaeochannel system. Regardless of the basement topography, the aerial extent of the LAU dictates the potential of any connection. The uppermost sand unit of the Elandsfontyn is not connected between the LRAS and EAS (Timmerman, 1988). Groundwater is intercepted locally in the Malmesbury basement rocks, where the Malmesbury is transacted by regional dykes and faults (for example in the Swartland and on the Cape Flats). But at the regional scale the volumes of water involved in this process are assumed negligible and the basement is assumed an impermeable base to the aquifer systems.

The relatively impermeable clays of the uppermost Elandsfontyn Formation confine the lower aquifer. The clays underlie a wide area over the centre of the LRAS and EAS and north of the

Berg River. The clay formation has, however, been eroded along the lower course of the Berg River itself, and within ~5 km of the southwest coastline (Timmerman, 1988, Map 3.8). The basal gravels are considered continuous along the length of the palaeochannel and therefore the permeable aquifer units locally sub-outcrop beneath only a thin cover of younger aeolian sands. North of the Berg River the muddier Papkuils member (Bredasdorp) contributes to the aquitard (Timmerman, 1985b).

The aquifers in the Bredasdorp and Varswater formations are unconfined to semi-confined and continuous (not necessarily homogenous) over the whole study area (unlike the discontinuous LAU). These aquifers are thin in the LRAS and AAS (<20 m) but thicker in the EAS. Timmerman (1985b) lists the lower Bredasdorp within the EAS as semi-confined (**Table 2-5**). However he also notes that the UAU in the EAS is “a very complex system where the occurrence of aquifers is not related to specific geological units but to the composition of a given geological succession at any particular place” (Timmerman 1985b, op cit p10). Therefore over the regional scale it is likely that the whole upper Bredasdorp can be represented by an equivalent homogeneous (unconfined) hydraulic conductivity.

A summarised stratigraphy is shown in **Figure 2-8** below. Geological features have been averaged to one typical section, which can be applied across the model domain.

**Table 2-5 Hydrostratigraphy (Timmerman, 1985b)**

Aquifer Unit	Lithostratigraphic unit		Aquifer type	Thickness (m)
	Formation	Member		
Adamboerskraal Aquifer System	Bredasdorp	-	Unconfined	10-20
	Elandsfontyn	1 Clay	Aquitard	20-30
		2 Sand and Gravel	Confined	20-40
Langebaan Road Aquifer System	Bredasdorp	Langebaan Limestone	Unconfined	10-20
	Elandsfontyn	1 Clay	Aquitard	10-20
		2 Sand and Gravel	Confined	40-60
Elandsfontein Aquifer System	Bredasdorp	1 Springfontyn	Unconfined	5-20
	Varswater	2 Noordhoek	Aquitard	5-60
		1 PPM	Aquitard	0-20
		2 QSM	Semi-confined	0-30
				<u>TOTAL UAU</u>
				<u>10-130</u>
	Elandsfontyn	1 Clay	Aquitard	10-30
		2 Sand and Gravel	Confined	10-30

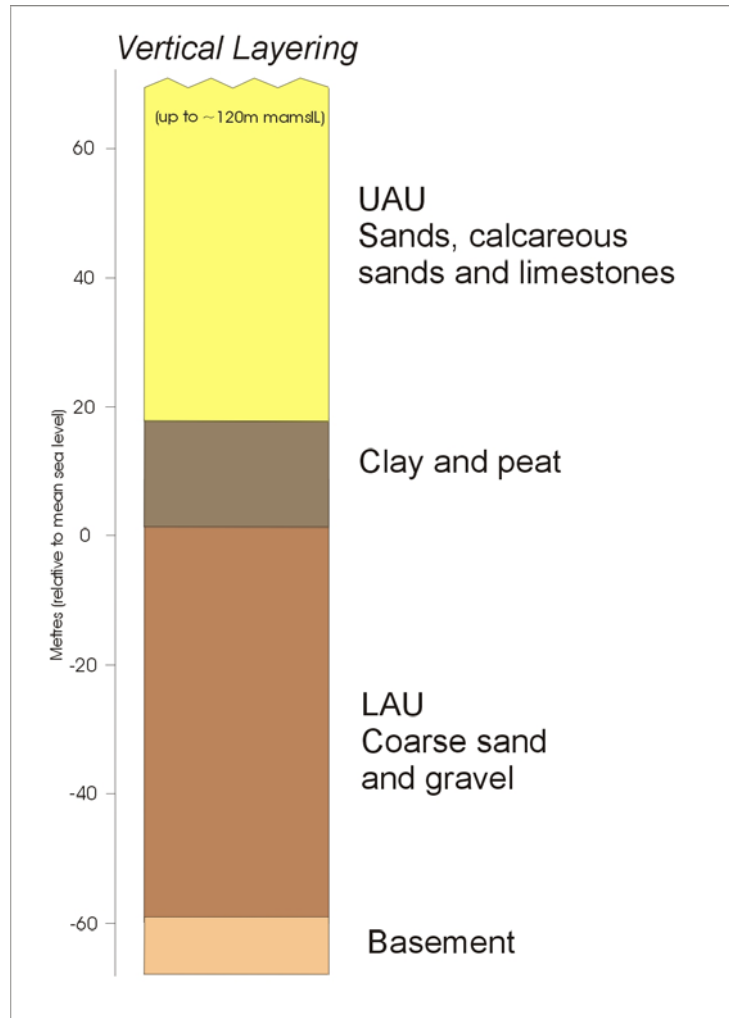


**Figure 2-8 Geological summary**

*The typical stratigraphic elevation of each of the layers is shown. The stratigraphic height of the top of the units is determined from assuming that the layers are sub horizontal and taking one level for each surface, from each of the sections shown in the cross sections in **Figure 2-6**. The levels were then averaged. The typical thickness of the clay was also taken from the thickness ranges given in Table 2.5 and averaged between the LAS and EAS. This gave a similar result (only 1 m difference) as calculation from the cross sections.*

*The thickness of the UAU depends on topography. The top of the clay sits at 18 mamsl, and base at 1.5 mamsl. the average thickness of the unit is ~16.5 mamsl. The average thickness of the LAU is 35 m, depending on the basement depth.*

## 2.4 HYDROGEOLOGY

### 2.4.1 The flow regime

The significant features from the hydrostratigraphy and the palaeotopography that dictate the flow regime are:

- The lower (semi-) confined aquifer unit occurs in the palaeochannels and is unlikely to be connected between the LRAS and the EAS, as a basement elevation of at least 0 mamsl separates the two palaeochannels.
- The upper aquifer unit (UAU) is continuous across the area.
- The clay unit confining the LAU is absent along the SW coastline and in the vicinity of the Berg River.

Woodford et al (2003) report that groundwater flow patterns are similar in the lower and upper aquifer units. However this is unlikely to be completely accurate due to the different nature of the 2 aquifers and their different aerial extents. It is suggested that the flow in the LAU is controlled by the bedrock topography and flow occurs along the axis of the palaeochannels, towards their exits on the SW coastline. Flow in the UAU is more likely to be topographically controlled. The UAU is directly recharged from rainfall, which is concentrated in the dune areas west and southwest of Hopefield, where topography, and water levels are highest (**Figure 2-1** and **Figure 2-9** and **Figure 2-12**).

The water level map presented (**Figure 2-9**) is not aquifer-specific. The points are a mixture of single water level records and averages for time-series data. Due to lack of information in the NGDB regarding where the boreholes are screened, it is not possible to generate an aquifer-specific contour map with any real confidence. But, for calibration purposes, aquifer-specific data is required. For a selection of the point data the aquifers are separated based on assumption only that their drill depth determines which aquifer they are screened in (described in section 5.3). The signal shown in **Figure 2-9** is a mix of the 2 aquifers, however it is possible to detect imprints of the behaviour of the LAU and UAU. (Note: The contouring package used in **Figure 2-9** has automatically closed contours towards the coast at Veldrif. The groundwater contours should reduce to zero towards the coast.)

The flow direction from the water level high SW of Hopefield is semi-radial towards the east, north, west and southwest. The flow to the north crosses from the area of EAS to the LRAS. This flow path is an imprint of the UAU which is geologically continuous between the aquifer systems. The flow path which continues north from the recharge mound, flowing to the Berg River is interpreted as an imprint of the UAU due to the absence of the LAU in this position (Timmerman 1988) and because flow in the LAU is controlled by the bedrock topography and therefore would flow SW from this position. The flow from the recharge mound to the SW may reflect the movement of groundwater in the UAU and LAU combined. The LAU has higher hydraulic conductivity, which may generate the low water levels over the LRAS. The abstraction from the LAU may also generate the lower levels. It is unlikely that water in the northeast of the LRAS palaeochannel will flow uphill towards the Berg River, hence the contours in the northeast of the LRAS which show the Berg River gaining, are an imprint of the UAU.

The flow directions indicate many flow divides. One such divide exists between the Langebaan Lagoon and Saldanha Bay, trending northeast. The divide separates the LRAS and the EAS, however it only extends 15 km inland from the southwest and hence there is flow across this

boundary, from the EAS southeast of the divide to the LRAS in the UAU (from the recharge mound in the south of the study area, as described above).

Recharge for the UAU concentrates in this area southwest of Hopefield, but also exists across the region (**Figure 2-12**). The UAU discharges to the Berg, and to the coast in Saldanha Bay and to the coastline south of the lagoon. The LAU is recharged in areas where the head difference between upper and lower aquifer is large enough to drive vertical recharge downwards (via leakage through clay if a clay layer is present). The LAU also discharges to the coast in Saldanha Bay and to the coastline south of the lagoon.

According to Timmerman (1985b) a groundwater divide exists from the Darling granite hills in the south to the Berg River Station (Timmerman 1985b, fig 5, or along the elongate contours from the recharge mound in **Figure 2-12**). **Figure 2-9** suggests that there is a flow divide in the UAU from the recharge mound oriented NNE across the contours. The Sout River flows ~northeast to the southeast of the recharge mound, and therefore along the recharge mound there must be a divide separating drainage which flows away from the area to the Sout River. The model boundary in the southeast is based on this approximate divide.

Without aquifer specific piezometric maps it is difficult to be more accurate with regard to the hydraulic nature of the aquifer than the above discussion. It is important to note that **Figure 2-9** was contoured with all available water level records in the NGDB, however the number of NGDB points which have geology data and water level information are much less. Comparison of a piezometric map of each aquifer would show areas where the LAU is artesian, areas where the artesian conditions ease and there is downward flow (recharge) from the UAU to the LAU.

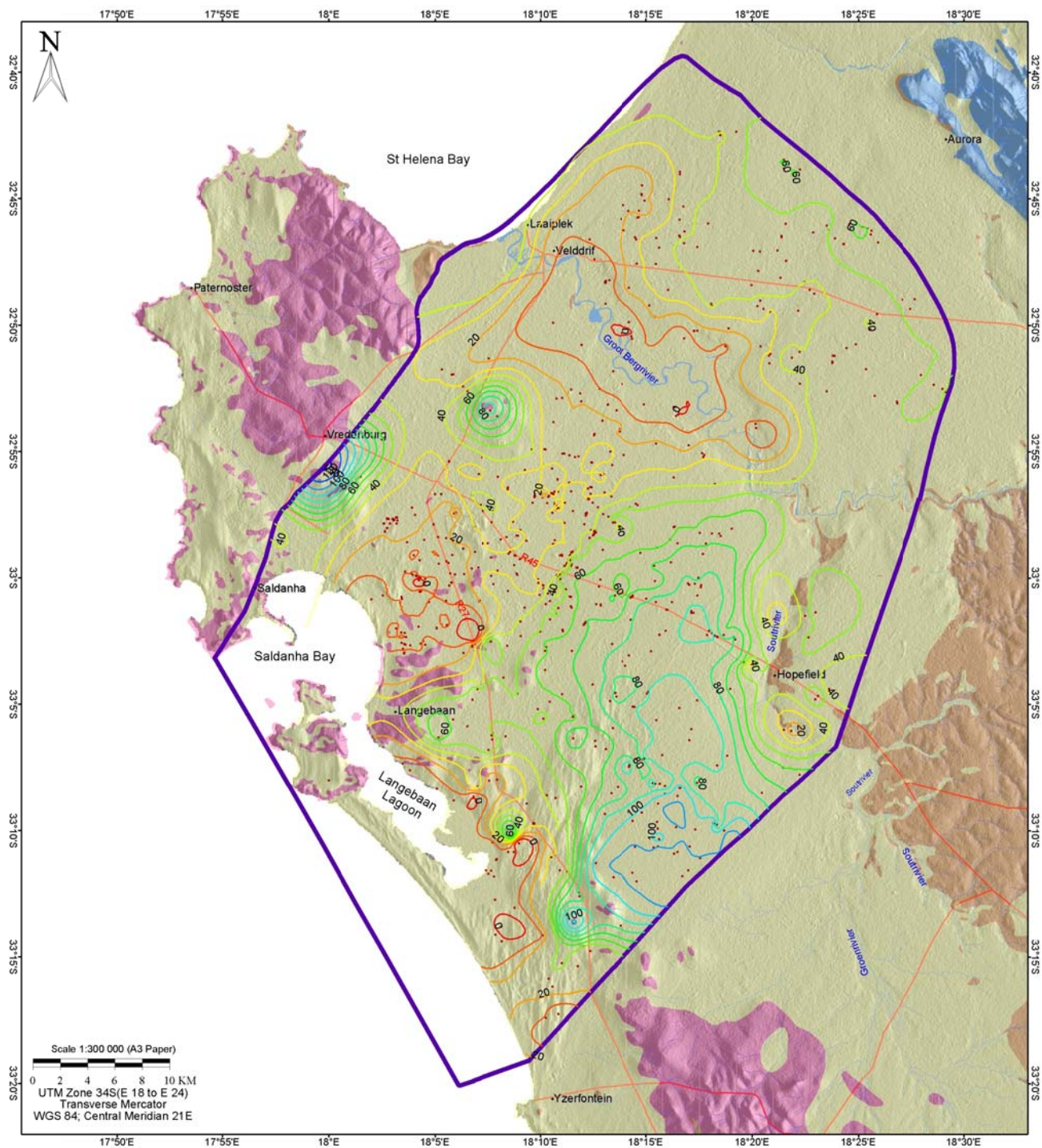
The degree to which the LAU is confined is likely to be highly variable across the area, with thickness of the clay layer varying from 0-30 m. Analysis of NGDB data reveals numerous boreholes that were drilled to the LAU having water levels recorded as equal to groundlevel. The following data observations give an indication of the variability:

- At the West Coast Fossil Park, located at Langebaan Road in the centre of LRAS, perennial ponds have developed in the excavation depressions. These ponds are assumed to be groundwater fed from the UAU. There is a borehole situated in the centre of one such pond that has recently (October 2007) become artesian (**Figure 2-10**). The flow rate is ~0.5l/s which is interpreted to represent ~3 m head of water difference between the 2 aquifers (pers comm. L Groenewald, 2007).
- There are very few water level data points from the 2 aquifers at the same point. Ideally multi-level piezometer measurements are required. The available data shows a difference of 11m between the 2 aquifers (LAU 11 m higher than UAU) close to the palaeochannel mouth in the EAS. This measurement is from 2 boreholes in close proximity. Boreholes located 4 km inland from Saldanha Bay in the LRAS show only 0.86 m difference (again LAU higher than UAU). The geology logs (NGDB) show that the clay and the gravel Elandsfontyn formations are present in both these positions. The difference in confinement is possibly caused by differing thickness of the clay formation, but thicknesses are not clear in the logs as geology is only recorded at the depths where samples were taken. Site-specific heterogeneity will also affect these measurements and many more than one is required to analyse the degree of confinement.

North of the Berg River the water level map (**Figure 2-9**) shows the flow direction broadly following the basement elevation and flow is from the higher land in the east, towards the coast

---

and towards the Berg River. Timmerman (1985a) describes this pattern as towards the sea in the northern part of the area, towards the Berg River in the southern part, and in both these directions in the central part. The contour spacing (Timmerman 1985a, figure 15) suggests slower 'sluggish' flow 15km inland (under a gradient of 0.001) which speeds up to the coast and Berg River.



## LEGEND

- Towns
- Water Level Points
- Roads
- Rivers
- Model Domain

## WATER LEVEL (mamsl)

- 0 - 5
- 5 - 10
- 10 - 20
- 20 - 30
- 30 - 40
- 40 - 50
- 50 - 60
- 60 - 70
- 70 - 80
- 80 - 90
- 90 - 100
- 100 - 110
- 110 - 120

## PROJECT NAME

BERG WATER AVAILABILITY  
ASSESSMENT STUDY

## CLIENT



DEPARTMENT OF WATER  
AFFAIRS & FORESTRY

## CONSULTANT

UMVOTO

## TITLE

WATER LEVELS

FIGURE 2.9



**Figure 2-10 Artesian Borehole in groundwater fed pool: Evidence of 2 water tables**

*Photograph taken at the West Coast Fossil Park at Langebaan Road, the site of a disused quarry. A perennial groundwater fed pond is shown which has developed in the excavation depression (fed from the UAU). A deep (80m) borehole situated in the centre of the pond has recently (October 2007) become artesian. This is evidence for 2 separate aquifer systems: an upper unconfined and a deeper confined aquifer.*

### 2.4.2 SW-GW interaction

Quantifying the interaction of surface and groundwater is required for the Berg River, the main river of interest in the area. The water level contours (**Figure 2-9**) are generated from averages of all recorded water levels at each borehole with records. They indicate flow towards the Berg River and a sink to the groundwater in the area of the Berg River. Groundwater may be discharged to the Berg River (a gaining river, see **Figure 2-11**) or possibly discharged by direct evaporation where groundwater is shallow close to the river, or to evapotranspiration in the riparian zone. In the model the sink is represented together, as the 'river boundary condition', because it is not possible to independently quantify the evaporative losses. Also, it is assumed that evaporative losses are minor in comparison to the river and thus the dominant sink is considered to be the river. Therefore this groundwater sink is referred in the report text as the river gaining from groundwater.

Key to understanding the GW-SW interaction is whether this hydraulic signature of a gaining river is generated by interaction between the Berg River and the UAU, or whether the LAU is also hydraulically connected to the Berg River. Connectivity of the LAU and the Berg is dependent on the basement elevation beneath the Berg and surrounding the Berg, the depth of incision of the riverbed, and the geological extent of the basal aquifer and its overlying aquitard. Discussion in the previous sections has shown:

- The LAU is not continuous across the Berg River. The confining clay over the LAU is also not continuous.
- The basement beneath the Berg River is relatively shallow; around –20 to 0 mamsl, and a local basement high disconnects the LAU within the LRAS and EAS from deposits underlying the Berg River.

It is assumed here that only the upper aquifer interacts with the Berg River.

Data from a DWAF flow gauging station at Jantjiesfontein show typical annual fluctuations of 1.6 m between summer and winter levels. The data show peak river flows are up to 2 m above the annual average stage (data supplied by Frans Mouski, DWAF). During these floods the river will increase in width and cover its flood plains. At these times the hydraulic gradient towards the Berg River is likely to be reversed, at least in close proximity to the Berg River, and the river will recharge the aquifer. The regional groundwater gradient is likely to remain towards the Berg River, but locally the flow direction will be reversed. Where these conflicting flow directions meet (likely on the flanks of the flood plain) water will enter the ground as recharge (if the volume of excess water exceeds the potential evaporation). Following the above reasoning, the recharge is likely to occur to the UAU only. Recharge of river floodwaters to the LAU will occur via the UAU, in places where artesian conditions are reduced to allow downward flow.

Wetlands exist at the southern point of the Langebaan lagoon. The wetlands are groundwater fed; this area is a significant groundwater discharge zone as for the EAS as confirmed by the groundwater contours (**Figure 2-9**). The floodplain of the Berg River becomes very wide towards the mouth as the river meanders – up to 3.5 km wide near the Jantjiesfontein farm, and becomes marshland. Some minor (<0.5 km wide) ephemeral ponds are mapped at 1:50 000 scale (e.g. topography sheet 3218CD, in the area of Drommel Valley). These are interpreted as outcrops of groundwater from the UAU in topographic lows. They do not impact on the regional

flow pattern and are not considered in the model, although they are sites of either enhanced recharge or discharge depending upon the groundwater level at any time.

Large volumes of seawater are held at the surface at numerous salt works around the Berg River mouth and close to Yzerfontein south of the area. But it is assumed that these have no effect on the regional flow regime. Water loss from the pans through downward flow (i.e. artificial recharge of seawater to the aquifer from the pans) would be minimised for economic reasons. The pans are likely to be clay lined to avoid this potentially likely pathway considering holding water on top of an unconfined sand aquifer. Additionally, any artificial recharge that did occur would generate a local recharge mound. The pans are so close to the coast – i.e. where the aquifers discharge – that any recharge generated would not affect the regional flow regime.

The EC of the UAU groundwater is much higher in the LRAS than in the EAS (Woodford et al 2003, **Figure 2-15**). Low values (<300 mS/m) are presented for the whole EAS area, likely to be an imprint of the recharge zone here, whereas a high of >1000 mS/m is plotted extending 7.5 km inland from Saldanha Bay. With the hydraulic gradient towards the coast it is difficult to see how a seawater influence could reach this far. More confusing is the high (again > 1000 mS/m) mapped to cover the northern LRAS connecting from the Berg River to just north of where the high from Saldanha Bay extends. This is too far for direct influence of SW and groundwater (i.e. a mixing zone), especially again as the hydraulic gradient is towards the ocean. It is also too far from the Berg River to be caused by salinisation due to direct evaporation from a shallow water table. One possible explanation is that the tidal influence within the Berg River reaches very far inland, and then this water enters the aquifer during times of the year when the regional hydraulic gradient is reversed and the UAU gains from the surface water, not through Berg River Flood events, but through normal river levels in summer (kept high by influxing seawater) which is when the aquifer levels are lowest. If this is correct then the aquifer must be highly seasonal, discharging to the river only in winter but gaining from the river when the river floods, and recharging from the saline river in summer months.

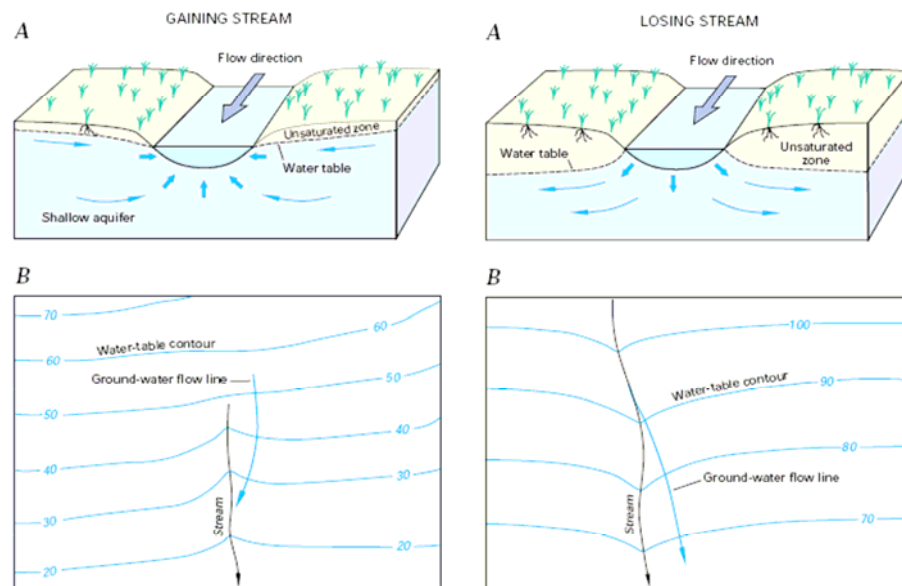


**Figure 2-11** Schematic diagram displaying hydraulically connected gaining and losing rivers (Winter et al 1998)

### 2.4.3 Recharge

Salient points regarding recharge to the aquifer described in sections above are:

- The UAU receives recharge directly from rainfall across the area.
- Recharge occurs to the UAU from Berg River during flood events and from the Berg River during the summer when the aquifer is lowest.

Rainfall decreases from west to east and from south to north (**Figure 2-12**). Thus the southern parts and higher lying parts are favourable to recharge to the UAU and a recharge mound is located southwest of Hopefield, from where water flows out to the UAU of the LRAS. Lateral recharge of run-off and shallow interflow from the granite koppies is not quantified.

The confining clay unit over the LAU is considered extensive across the area. The clay is only known to be absent over of the LAU within 5 km of the coast. This raises the question of how the LAU is recharged considering it does not outcrop anywhere (Rogers, 1980). Recharge must therefore occur through leakage via the UAU in areas where the head difference between upper and lower aquifer is large enough to drive vertical recharge downwards (via leakage through clay if a clay layer is present). This will be away from areas where the artesian conditions are observed, likely to be the central palaeochannels, and possibly at the UAU recharge mound where the head in the UAU is highest. Woodford et al (2003) note that the groundwater quality of the LAU deteriorates towards the west and suggests that this signal is due to recharge from the overlying UAU, “because of the clay layer becoming more permeable towards the west and it’s eventual disappearance” (Woodford et al, 2003, op cit p40).

The GRAII database provides non-aquifer specific recharge estimates per quaternary catchment (Volume 2 of this report, DWAF, 2007a). These have been re-calculated to apply to specific aquifers and the method applied to rainfall data at a sub catchment scale, thus a distribution across the area is available (Volume 2 of this report, DWAF, 2007a). The various recharge estimation methods are described and compared in Volume 4 of this report (DWAF, 2007c). Various estimations are shown in **Table 2-6** including those from local studies.

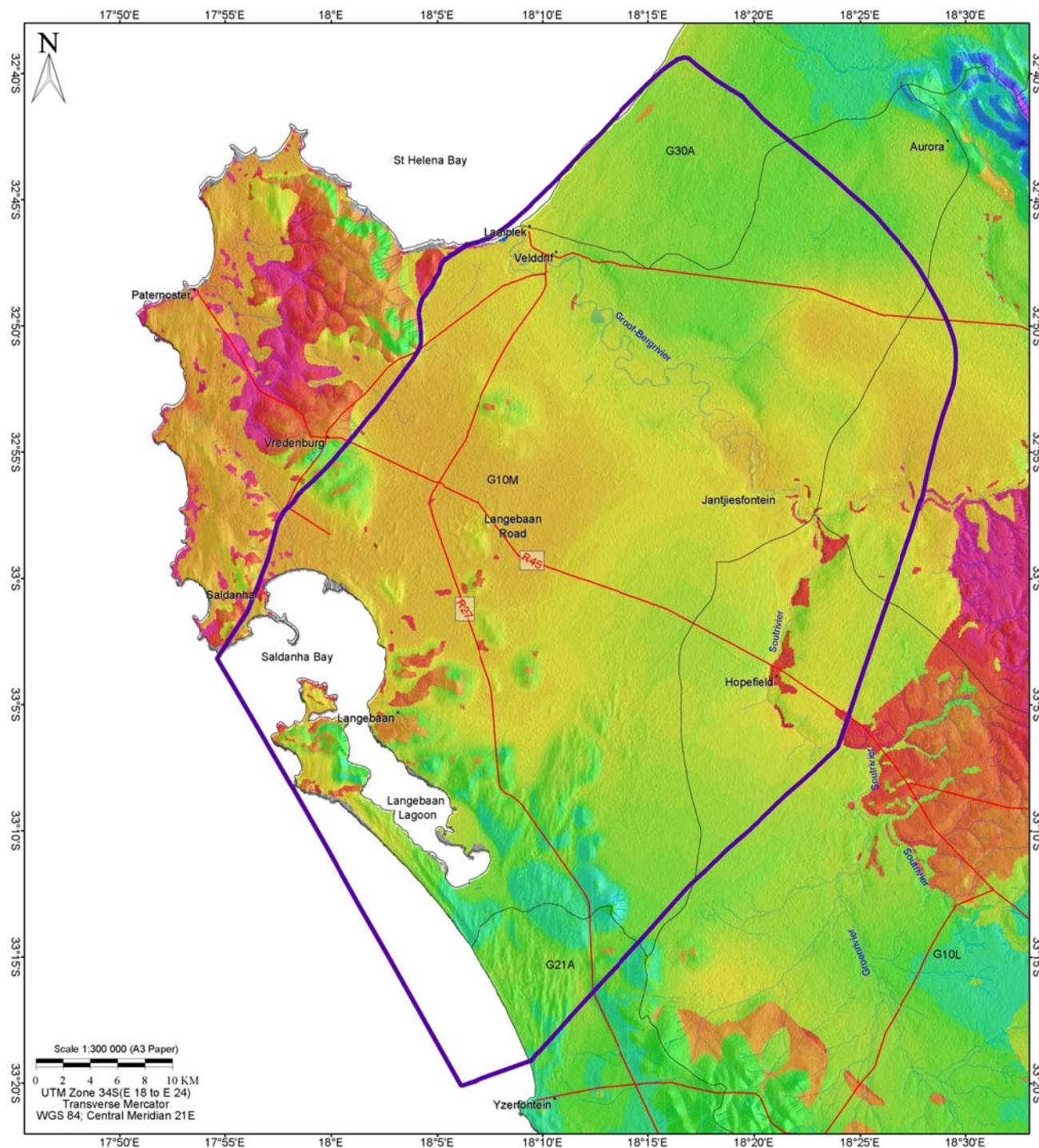
Woodford et al (2003) used a GRID-based GIS modelling technique to estimate effective annual recharge, which relates to an average effective recharge of 3.9% of annual rainfall. The GRAII, BRBS, and Water Balance Model (Volume 4 of this report, DWAF, 2007c) methods all generate recharge estimates that are ~5% of the rainfall, and at a maximum at 8% (Volume 4 of this report, DWAF, 2007c).

**Table 2-6 Recharge estimations in the Study Domain from previous studies and standard methods**

<b>Catchment</b>	<b>BRBS Method¹ (DWAF, 2002)</b>		<b>GRA II Method¹ (2005)</b>		<b>Berg WAAS Water Balance Method¹ (DWAF, 2007)</b>		<b>Local Studies: SRK² (2003)</b>	
	<i>Mm3</i>	<i>mm</i>	<i>Mm3</i>	<i>mm</i>	<i>Mm3</i>	<i>mm</i>	<i>Mm3</i>	<i>mm</i>
G10K	4.75	10.78	4.48	10.16	5.15	11.67	16.90	38.32
G10L	11.70	12.30	12.79	13.44	12.60	13.24	23.60	24.80
G10M	17.76	10.11	21.98	12.51	19.47	11.08	21.20	12.06
G21A	10.45	28.79	8.97	24.72	5.55	15.31	8.70	23.97
G30A	9.54	13.44	11.35	16.00	10.15	14.31	-	-

1) Aquifer-specific values are available for a sub catchment distribution, and here summed for intergranular aquifer per catchment. All values from Volume 4 of this report (DWAF, 2007c)

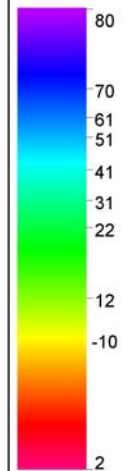
2) Values given for whole aquifer (not aquifer specific)



## LEGEND

- Towns
- Roads
- Rivers
- G21A Quaternary Catchments
- Model Domain

RECHARGE (mm/a)



PROJECT NAME

BERG WATER AVAILABILITY  
ASSESSMENT STUDY

CLIENT



DEPARTMENT OF WATER  
AFFAIRS & FORESTRY

CONSULTANT

UMVOTO

TITLE

RECHARGE  
(After DWAF, 2002)

FIGURE 2.12

#### 2.4.4 Groundwater use

Data regarding water use is available from GRAII and from WARMS (Volume 2 of this report, DWAF, 2007a). Water use, summed for each type of use, for each catchment is given in **Table 2-7** below.

**Table 2-7 GW use per catchment after GRAII**

Quaternary Catchment	Groundwater Use [Million m ³ /a]							
	Total	Rural	Municipal	Agric. Irrigation	Agric. Livestock	Mining	Industry	Aqua
G10K	2.6975	0.0240	0.0000	2.4656	0.2079	0.0000	0.0000	0.0000
G10L	0.4196	0.0100	0.2406	0.0000	0.1690	0.0000	0.0000	0.0000
G10M	1.9990	0.0070	0.0837	0.0000	0.4073	0.0000	1.5010	0.0000
G21A	0.1953	0.0020	0.0000	0.0000	0.1933	0.0000	0.0000	0.0000
G30A	2.7694	0.0040	0.0000	2.6167	0.1487	0.0000	0.0000	0.0000

The WARMS and GRAII data sets indicate large discrepancies regarding the different sectors of water use, but the total water usage appears similar; the GRAII data indicates a total groundwater use of 2.6139 Mm³/a and the same data from WARMS shows groundwater use of 2.27 Mm³/a for the model domain.

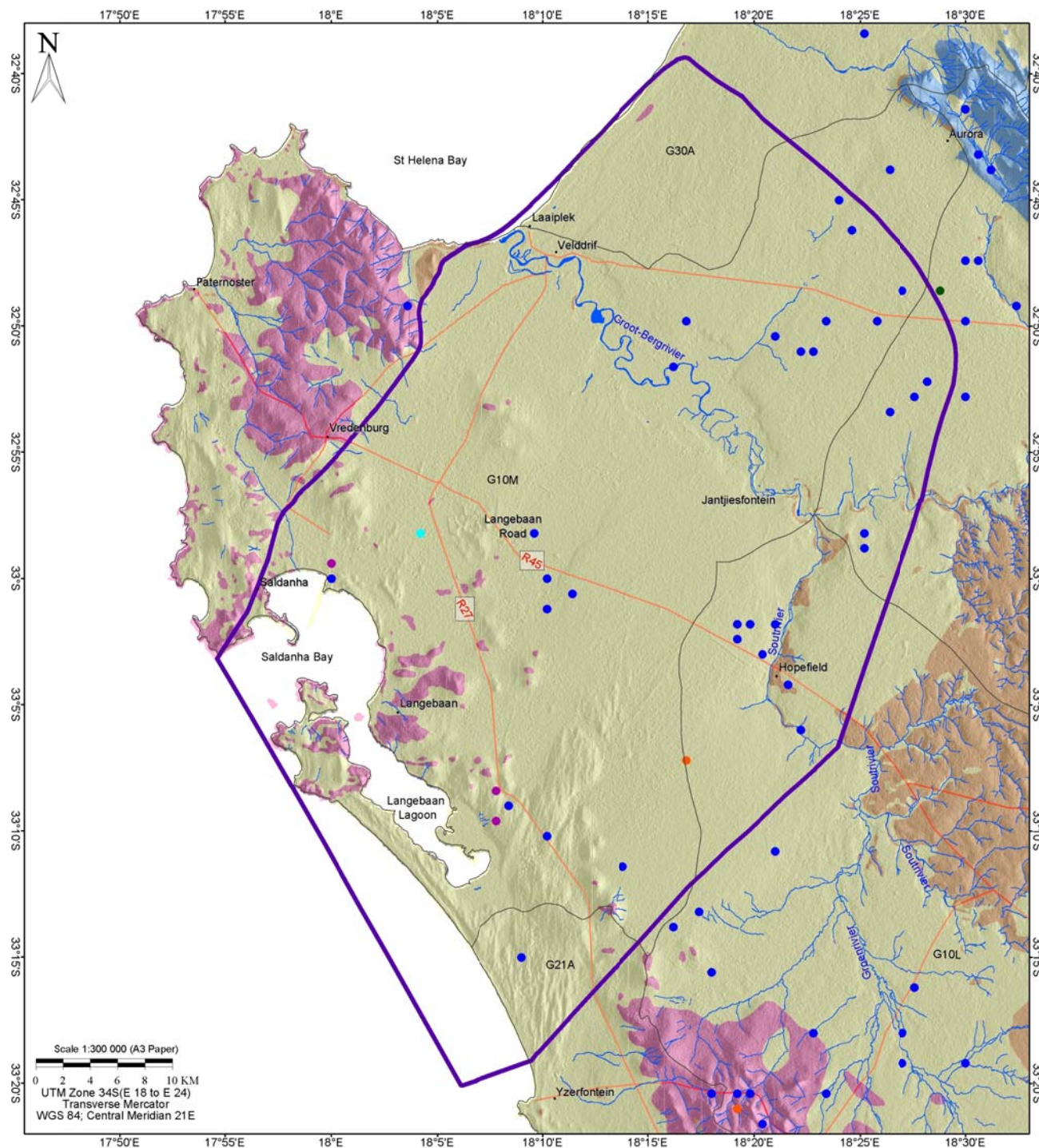
Water use above Schedule 1 must by law be registered with the DWAF and is captured in the WARMS database. Groundwater allocation is normally authorised, registered and stored per user or farm, which means that the spatial information about the number and location of boreholes is lost. A detailed analysis of the database entries and linkage with the spatial attributes stored in GRAII or NGDB can minimise any uncertainty this lack of information may introduce. However on the regional scale of the model the exact location of boreholes within a farm (relatively small with respect to the regional area) is likely to be unimportant.

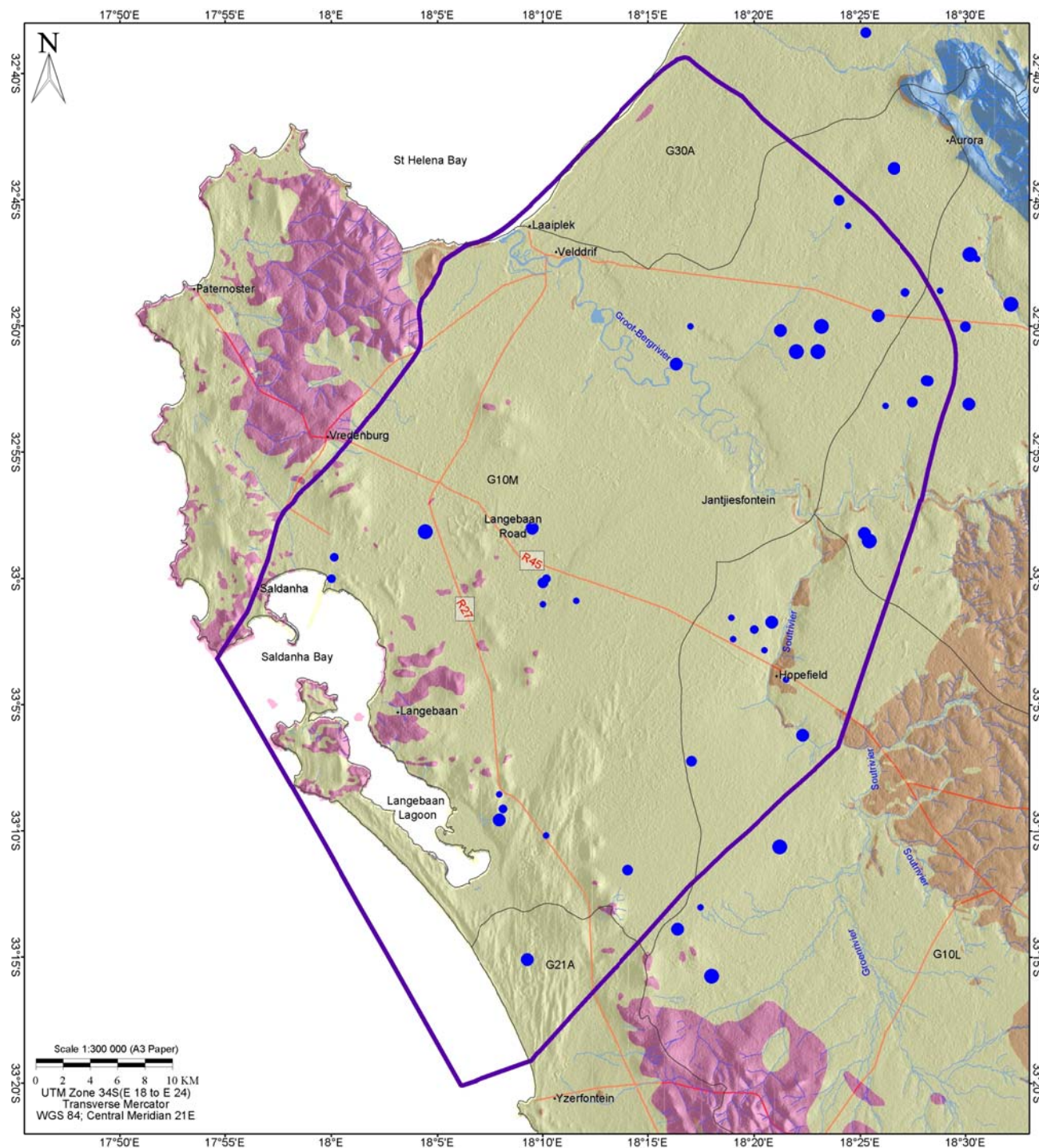
Registered groundwater use from the WARMS database indicates that most groundwater use for irrigation takes place in the G10L quaternary catchment for the study domain and is centred around Hopefield. Irrigation also takes place around Langebaan Road. Industrial use is indicated for at the Saldanha Steel plant and also at the southern end of the Langebaan Lagoon.

If using the WARMS database for usage, information on the depth of borehole, geology and therefore inference of the aquifer from which the abstraction is taking place, is lost. This information could be inferred from combining the use with GRAII and NGDB borehole data and analysing the NGDB logs. However, even going to this length will not conclusively indicate which aquifer the borehole abstracts from, because there is not information on where the borehole is cased and screened. It is assumed here that each WARMS data entry represents a single borehole (so the abstraction over a few boreholes may be summed to one point on the farm) and that all boreholes are fully penetrating and screened over the aquifer that they penetrate, as dictated by their location only. For example, a WARMS data point located in a position where the basement is deep and thick deposits of LAU exist, will be assumed as penetrating to the LAU and being cased off in the UAU and clay and only screened in the LAU. It is very likely that in drilling a borehole on a farm the intention would be to maximise the water availability and thus drill through to the basal gravels.

Large-scale groundwater abstraction occurs from the LAU at the West Coast District Municipality Wellfield. The wellfield is situated 5 km to the east of Langebaan Road. The rate of abstraction from the wellfield is ~4000 m³/day which has been suggested as the sustainable yield from the LAU (Woodford et al, 2003). Water levels in the area have reduced by ~10 m in the LAU since pumping began in December 1999, and the system is no longer artesian in the area. The shallow waterlevels in the UAU have not been significantly affected because the clay aquitard is ~25 m thick in the area (Woodford et al, 2003; figure 12). The drawdown cone from the WCDM has extended up to 10 km from the site (Woodford et al 2003).

The WARMS groundwater use is shown in **Figure 2-13** below, for the type of use and the registered volume.





## LEGEND

- Towns
- Roads
- Rivers
- G21A Quaternary Catchments
- Model Domain

### VOLUME (m³)

- 2140 - 20 000
- 20 000 - 50 000
- 50 000 - 100 000
- 100 000 - 200 000
- > 200 000

## PROJECT NAME

BERG WATER AVAILABILITY  
ASSESSMENT STUDY

## CLIENT



DEPARTMENT OF WATER  
AFFAIRS & FORESTRY

## CONSULTANT

UMVOTO

## TITLE

GROUNDWATER VOLUME  
(WARMS)

FIGURE 2.13b

## 2.5 WATER QUALITY

Groundwater in the Langebaan Aquifer has a Na Ca \ Cl, alkaline character with most pH falling in the range of 6.37 to 10.23 and average pH of 7.98. Average EC of groundwater is 342.01 mS/m and range between 24 and 4548 mS/m (**Figure 2-14**; NGDB data set).

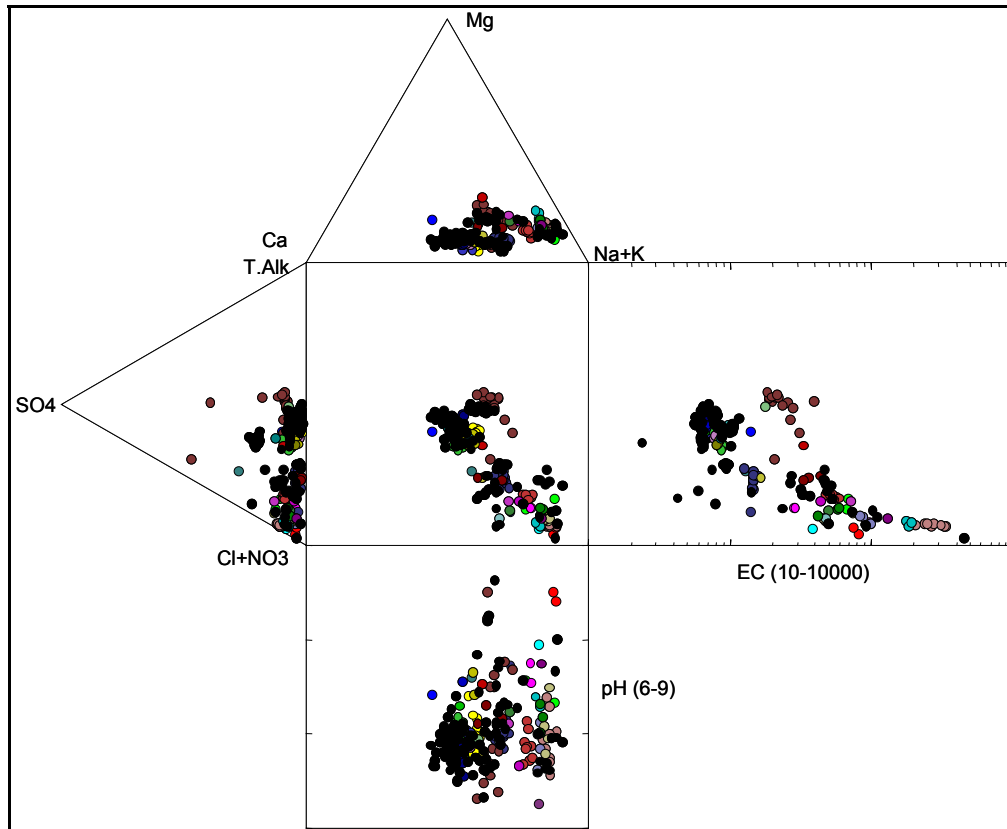


**Figure 2-14** Durov diagram; all data

The groundwater quality is variable spatially and vertically in the different aquifer units. Good quality water (TDS<500 mg/l) occurs in the centre of the LRAS and EAS. Towards the Berg River and the coast the groundwater becomes poorer (TDS 2000-15000 mg/l) (Timmerman 1985).

The spatial variability in water quality is shown in **Figure 2-15** below, reproduced from Woodford et al (2003). The broad pattern shows a low EC signal in the south and southeast (the recharge zone) and poor quality water towards the NW and the Berg River mouth. The pattern may be contributed to by tidal seawater influence (discussed above in section 2.4.2). The distribution is unlikely to be attributed to direct evaporation from a shallow water table in the riparian zone, as the poor quality water also exists in areas where groundwater is >5 m deep (eg NW of Langebaan Road). Direct evaporation of groundwater may well be occurring in the riparian zone but it is unlikely to occur in significant volumes, and unlikely to be enough to salinise the aquifer. There are wide-spread example in literature of salinisation of aquifers from irrigation enhanced evaporation, but none where a natural system of evaporation in the riparian zone causes aquifer salinisation.

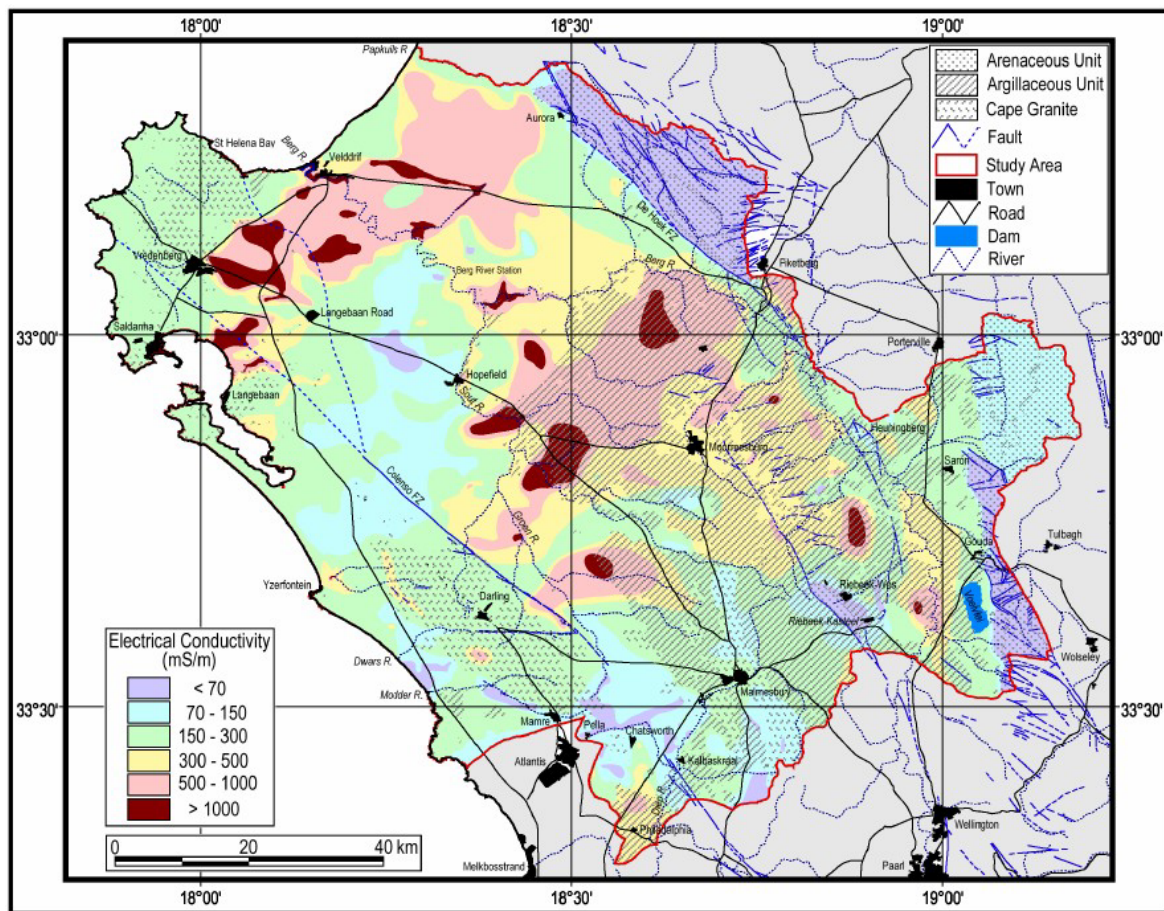


**Figure 2-15 Spatial variability of groundwater quality (Woodford et al, 2007)**

The groundwater quality differs between the upper and lower aquifer. Groundwater quality is good in the LAU with EC's <120 mS/m (Woodford et al, 2003). The quality deteriorates from east to west due to influence from the overlying aquifer. The groundwater in the UAU is much poorer than the LAU (SRK, 2003). **Figure 2-16** shows that groundwater from the confined aquifer has a mixed Na Ca/ Cl alkaline character with an EC generally lower than 70 mS/m. Groundwater from the upper aquifer has a Na/Cl character with higher EC.

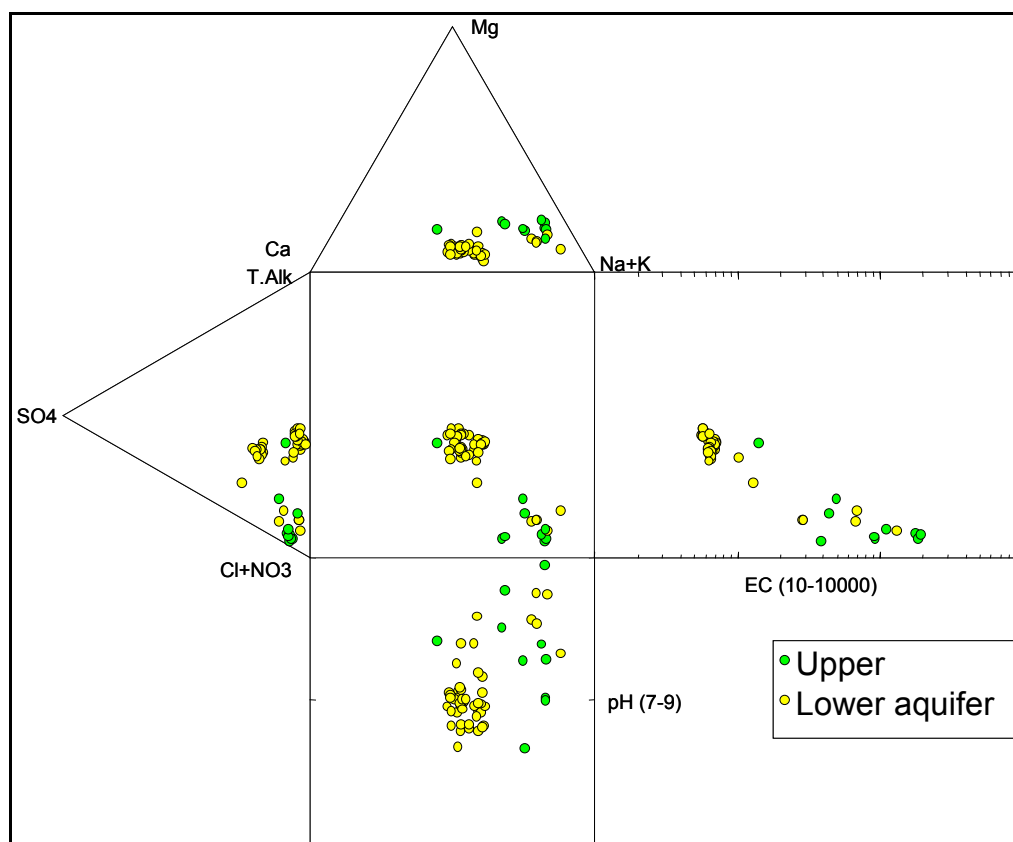
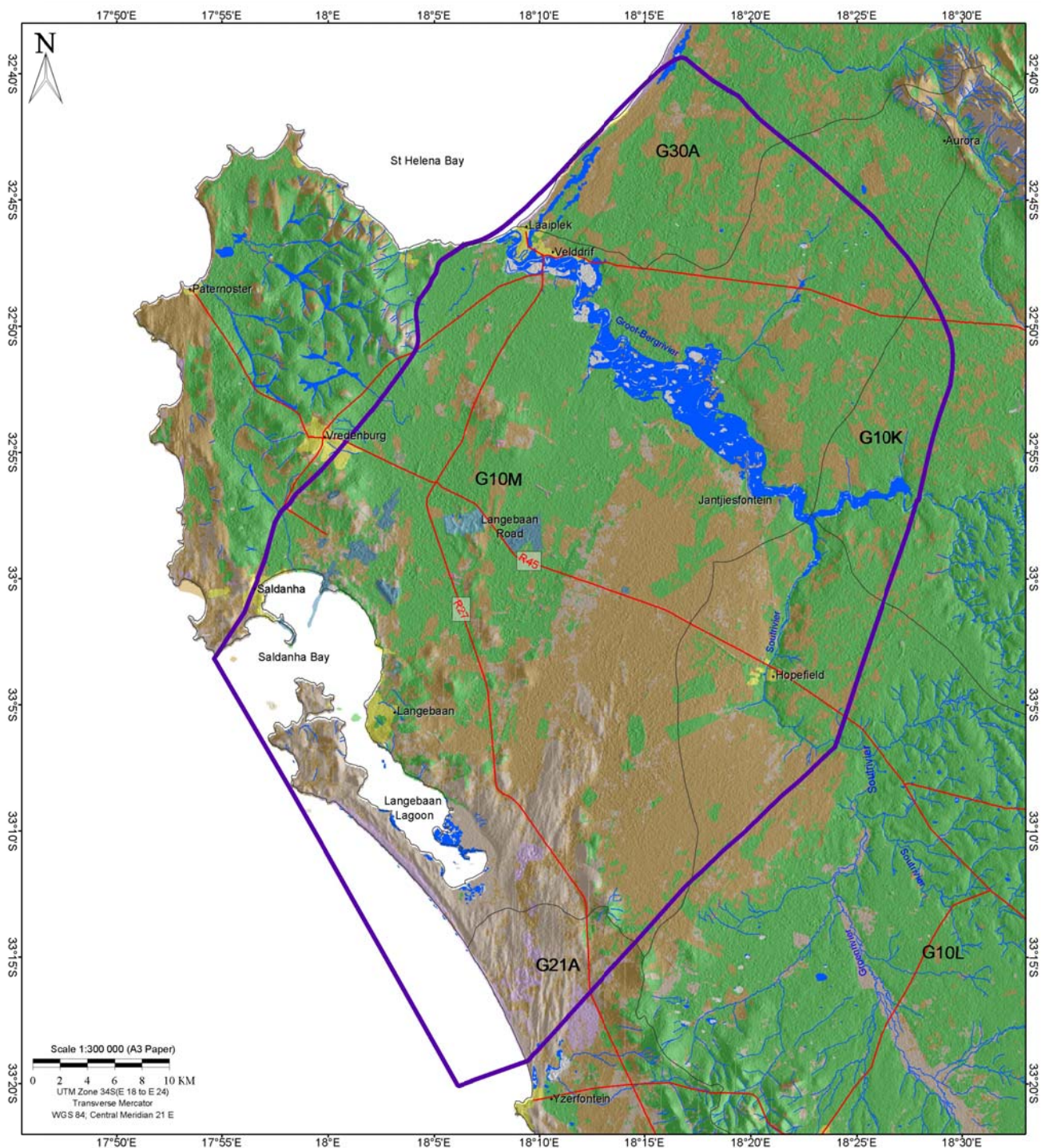


**Figure 2-16 Durov diagram; upper and lower aquifer separated**

## 2.6 LANDUSE

The landuse as mapped from the NLC2000 (CSIR Environmentek, ARC, 2000) is shown in **Figure 2-17** below. Open shrubland and low fynbos dominates the area and commercial cultivated land (large commercial farms) is the major landuse. Built-up areas occur in the small towns of the area, which include Saldanha, Langebaan, Velddrif and Hopefield. Industrial areas occur in the centre of Saldanha Bay and near Langebaan Road.

The natural vegetation of the coastal plain consists of Coastal Macchia, except for a narrow strip of “Strandveld” along the beachfront and in the floodplain of the Berg River (Timmerman, 1985b). Farming concentrates in the area just south of the Berg River with wheat, barley and dairy farming prominent in the Langebaan Road and Velddrif area.



## LEGEND

- Towns
- Roads
- Rivers
- G21A Quaternary Catchments
- Model Domain
- LANDUSE**
  - Bare Rock & Soil
  - Cultivated & commercial
  - Improved Grassland
  - Shrubland & Low Fynbos
  - Thicket, Bushland
  - Built-up
  - Industrial
  - Mines & Quarries
  - Waterbodies, Wetlands

## PROJECT NAME

BERG WATER AVAILABILITY  
ASSESSMENT STUDY

## CLIENT



DEPARTMENT OF WATER  
AFFAIRS & FORESTRY

## CONSULTANT

UMVOTO

## TITLE

LANDUSE  
(NLC2000)

FIGURE 2.17



### 3. CONCEPTUAL MODEL

#### 3.1 CONCEPTUAL MODEL OF GROUNDWATER FLOW SYSTEM

The aim in setting models up is to represent processes as simply as possible, without losing detail of the physics. Physical features and processes that dictate the groundwater flow system form the basis of the conceptual model. The salient conclusions for the groundwater flow system, as detailed in chapter 2, are summarised here. The conceptual model of the groundwater flow regime in the LRAS and EAS is formed on the assumptions that follow.

*The hydraulic nature of the aquifer:*

- It is assumed that the palaeotopography is representative of ancient fluvial systems and therefore automatic contouring of basement data is inappropriate as it generates isolated basins. The deep palaeochannel of the LRAS is assumed to correlate with deep basement measurements offshore and a continuous palaeochannel is inferred.
- The geology can be interpreted as 3 distinct hydrostratigraphical units:
  1. The upper unconfined aquifer unit comprising the Bredasdorp formation sediments and Varswater sediments if present;
  2. The confining layer (Upper Elandsfontyn clay)
  3. The lower (semi-) confined aquifer unit (Elandsfontyn sediments)
- It is assumed that the complex internal geology of the Bredasdorp and Elandsfontyn Formation can be averaged by an equivalent hydraulic conductivity over the depth of the deposit. Varying thicknesses of interbedded layers – such as peat within the Varswater of the UAU, will generate a lower equivalent hydraulic conductivity over the area that it extends and therefore these heterogeneities will be accounted for in the calibration of a heterogeneous equivalent K.
- The basement (Malmesbury and Cape Granite suite) is assumed an impermeable base to the LRAS and EAS.
- The LAU is present within both the LRAS and the EAS and is confined within the lateral limits of both palaeochannels. It is not continuous between the aquifer systems (LRAS and EAS) due to a small basement divide, and not continuous under the Berg River.
- The LAU is capped everywhere by a variable thickness of clay of the Upper Elandsfontyn Formation.
- The UAU is extensive across the entire area occurring over the LRAS and EAS.

*Sources, sinks, flow direction:*

- The UAU is recharged directly from rainfall.
- Recharge to the LAU occurs in places where the head difference between upper and lower aquifer is large enough to drive vertical recharge downwards (via leakage through clay if a clay layer is present)
- Flow in the UAU is topographically controlled and occurs away from the recharge mound to the SW of Hopefield, north to the Berg River, north and west into the LRAS, and directly southwest into the EAS.
- The UAU discharges to the Berg River, to the coastline at Saldanha Bay and the coastline at Langebaan Lagoon and south of the lagoon.
- On average the Berg River gains from the aquifer as there is a strong hydraulic gradient towards it. However during summer it is possible that the Berg River recharges the UAU.

- The Berg River acts as a recharge source to the aquifer during flood events.
- Flow in the LAU is basement controlled and occurs along the axes of the palaeochannels.
- The LAU discharges to the coastline at Saldanha Bay and the coastline at Langebaan Lagoon and south of the lagoon.

*SW-GW interaction:*

- The Berg River is in direct hydraulic connectivity with the UAU only.
- All groundwater which flows towards the Berg River interacts with the river. There is no through flow of water from north of the Berg River, to recharge the deep aquifer south of the river.
- The Sout and Groen rivers are non-perennial. The river reaches within the model area are small and thin and are assumed unimportant to the regional flow regime. They are not explicitly modelled in the numerical model.
- Saltpans do not affect the regional flow regime.

### 3.2 TRANSLATION INTO NUMERICAL MODEL

The numerical model is described with a focus on the model boundaries below. Other features of the modelling, for example the representation of the Berg River as a 'transfer boundary', and the input data for model layering, are described further in Section 4. The system is modelled with a finite element groundwater software package Feflow. The mathematics of the finite element package used is beyond the scope of this report and the reader is referred to the Feflow manual (Diersch et al 2006).

Numerical model boundaries are required to be set at positions where a known hydraulic head, known flux of groundwater, or known loss of groundwater from the system can be specified and input to the model. Positions of known fluxes within the model area are also specified as internal boundary conditions.

The boundaries of the model are described in the table below:

**Table 3-1 Description of model boundaries**  
(Numbers refer to numbered boundaries in Figure 3.1)

Location	Conceptual Description and assumptions	Numerical Translation
1. North west boundary, portion south of the Berg River mouth	The boundary follows a smoothed line of the aerial extent of the UAU outcrop. It is assumed that areas where sand outcrops beyond the model boundary are not significant to the regional flow regime as basement elevation and topography comparisons show the thicknesses here are <10 m.	It is assumed that there is no flux across the boundary of the sands outcrop, which is numerically modelled as a no-flow boundary.
2. North west boundary, portion along coast line	The LAU is absent along this coast line. The UAU outcrops to the coastline and is in hydraulic contact with the ocean which numerically means that the ocean is a constant source/ sink of water at a hydraulic head of 0 mamsl.	A constant head boundary condition is applied along the coastline.

Location	Conceptual Description and assumptions	Numerical Translation
3. Northeast boundary, north of the Berg River	The Berg River is a point of interest in the model therefore for numerical robustness it is not used as an external model boundary. The details of the flow regime north of the Berg River are not of interest; therefore the main requirement of the northern boundary is for it to be far enough from the Berg River that its conditions do not affect behaviour at the river. The boundary is based on an approximate location of a surface flow (or UAU) divide, to the Berg River and to the Papkuils and Kuilders Rivers.	It is assumed that there is no flux across the surface-flow divide; modelled as a no-flow boundary.
4. East boundary, north of Sout River	The Cenozoic deposits beyond the boundary are assumed thin and not significant to the regional flow regime. The boundary is far enough from the central areas of interest (i.e. the LAU within the LRAS and EAS) that potential implications of this assumption are reduced.	It is assumed that there is no flux across the boundary; modelled as a no flow boundary.
5. Southeast boundary, south of the Sout River	The boundary is based on an approximate location of a surface flow (or UAU) divide, between flow towards the north away from the recharge mound on dunes southwest of Hopefield, and flow towards the Sout River.  Any potentially deep influx across the boundary is assumed negligible because the contoured basement here is ~10 mamsl, so it is unlikely that there is a significant thickness of the basal gravels.	It is assumed that there is no flux across the boundary; modelled as a no-flow boundary.
6. Southwest boundary around coastline	The UAU is in hydraulic contact with the ocean; a constant source/ sink of water at a hydraulic head of 0mamsl.  The clay aquitard is thin or absent at the coastline therefore it is possible that the pressure difference between the UAU and LAU dissipates and the LAU is also hydraulically connected to the ocean. In this case a constant head of 0 mamsl at the coastline, also applies to the LAU.  But to allow for the possibility that the LAU is still under a degree of confinement at the geographic coastline, the boundary is set at a distance out at sea, far enough that all deep groundwater will be allowed to discharge.	The geographic coastline is set as a constant head to the UAU.  Boundary conditions of constant head at the coastline and at the model extent will both be tested for the LAU.
7. Internal Boundary: Berg River	The Berg River is assumed to be in contact with the UAU, and not to be deeply incised.	The river is modelled as a transfer boundary.

---

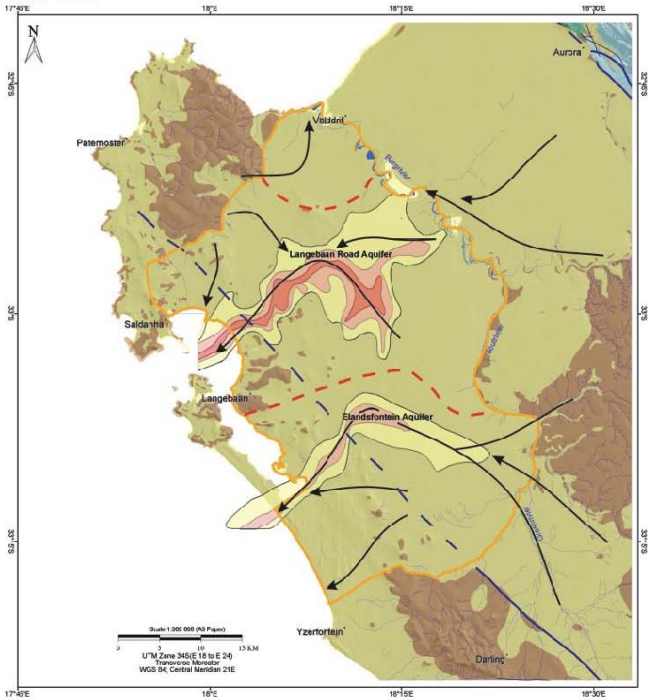
**Figure 3-1** illustrates the translation of the conceptual model into the numerical model.

The boundary conditions are shown in **Figure 3-2** and **Figure 3-3**. The model mesh excludes the basement outcrop area that separates the LRAS and EAS at the coast. Because the basement is assumed impermeable this area is negligible to the flow regime. The same approach cannot be used for internal outcrops of basement because the model software does not cope numerically with there being 'holes' within the model domain. The internal outcrops are ignored as irrelevant to the regional flow regime, and they are simply dealt with by ensuring the total model thickness is at a minimum where they are present (5 m).

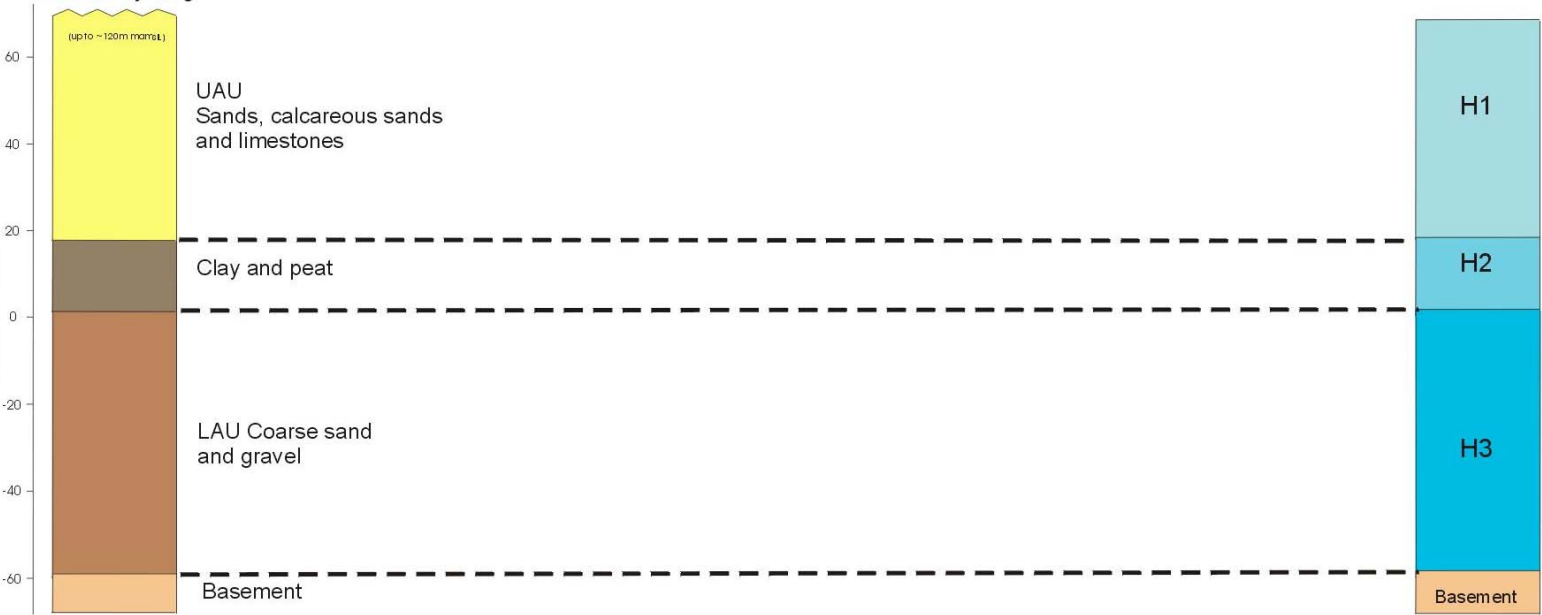
The model set up as described above, is used for calibration of both the steady-state and the transient model. The calibrated steady-state model parameters are input to the transient model. The calibration process is described in Section 4.

Conceptual Model

Plan View

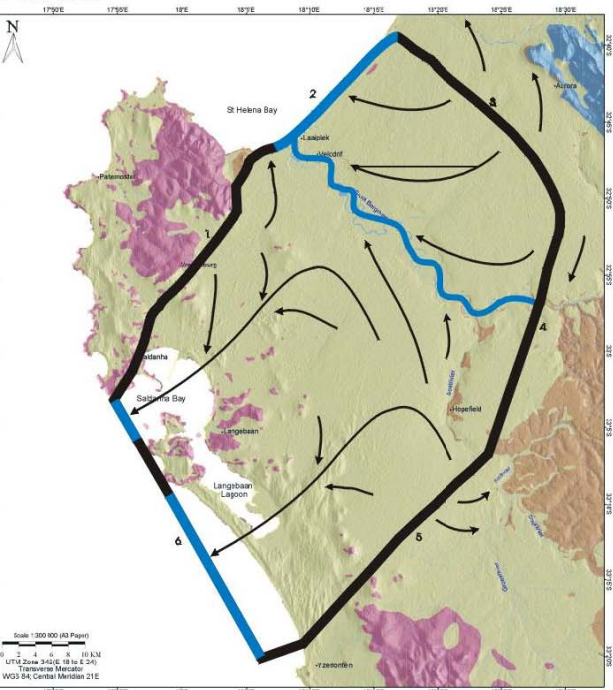


Vertical Layering



Numerical Model

Plan View



LEGEND

- Towns
- Rivers
- Faults
- Hydrotects
- Langebaan Study Domain
- Compartments Langebaan Model Domain
- Bedrock Elevation (mamsl)
  - <-40
  - 20_-40
  - 0_-20
- Model Groundwater Flow
- Constant Head Boundary
- No Flow Boundary

PROJECT NAME

BERG WAAS

CLIENT



DEPARTMENT OF WATER  
AFFAIRS & FORESTRY

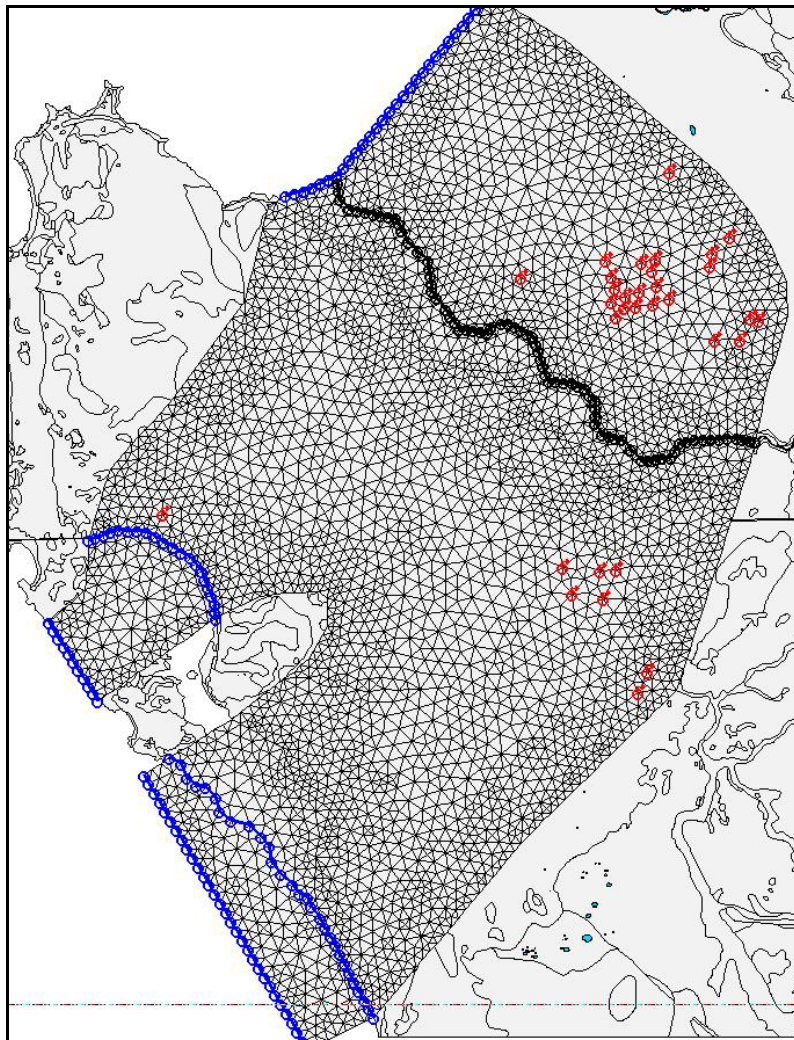
CONSULTANT

UMVOTO

TITLE

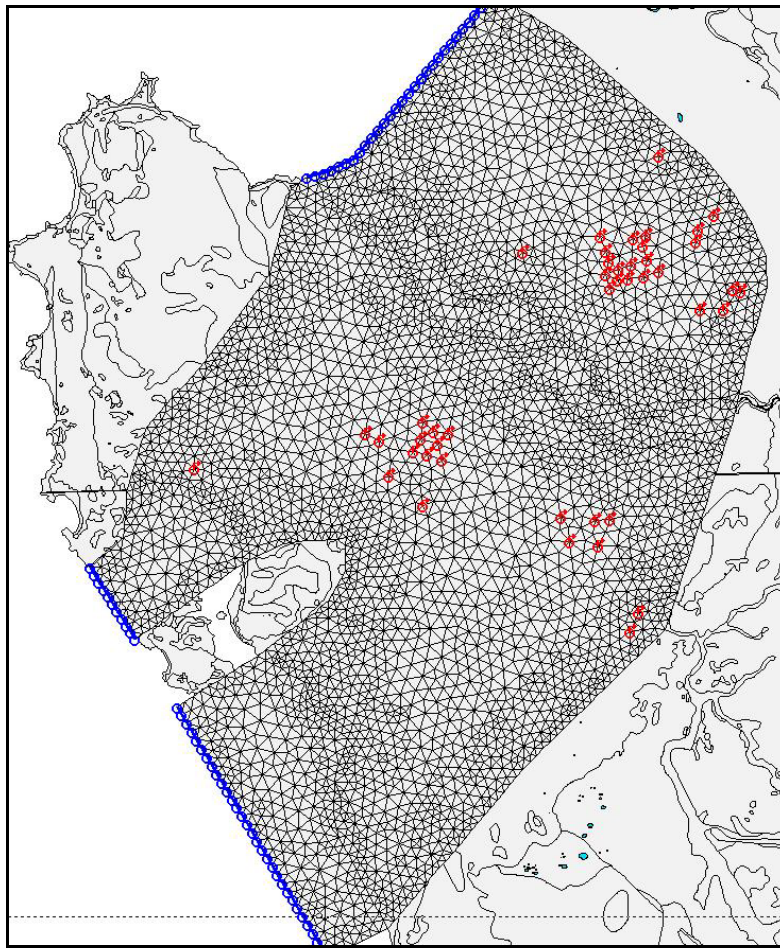
CONCEPTUAL MODEL OF  
GROUNDWATER FLOW IN THE  
LANGEBAAN ROAD-ELANDSFONTEIN

FIGURE 3.1



**Figure 3-2 Boundary conditions and the model mesh: the Upper Model Surface**

*Red nodes indicate abstraction wells, black nodes represent transfer boundaries and blue nodes indicate constant head boundaries. (N.B. The abstraction boundary conditions are explained fully in section 4.8)*



**Figure 3-3 Boundary conditions and the model mesh: the Lower Model Surface**

*Red nodes indicate abstraction wells, black nodes represent transfer boundaries and blue nodes indicate constant head boundaries. (N.B. The abstraction boundary conditions are explained fully in section 4.8)*

## 4. MODEL INPUT DATA

### 4.1 REQUIRED PARAMETERS

A numerical groundwater model requires data for:

- Physical 3D dimensions of the area to be modelled, therefore requiring data on the aquifer top surface (in this case topography), aquifer bottom (basement) and physical boundaries of the modelled aquifer.
- Internal aquifer geometry, for example if the aquifer is homogeneous or multi-layered, which is dictated by the geology and governs the hydraulic properties assigned.
- Hydraulic properties including hydraulic conductivity and specific storage. Porosity data affects the speed of groundwater flow and is thus required for contaminant transport modelling.
- Definition of all sources and sinks of water to the aquifer, including recharge, abstraction
- Actual field water level measurements are required as calibration data. For transient calibration a time series of water level data is required.

**Table 4-1 Summary of required input parameters**

Model Input Parameter	Source	Type
Topography	100 m DEM	Fixed
Bedrock topography	Literature and NGDB	Fixed
Layering	Based on geology and numerical requirements	Fixed
Hydraulic conductivity	1 st approx from typical literature values	Steady-state calibration
Storage	1 st approx from typical literature values	Transient calibration
Porosity	Typical literature values	Fixed
Recharge	BRBS method (DWAf 2002) at 100 m grid scale	Fixed for steady-state calibration, varied in transient scenario testing
Abstraction	WARMS	Fixed for steady-state calibration, varied in transient scenario testing
River stages	Assumption based on DEM and 1:50,000 topo sheets	Calibration
Transfer rate	Assumption based on data	Calibration

### 4.2 THE MODEL MESH

Using the boundary conditions as described in section 3.1 the modelled area amounts to ~2000 km². The Feflow software functions on a triangular mesh. The problem is full 3-dimensional and contains 7135 triangular prisms. The length of the side of the triangles is between 500-1200 m.

The model functions by solving the groundwater flow equation at the nodes of the triangles only. The solution for head is then averaged by linear interpolation between nodes to produce a smooth appearance to the contours, and to generate a hydraulic head at every point in the model, including away from a node. Therefore the solution is accurate to the scale of ~1000 m. The length scale of the problem is at least one order of magnitude greater than this scale of accuracy and therefore it is deemed sufficient.

All data in the model is handled in this way. Input data can be imported as point data and a data regionalisation is carried out, through which point data which may not coincide with the position of the nodes, is applied to the nodes through a user-selected interpolation technique. The data is then averaged by linear interpolation between nodes to produce a smooth appearance to the data contours, and to generate data at every point in the model, including away from a node.

### 4.3 TOPOGRAPHY

A 100x100m DEM was used to construct the model surface topography. In the GIS software TNT MIPS a grid file-containing point data for each cell of the DEM was created. The point data, because it is based on a 100x100 grid, is much denser than the model mesh, which has nodes separated by ~1000 m distance. During data regionalisation a nearest neighbour inverse distance weighting method was used in order to apply topographic data points to the nodes.

DEM data is available for the area at 20x20m scale. This scale of information is used in converting measurements from depth below collar to mamsl (e.g. for NGDB water levels and for geology logs). The 100x100 m grid is used in the model for ease of data manipulation.

Because the input data is denser than the nodes, it is possible that small errors arise. For example an aerially small rise in topography might lie close to a node and be translated to that node. Then this nodal topography is averaged by linear interpolation between nodes to apply data to all points in the model and hence the topography that is averaged between two nodes is artificially raised. With a finer mesh the detail of the input data can be higher. For example a 100 m element size and a 100m DEM, or a 20 m element size and 20 m DEM, would describe all minor topographic variations. At the regional scale of this model this is not necessary.

Topography ranges within the model area, from 0 mamsl at the coast to a maximum of 226 mamsl in the south, at the granite outcrops at Betjieskop and Swartberg. Only ~1.5 km away from the centre of these granite Koppe's the topography is much lower; ~120 m high. This is more typical of the raised dunes in the area. The granite basement is assumed impermeable. The outcrops are therefore not entered into the model in anyway as they do not affect the flow regime. The upper surface is manually entered as if the Koppe's were not present. For example in this area, a value of 120 m is assigned.

### 4.4 BEDROCK

The following data sets were used to construct the bedrock topography:

- Borehole depths from the NGDB data set, using records of shale and granite as indications of basement rocks.
- Offshore basement data of De la Cruz (1978).
- Spot heights on bedrock outcrops as shown in the 1:250 000 geological maps.

The bedrock elevation from the NGDB, as mamsl rather than depth below surface, was computed by simply subtracting the borehole elevation from the topographic elevation at each borehole data point/position (using a 20x20 m DEM). The above data sets were combined. The contours were manually forced along the axis of the palaeochannels to force a gradual decrease (described in section 2.3.2), the interpreted bedrock surface, used as input to the model shown in shown in **Figure 2-7**.

#### 4.5 INTERNAL AQUIFER GEOMETRY

The stratigraphy requires at least 3 layers in order to represent the different hydraulic characteristics (**Figure 2-8**); an upper layer 1 representing the UAU, a 2nd representing the clay aquitard and a 3rd representing the LAU. But representing the upper and lower aquifers with only one layer each, would force large differences in thickness over small distances – e.g. at the edges of the palaeochannel or around the dunes. Therefore 2 model layers represent the UAU and 2 represent the LAU.

Exact representation of the geological layers is limited by the numerical requirement that layers must be continuous across the model. The complex geological layers with varying thicknesses must be averaged to a sloping plane or a fixed elevation. A geological unit that is not continuous across the domain is numerically treated as continuous, reducing to a small thickness where the unit is not present and masking its presence hydrogeologically by assigning it the same hydraulic conductivity as geological layers above or beneath it that are present. For example, the basal layer (layers 4&5) will have a higher hydraulic conductivity than the layers above it. The bottom model layers in areas of the model outside of the palaeochannels, where the basal gravels are not present, will have a hydraulic conductivity of layer 3 (the clay) if the clay is present in that area. In positions where the Elandsfontyn Formation is not present, the lower 3 layers will have a hydraulic conductivity the same as layers 1&2.

The model layering is shown in **Table 4-2**. The stratigraphic summary given in section 2.3.3 above informs where layers are assigned (see **Figure 2-8**). A minimum model thickness of 5 m is set, and each layer has a minimum of 1 m where it is forced to pinch out.

**Table 4-2 Model Layering**

Layer	Surface	Top	Bottom
1	Top =1 Bottom =2	Topography	Half way between topography surface 3
2	Top =2 Bottom =3	Half way between topography and surface 3	18 mamsl. Or surface 4 +1 m where surface 4 > 18 mamsl
3	Top =3 Bottom =4	18 mamsl. Or surface 4 +1 m where surface 4 > 18 mamsl	1.5 mamsl. Or 1.5 mamsl + 2 m where basement > 1.5 mamsl
4	Top =4 Bottom =5	1.5 mamsl. Or 1.5 mamsl + 2m where basement > 1.5 mamsl	Half way between surface 4 and basement
5	Top =5 Bottom =6	Half way between surface 4 and basement	Basement topography

Because each and every change in vertical sequence is not represented in the model layers, the calibrated hydraulic conductivity values for each layer is an “equivalent hydraulic conductivity”. They cannot be interpreted as the hydraulic conductivities for specific geological formations identified in borehole logs. They do however adequately represent the spatially average hydraulic conductivity of the combined units that comprise the UAU and the LAU.

## 4.6 AQUIFER HYDRAULIC PROPERTIES

### 4.6.1 Hydraulic conductivity, K

Hydraulic conductivity values vary over more than 10 orders of magnitude in nature (Calver 2001). Typical hydraulic conductivity values are:

- For an unconsolidated silty sand to gravel – 0.01 to 10,000 m/d (Freeze and Cherry 1979)
- For fluvial deposits (alluvium) – 0.1 to 1000 m/d (Hiscock, 2005)
- For lacustrine silt and clay –  $1\text{E}^{-8}$  to  $1\text{E}^{-4}$  m/d (Hiscock, 2005).

Timmerman (1985b) gave estimates for transmissivity (T) (hydraulic conductivity x thickness) of the sand deposits on the area from hydraulic testing, shown in **Table 4-3** below (where S is storage parameter).

**Table 4-3 Hydraulic conductivity estimates for the Langebaan area from Timmerman (1985b.)**

Aquifer Unit	Lithostratigraphic unit		T (m ² /d)	K ¹ (m/d)	S (-)
	Formation	Member			
Adamboerskraal Aquifer System	Bredasdorp	-	100	5-10	-
	Elandsfontyn	1 Clay	-	-	-
		2 Sand and Gravel	500	12.5-25	$1.0 \times 10^{-3}$
Langebaan Road Aquifer System	Bredasdorp	Langebaan Limestone	<100	<5	-
		1 Clay	-	-	-
	Elandsfontyn	2 Sand and Gravel	1000	16.7-25	$3.1 \times 10^{-3}$
Elandsfontein Aquifer System	Bredasdorp	1 Springfontyn	300	15-60	-
		2 Noordhoek	-	-	-
	Varswater	1 PPM	-	-	-
		2 QSM	500	16.7	$3.6 \times 10^{-4}$
	Elandsfontyn	1 Clay	-	-	-
		2 Sand and Gravel	600	20-60	$1.0 \times 10^{-3}$

¹K is calculated from reported transmissivity and thickness values.

The hydraulic properties shown above are reported to result from exploration work carried out by DWAF between 1984-1985, during which numerous holes were drilled and hydraulic tests conducted (pump tests, stepped drawdown tests). However Timmerman (1985b) reports that numerous issues affected the process. These include:

- Gravel packs seldom being placed in the correct positions, hence the possibility that unknown units are targeted in the pumping

- Incorrect well and screen design causing sand infiltration into the holes and sand blocking screens artificially reducing the hydraulic conductivity of the formation surrounding the hole.

The pump test results are therefore unreliable. There appears to be little variation between the units, all within the range of 5-60 m/d, which is narrow for the varying nature of the sediments. It is likely that individual units were not accurately targeted and that these hydraulic conductivities represent averages. The results will only be used as a guide.

An initial hydraulic conductivity of 10 m/d will be applied across the model, to all layers. The hydraulic conductivity is the foremost calibration parameter.

#### 4.6.2 Storage properties

The volume of water released through gravity drainage, per unit decline in head in an unconfined aquifer is the specific yield (dimensionless). Water is also released elastically though this volume is much less, and is known as the specific storativity [ $L^{-1}$ ]. The normal range of specific yield in an unconfined aquifer is from 0.01 – 0.30 (Hiscock, 2005). A confined aquifer does not dewater, there is no gravity drainage and therefore the aquifer does not have a specific yield. Because of the lack of dewatering, the changes in pressure in the confined aquifer force more water to be released from elastic storage in a confined aquifer, therefore the specific storativity (elastic storage) is important. The storativity of an aquifer is the specific storativity [ $L^{-1}$ ] x the thickness of the aquifer. This property is reported in **Table 4-3** above.

In agreement with typical literature values the specific yield was assigned to 0.2 for the unconfined layers and the specific storage to  $1E^{-4} m^{-1}$  for all layers. Storage parameters affect the transient numerical model, and are described further in section 6.

#### 4.6.3 Porosity

Porosity for fluvial alluvium varies from 0.05 – 0.35 (Hiscock, 2005). The porosity affects only the speed of groundwater flow (important in particle tracking and contamination problems), and is required when calculating stored yield. The porosity can be assumed to be similar to the specific yield.

### 4.7 RECHARGE

The recharge for the area calculated with the BRBS method (DWAF, 2002) is shown in **Figure 2-12**. This method is based on rainfall and geology and takes no account of the land use (the method is described in more detail in Volume 4 of this report, DWAF, 2007c).

The dominant land use is shrubland, fynbos and commercially cultivated land, which would not significantly decrease the permeability at the surface. The recharge distribution from the BRBS method is assumed representative for the area and is input as a fixed parameter. The total recharge over the model area is 21.69  $Mm^3$ /annum, and averages ~9 mm/yr.

Losses of water to evapotranspiration are not quantified individually, the low % of rainfall that is used within the BRBS method (~5%) is assumed to represent only the rainfall that infiltrates to the subsurface. The recharge is assumed to be effective recharge. This is assumed adequate because for the following 2 reasons. The fynbos is unlikely to abstract significant amounts of

water from the aquifer, as it is adapted to dry conditions, surviving on opportunistic water supplies when there is excess winter rain. Alien vegetation in the area is minimal, existing only around certain farms and also along the banks of the Berg River at certain stretches. On the regional scale their abstraction is assumed negligible.

#### 4.8 ABSTRACTIONS

The current abstraction in the area, as given by WARMS, is shown in **Figure 2-13**. Abstractions are input to the model as boundary conditions applied to a node, specifying the abstraction rate. This model is concerned with the affect of the current abstraction on the regional flow regime and water levels, not on predicting drawdowns at a specific position. It was therefore deemed sufficient to use the WARMS usage data, regardless of the fact that the use is registered per farm and so its coordinated may not represent the individual boreholes. For the steady-state simulation the registered abstraction was divided by 365 for an averaged daily rate. In the transient simulation a more realistic summer abstraction pattern is applied.

Abstraction boundary conditions are entered in the model to represent wells. A maximum typical daily abstraction of 500m³/d was applied. Registered volumes which exceeded this were divided in 2 and the registered volume abstracted form 2 boundary condition abstractions. Volumes that still exceeded 500 m³/d when divided by 2, were divided by 3 and so on, keeping a maximum at 500m³/d. This resulted in total of 36 model abstraction points are entered to represent 21 WARMS points.

For wells that are situated in the palaeochannels, the abstraction condition is applied to the lower slices of the model only, based on the assumption that these wells are only screened in the basal aquifer (section 2.4.4). Positions outside of the palaeochannel represent areas where the LAU is absent and so these wells exist ion every slice to represent full penetreatin in the UAU.

The WARMS data doesn't include the boreholes at the wellfield. These are entered into the model based on information given in Woodford et al, 2003. A summary of the abstraction is shown in **Table 4-4** below.

**Table 4-4 Abstraction input data**

Data	Abstraction	Number of Boreholes	Total Abstraction	
			m ³ /day	Mm ³ /annum
WARMS	Average registered abstraction 356 m ³ /day	21	6 218	2.27
Woodford et al, 2003	Average registered abstraction 4000 m ³ /day	8 (assumed)	4 000	1.46
Modelled	Average borehole abstraction 152 m ³ /day	44 (36 to represent WARMS data and 8 points representing the wellfield)	10 218	3.73

## 4.9 RIVERS

### 4.9.1 Positions and river stages

The Berg River is modelled as a transfer boundary. A transfer boundary condition enters a source or sink of water to the selected element based on a simple Darcy calculation between the head in the aquifer beneath the river ( $H_A$ ) and the river stage ( $H_S$ ), and the conductance, as follows:

$$Q = \frac{K A}{B} (H_A - H_S)$$

Where;

$Q$  = flow [ $L^3 T^{-1}$ ],

$K$  = hydraulic conductivity of bed sediments [ $L T^{-1}$ ],

$B$  = bed thickness [ $L$ ]

$A$  = cross sectional area of flow [ $L$ ].

The ( $K/B$ ) term is the conductance of the river, and in Feflow is termed the “transfer rate”.

The river stage  $H_S$  and the transfer rate must be entered for each transfer boundary node.

In a river scenario the cross sectional area of flow is taken as the horizontal area of the riverbed –the river width times its length. In the classical and simplest representation of SW-GW interaction, applicable at regional scales such as the Cape Flats, this represents the area over which groundwater and surface water can exchange (Rushton and Tomlinson, 1979). In finite difference models such as Modflow it is possible to set this area and within the cells the transfer boundary is entered. However in Feflow the area cannot be manually set. The river outline follows the actual trace of the river and so the length of the modelled transfer boundary is realistic. In Feflow transfer boundaries must be set at adjacent nodes so that these connect to form an area of the river (not simply a length). The distance between two adjacent nodes will then represent the width of the river.

To satisfy this requirement in a model on regional scale such as the Langebaan Aquifer would require an aerial mesh with element dimensions in the order of 10 m at the river. Over an area of 2000 km² this mesh would require significant computational effort. The transfer boundaries are set along the positions of the rivers as mapped by the Chief Directorate Surveys and Mapping (CDSM). But the trace of the river length has been highly smoothed for the numerical model (evident in **Figure 3-2**) to avoid numerical error. To model exact meanders in river length local-scale models would be required. Therefore to account for the length of river not being replicated exactly, the width is increased to well beyond the actual 10 m, allowing the required discretisation for aerial representation of the river areas workable.

The data shows and the model assumes that the Berg River is gaining from groundwater on average. The river stages must be assigned levels lower than the modelled groundwater level.

As an initial estimate of the modelled groundwater levels the topography and the measured water level distribution was used (**Figure 2-9**) and river stages were input relative to this water level distribution, between 1-3 m below it. Flow gauging station data received from DWAF is measured relative to the notch of the flow gauge, which are not surveyed. It is not possible to convert their measurements into mamsl (pers comm. Frans Mouski, November 2007). The variation in these records can simply be used as a guide as to the fluctuation from a mean stage. The steady-state calibrated stages are taken as a mean and the typical fluctuation applied in the transient simulation.

#### 4.9.2 Hydraulic connectivity

The transfer rate accounts for the hydraulic conductivity of the bed sediments divided by the thickness of the bed sediments. A transfer rate of zero signifies zero hydraulic conductivity and the transfer node essentially represents a no-flow boundary. As the transfer rate increases the hydraulic connectivity increases and flux between the aquifer and river flows more freely.

The transfer rate is used as a calibration parameter that can be varied to account for changes in bed sediment thickness and hydraulic conductivity. The parameter is also used as a compensation factor to account for changes in river widths that aren't captured in the representation of the river trace by the transfer boundaries.

Where river reaches are natural they are likely underlain by low hydraulic conductivity riverbed sediments such as fine sand and mud (<1 m/d) especially as the Berg River flows over areas of Malmesbury shale rocks, likely to be in a thickness of 0.5 – 1 m overlying the sand aquifer. In these areas transfer rates could be in the order of:

An initial transfer rate of 1 m/day was set ( $\text{Transfer rate} = K / B = 1 \text{ m/d} / 0.5 \text{ to } 1 \text{ m} = 1\text{-}2 \text{ d}^{-1}$ ) and varied in calibration.

#### 4.10 INPUT PARAMETER SUMMARY

The initial input parameter are summarised in **Table 4-5**.

**Table 4-5 Input parameter summary**

Model Input Parameter	Value	Type
Topography	Range 0 mamsl to 125 mamsl	Fixed
Bedrock topography	Range -70 amsl to 100 mamsl	Fixed
Layering	5 layers (Table 4.2)	Fixed
Hydraulic conductivity	10 m/d	Calibration
Storage coefficient	1E-4 m-1	Transient Calibration
Specific yield	0.2	Transient Calibration
Porosity	0.15	Fixed
Recharge	Range	Fixed for steady-state calibration, varied in scenarios
Abstraction	N/A	Fixed for steady-state calibration, varied in scenarios
River stages	1-3 m below real groundwater levels	Calibration
Transfer rate	1	Calibration in natural river sections

---

## **5. NUMERICAL MODEL: STEADY-STATE MODELLING**

### **5.1 CALIBRATION PROCEDURE**

The procedure adopted for calibration is standard to modelling investigations; the simulated steady-state heads and flows (“modelled” data) are compared against field-measured values (“real”, or “observed” data). This is conducted first for steady-state simulations and subsequently for transient simulations (chapter 6). Aquifer parameters are varied until a reasonable fit is generated between modelled and real data selected as calibration data. The procedure and principles are consistent in all the model tasks undertaken on this project.

The calibration of the model is described in Section 5.4. Numerical modelling started with conceptual model testing. The complex hydrogeological details (e.g. the multi-layering) were ignored and the major flow paths were generated with a homogeneous recharge and hydraulic conductivity. This allows the influence of the model mesh and the model boundary conditions to be understood. The full complexity of the system is then incrementally introduced to the model. When physically realistic behaviour is replicated at the boundary conditions calibration of the hydraulic conductivity (K) begins. Within this general process there is iteration that occurs. Regardless of the sequence of events, the parameters from the final model are described under each parameter Section of 5.4.

Parameter testing and evaluation of model sensitivity to different parameters is established. A range of values for one or more parameters are input to the model in order to understand the model response to a particular variable, coupled variables or even a group of variables because it is preferable, but not always possible, to establish a unique model solution. However the calibration is always assessed against what could be physically real. Given the inherent uncertainties in this model with respect to the exact nature of the bedrock topography, the rate of transfer between rivers and the aquifer, lateral continuity or otherwise of the confining layer at different depths and unknown vertical and lateral connectivity between the Berg River and various units, between the upper and lower aquifer unit, a unique model solution was not expected.

A unique model solution is also not necessary as a planning tool. This model aims to test various model scenarios and their effect on estimates of the long-term average flux to or from the different rivers, (SW-GW interaction), the ocean and the impact of abstraction on these fluxes.

### **5.2 CALIBRATION STANDARD**

There is no known standard protocol for quantitative evaluation of a model calibration (Anderson and Woessner, 1992). Point data is used here so that a quantitative evaluation is possible, rather than a qualitative visual comparison between contoured maps (which also include any interpolation errors induced on contouring real data). Point data allows scatter plots of the measured against simulated heads to be generated, which for a calibrated model would show a random distribution of points lying closely around the 1:1 line. The difference between the measured and simulated heads can be calculated, and the average of these absolute “errors” (“error” refers to the absolute difference between measured and modelled values) is a useful quantification of the goodness of the fit in the model run (Anderson and Woessner, 1992).

The maximum acceptable value of the calibration error depends on the magnitude of the change in heads over the problem domain (Anderson and Woessner, 1992). Although there is no convention, the following will be used as guidelines:

- All errors should be within 10% of the magnitude of the change in heads across the model (R. Mackay, Pers. comm. 2005). The water level surface for the model domain (**Figure 2-9**) shows the maximum water level within the model area is ~115 mamsl occurring in the southeast (ignoring the highest point in the west near Vredenburg as it is associated with granitic outcrops and extremely steep basement). The minimum is sea level, therefore 10% of this head drop suggests all point data should be met to within 11.5 m by modelled data in calibration.
- A “small ratio of the RMS error to the total head loss in the system” (Anderson and Woessner, 1992). Anderson and Woessner (1992) however provide no quantitative description of the small ratio.

The calibration point data is used in combination with all available knowledge (local knowledge of groundwater levels, knowledge gained through literature review). In addition to the point data, model runs will be analysed through comparison of certain “key indicators”. These calibration key indicators include:

1. Point data (see below) – the average error to point data and the range in the errors;
2. the maximum modelled water level, to indicate whether any parts of the model are “dry”;
3. modelled water levels as compared to ground level, to show if water levels are within a few metres of ground level or above ground level;
4. mass balance numbers including fluxes to the ocean and to and from the rivers.

The upper and lower aquifers are calibrated separately to different point data sets.

### 5.3 CALIBRATION DATA: STEADY-STATE WATER LEVELS

The available point data for the model domain is shown in **Figure 2-9**. These are a combination of single points and time series averages for the upper and lower aquifer together (see Section 2.4.1). Out of the 278 water level points that are available (**Figure 2-9**), 89 were selected; 54 from the Upper Aquifer and 35 from the Lower Aquifer.

This selection is limited to only those points that have a detailed geology log in the NGDB from which to determine whether the water level point is from the upper or lower aquifer. For the Lower Aquifer, points that are situated on the edges of hydrogeological model zones (at the very edge of palaeochannel) were avoided. The water levels at these points will be controlled by local heterogeneities in the basement elevation and are not considered representative of the regional groundwater surface. For both aquifers points that were in clustered positions were grouped; others were left as single points.

Out of the 54 individual points for the Upper Aquifer this generated:

- a set of 21 points acceptably spread across the model domain, all of which are shown in **Figure 5-1**
- 12 of the points represented a group of values
- 9 were individual
- 18 of these points were used in the final calibration of the model.

The 3 points discarded were the highest observed levels, which could not be replicated in the model (101.6, 93.6 and 78.2 mamsl in **Figure 5-1**). Whilst an acceptable fit was attained for the other points, the highest 3 continued to skew the results to suggest a bad fit. These 3 high points are all situated relatively close to the edges of the model and in areas of high and variable topography. It is interpreted that their water levels pertain to local topographically-driven highs in water level, which cannot be replicated on a numerical groundwater model because surface topography is not taken into account. The parameter calibration results presented refer to the point-data error calculated by excluding these points.

Out of the 35 individual points for the Lower Aquifer this generated:

- a set of 11 points acceptably spread across the north of the model domain all of which are shown in **Figure 5-2**. There is a lack of data from within the constraints of the palaeochannel that penetrates the Lower Aquifer.
- 9 of the points represented a group of values
- 2 were individual
- 10 of these points were used in the final calibration of the model.

The 1 discarded point was the highest observed level, which could not be replicated in the model (85.7 mamsl in **Figure 5-2**). Whilst an acceptable fit was attained for the other points, this one highest point continued to skew the results to suggest a bad fit. It is possible that the high observation point is generated by a local basement high “downstream” of the point that is not replicated by the smoothed modelled contour basement.

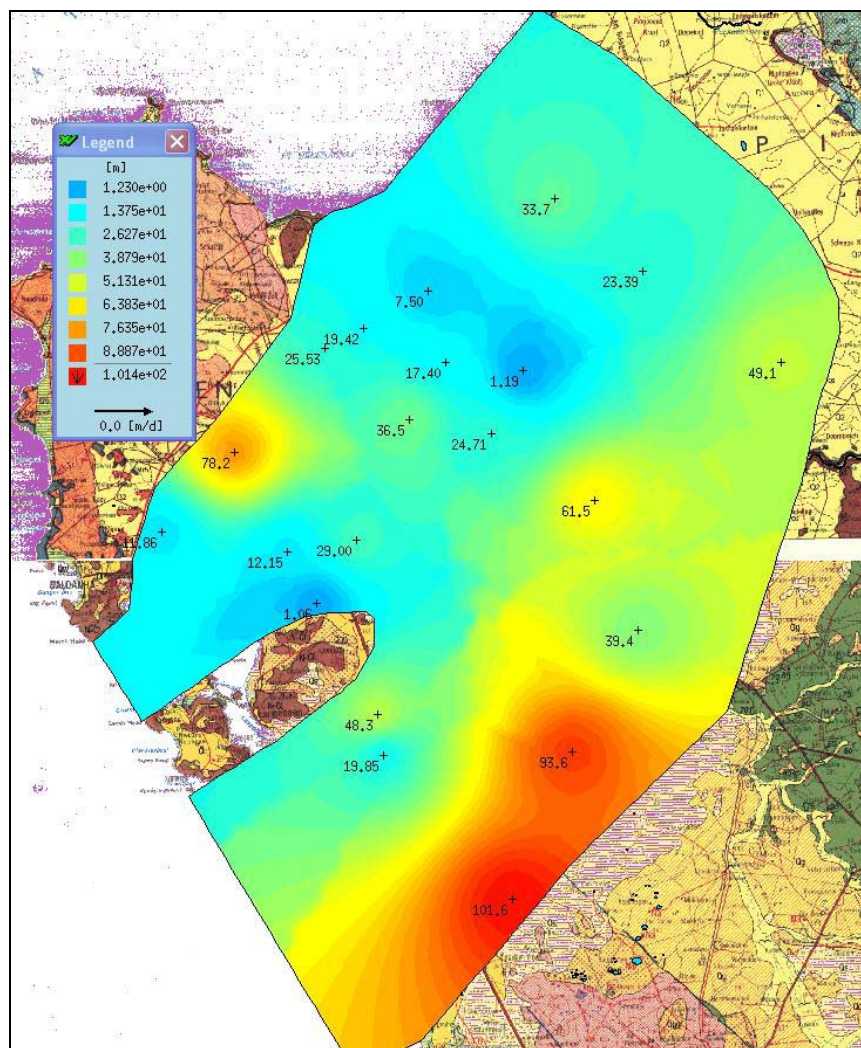


**Figure 5-1 Calibration data points: Upper Aquifer**

*The figure shows the data points used in the calibration and a colour field of water level surface interpolated from these points. This does not represent a true water level surface of the aquifer. It is based on these points only and simply included for display of the calibration data. The 1:250 000 geology map is used as the backdrop for orientation.*

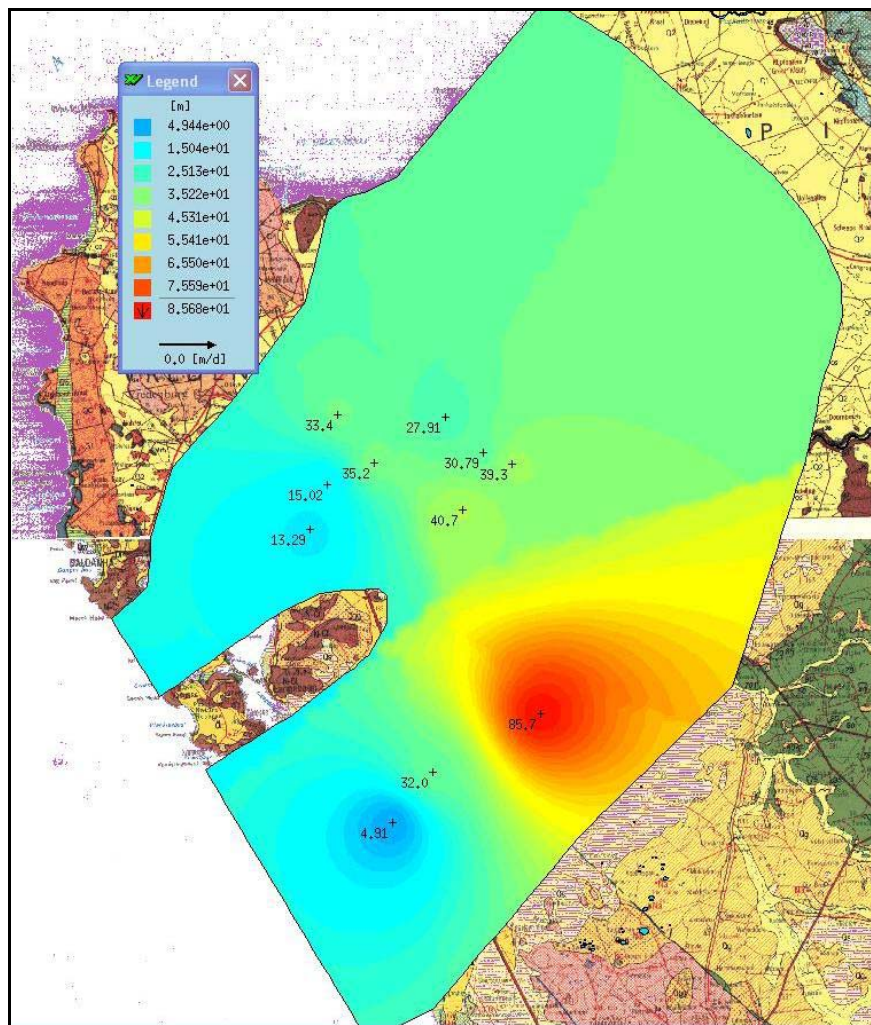


**Figure 5-2 Calibration data points: Lower Aquifer**

*The figure shows the data points used in the calibration and a colour field of water level surface interpolated from these points. This does not represent a true water level surface of the aquifer. It is based on these points only and simply included for display of the calibration data. The 1:250 000 geology map is used as the backdrop for orientation.*

## 5.4 PARAMETER CALIBRATION

### 5.4.1 River transfer rate

The transfer rate and hydraulic conductivity were varied simultaneously and independently to understand the coupling and independent effect of these parameters. Variations to the magnitude of the transfer rate in steady-state simulations have a significant effect on the flux of water in and out of the transfer nodes. The effect on the magnitude of the model water levels is less significant. But, although not impacting in the measurement of calibration error, it does impact on the modelled fluxes of water. Thus it is considered a calibration parameter and necessary to establish model sensitivity to variations in it. The transfer rate into and out of a river can be adjusted separately.

Given the understanding that there is often a greater resistance to flow into an aquifer from a river, than out of an aquifer (Rushton and Tomlinson, 1979) the transfer rate into the aquifer from the rivers was reduced by an order of magnitude compared to the transfer rate out of the

aquifer into the rivers (**Table 5-1** below). This maintained the realistic flow regime with regard to the modelled Berg River. Across the model, the Berg River acts as a sink to the Upper and Lower aquifers (discussed further in section 5.5 and 5.6 ).

**Table 5-1 Transfer rate calibration (magnitude)**

	Transfer Rate IN	Transfer Rate OUT
<b>Initial</b>	1 d ⁻¹	1 d ⁻¹
<b>Final</b>	0.1 d ⁻¹	1 d ⁻¹

#### 5.4.2 Hydraulic conductivity (K)

A summary of selected key model run results for various distributions of hydraulic conductivity is shown in **Table 5-2** below. Initial model runs where the conceptual model was tested and the internal layering ignored are not included. The Upper and Lower aquifer units were separated into 2 layers each for numerical model stability, and it is assumed that the aquifers are internally homogeneous, therefore these layers were treated together in the calibration. The confining layer was assigned a hydraulic conductivity initially of 0.1 m/d reduced to 0.01 m/d to increase the modelled water levels, thereafter the layer was assumed fixed.

The hydraulic conductivities are given in the standard m/d units. The units used in the modelling software Feflow are  $\text{E}^{-4}$  m/s. For simplicity the units are converted to the nearest significant figure in m/d. For example a hydraulic conductivity of  $1\text{E}^{-3} \times 10^{-4}$  m/s (blue in Figure 5.4) is quoted in the text as 0.01 m/d. Considering the accuracy of the model this is sufficient reporting of the model results. **Table 5-2** shows the key model fluxes that vary depending on the hydraulic conductivity scenario. The full model mass balance is shown in section 5.7. The main features to be drawn from calibration of hydraulic conductivity are:

- If homogeneity throughout the aquifer is assumed (i.e. each layer set with the same K), the best-fit K is 10 m/d. If K is above ~40 m/d the regional water table gradient generates water levels well outside the calibration error, and at 1m/d the water table is elevated well above observed. This suggests that the equivalent K taking the net effective of potential different K's in each layer is 10 m/d.
- With a homogeneous 10 m/d there is no separation of the water levels between the aquifers and the confined nature of the Lower Aquifer is not replicated.
- There is a relatively narrow range in K value in all layers, within which the model reproduces a reasonable regional water table and also an acceptable ratio of outflow to the ocean and into the rivers.
- There is a close relationship between the variations in K value in different model layers and the flux of water entering the rivers. The vertical anisotropy in the model impacts on the flux out of the aquifer into the river. The lower Kz the greater the flux to the rivers. The model showed a better calibration fit with Kz an order or magnitude lower than Kx and Ky. Kx and Ky were not varied with respect to each other.
- The numerical models showed that a heterogeneous K was required in order to calibrate to the observation data and hence K was varied between layers and also heterogeneously within layers.

- The numerical model results confirmed what was assumed in the conceptual model: that the low K clay aquitard is significant in the regional flow regime. Replicating this layer in the model, allowed modelled water levels to increase to match observed levels.
- Although it was expected that layers 4&5 might require a high K that only exists in palaeochannel areas (Volume 5 of this report, DWAF, 2007d), this was not the case based on the calibration point data. A better fit was attained when the K of 10 m/d was present throughout layers 4&5 (scenario 4 and 8 verses scenario 5, 6 and 7). If layers 4&5 were only high K in the palaeochannel there would be limited pathways for water from recharge. Therefore although it maybe more realistic that at depth high K only exists within the palaeochannel, the high k across the domain in layer 4&5 may represent addition of water to the layer that in reality may occurs through discrete positions where the clay is absent, areas which aren't modelled.
- It would appear that there is an upper limit to the K in the lower layers based on a model assumption that the rivers act as a sink on average over time. A basal layer of ~100 m/d, reasonable for a coarse clean gravel, lowers the water levels in the lower aquifer beneath observed water levels, and flattens the gradient to the ocean.

The model was considered calibrated for the following parameter set (Scenario 8 in **Table 5-2**);

- Kx and Ky of 10m/d in model layers 1 and 2 with certain areas at 1m/d.
- A very low Kx and Ky (0.01 m/d) in layer 3, set in positions where the layer is greater than 1 m thick. This corresponds to areas overlying palaeochannels (specifically where the basement is less than -0.5 mamsl) and where the topography is above 4.5 mamsl (see **Table 4-2**). This avoids the low K existing at or close to the surface, because the Upper Aquifer is extensive across the surface. In all other areas of the layer (e.g. on basement rises where the clay is not present but the layer must continue in the model) the Kx and Ky is 10 m/d.
- Kx and Ky of 10 m/d in model layer 4 and 5;
- Throughout the layers Kz is 0.1x these values.

There are potentially many permutations possible for combinations of K values that may be equivalent to that presented here. The K scenario described above was decided upon as a best fit, because it generated results which fall within the calibration standards set for this modelling exercise (**Table 5-2**). The heterogeneous K distribution for layers 1&2 and layer 3 is shown in **Figure 5-3** and **Figure 5-4** below. The point data results for the scenario chosen are similar to scenario 4. Scenario 8 was chosen for its lower range of errors.

The highest of the observation points were not matched and were discarded (described in section 5.3). Fixing these points as internal heads did not improve the calibration (Scenario 9).

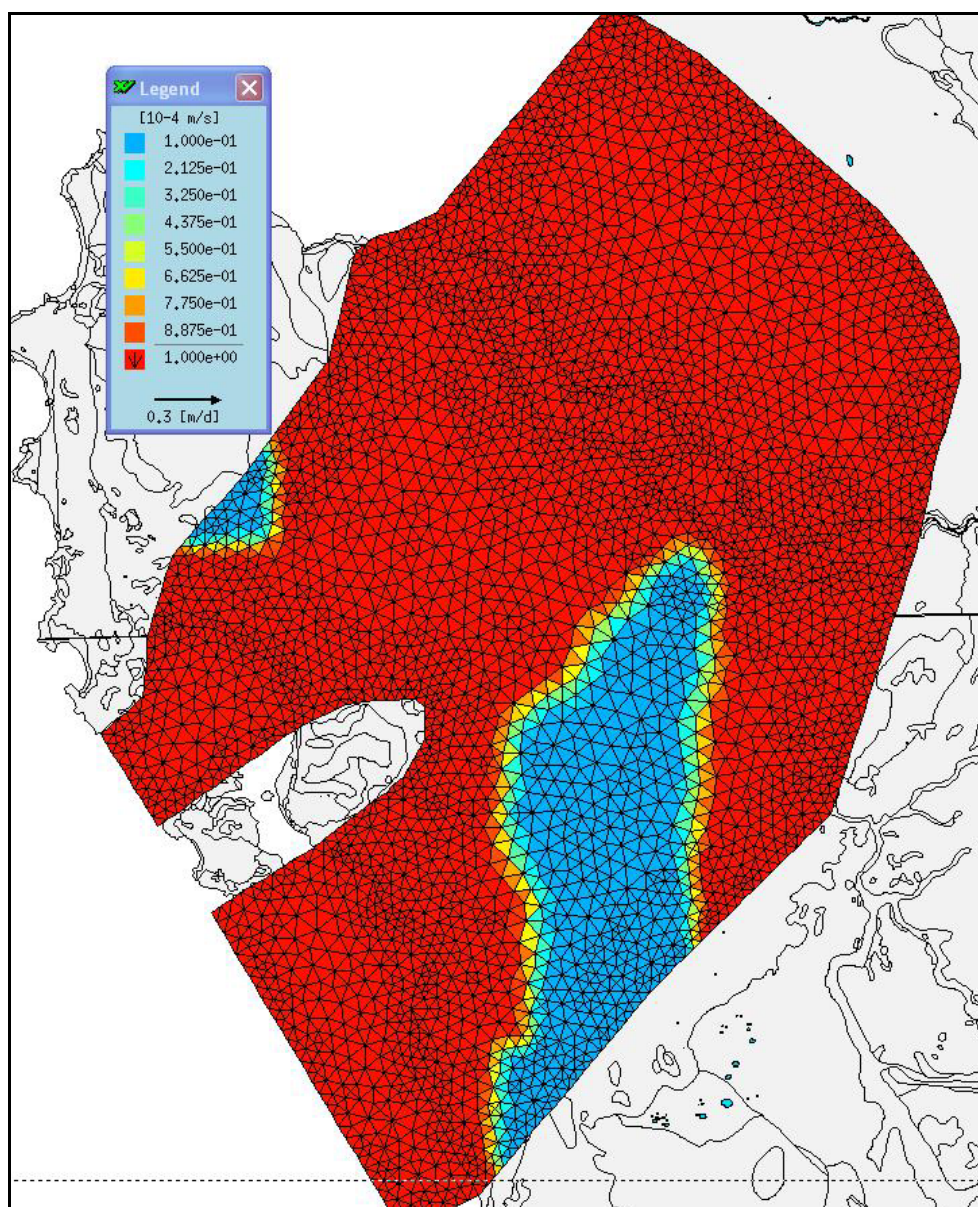


**Figure 5-3 Model hydraulic conductivity distribution for Layers 1&2 – the Upper Aquifer Unit (Kx is shown)**

*Blue represents areas of K ~ 1 m/d, red represents ~10 m/d.*

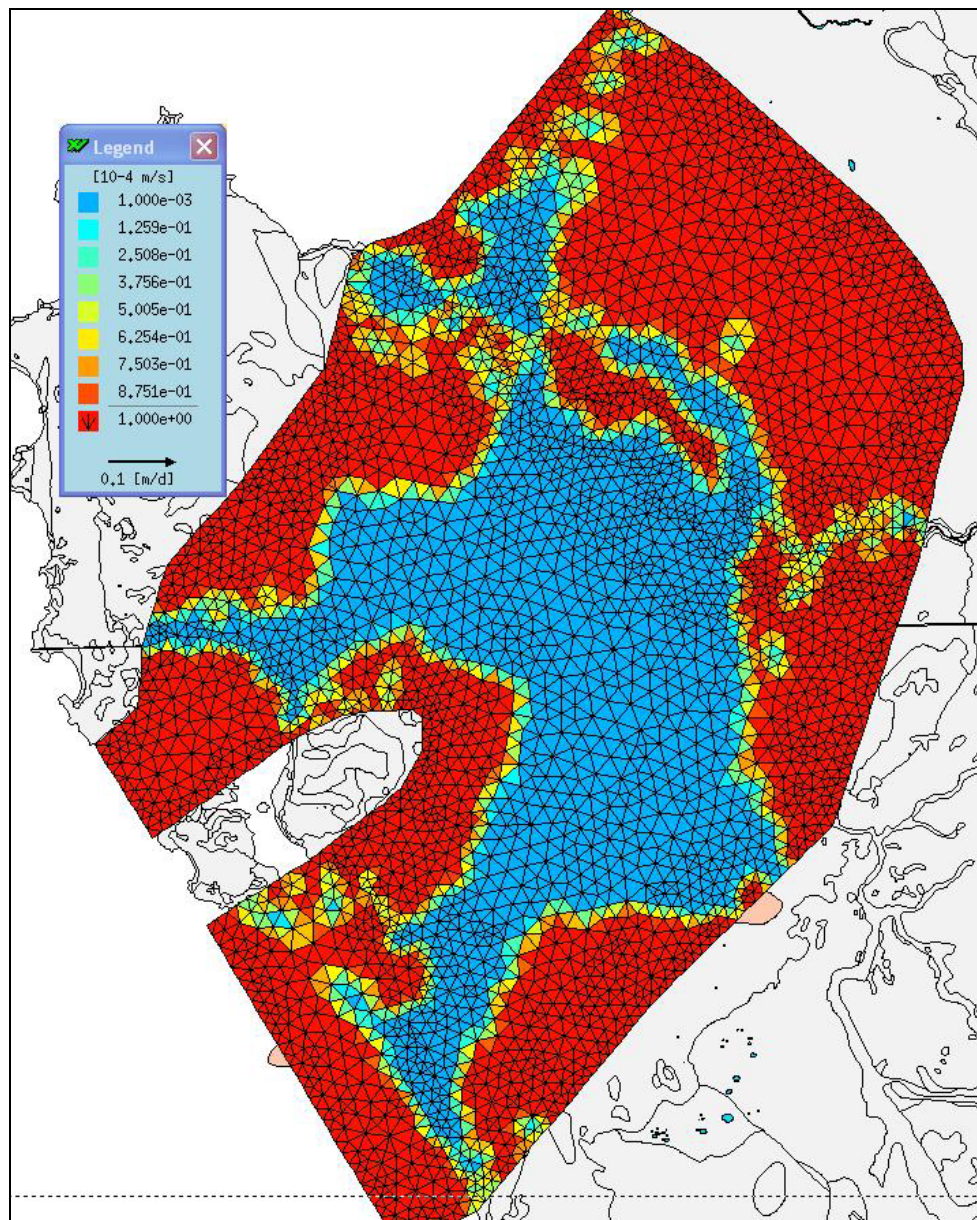


**Figure 5-4 Model hydraulic conductivity distribution for Layer 3 – the confining unit (Kx is shown)**

*Blue represents areas of  $K \sim 0.01$  m/d, red represents  $\sim 10$  m/d.*



**Table 5-2 Results of key indicators for various hydraulic conductivity scenarios, including results for final model scenario.***Bold indicates errors which are within the calibration standard suggesting a good model run, italics indicate poor model runs.*

Scenario	Description	K (m/d) Layer 1 & 2	K (m/d) Layer 3	K (m/d) Layer 4 & 5	UPPER AQUIFER Calibration point data		LOWER AQUIFER Calibration point data		Mass Balance (whole model) (m ³ /day)	
					Mean absolute error	Error range	Mean absolute error	Error range	To ocean	To rivers
1	Homogeneous within layers, anisotropic	1 / 1 / 0.1	0.01 / 0.01 / 0.001	10 / 10 / 1	25.6	88.8	16.8	14.2	31,000	19,000
2	Homogeneous within layers, anisotropic	10 / 10 / 1	0.01 / 0.01 / 0.001	10 / 10 / 1	12.0	46.0	<b>6.0</b>	19.6	31,400	21,700
3	Heterogeneous distribution in layer 1&2, anisotropic	10 / 10 / 1 and areas of 1 / 1 / 0.1	0.01 / 0.01 / 0.001	10 / 10 / 1	12.3	46.1	<b>6.2</b>	19.8	31,500	21,700
4	As 3, with a heterogeneous K distribution in layer 3	10 / 10 / 1 and areas of 1 / 1 / 0.1	0.01 / 0.01 / 0.001 over palaeochannel areas, otherwise 10/10/1	10 / 10 / 1	<b>10.3</b>	44.7	<b>5.5</b>	19.4	29,500	21,100
5	As 3, with a heterogeneous K distribution in layer 4&5	10 / 10 / 1 and areas of 1 / 1 / 0.1	0.01 / 0.01 / 0.001	10 / 10 / 1 over palaeochannel areas, otherwise 0.01 / 0.01 / 0.001	19.5	65.6	12.2	18.5	29,900	20,700
6	As 3 with heterogeneous distribution in layers 3 and 4&5	10 / 10 / 1 and areas of 1 / 1 / 0.1	0.01 / 0.01 / 0.001 over palaeochannel areas, otherwise 10/10/1	10 / 10 / 1 over palaeochannel areas, otherwise 0.01 / 0.01 / 0.001	14.6	47.4	<b>6.3</b>	18.5	30,200	20,100
7	As 5 with increased K in palaeochannel	10 / 10 / 1 and areas of 1 / 1 / 0.1	0.01 / 0.01 / 0.001	40 / 40 / 4 over palaeochannel areas, otherwise 0.01 / 0.01 / 0.001	13.5	51.2	13.5	26.1	34,000	16,200

					UPPER AQUIFER Calibration point data		LOWER AQUIFER Calibration point data		Mass Balance (whole model) (m ³ /day)	
8	As 4, with an increased area of low K in layers 1&2	10 /10 / 1 and areas of 1 / 1 / 0.1	0.01 / 0.01 / 0.001 over palaeochannel areas, otherwise 10/10/1	10 /10 / 1	10.3	44.4	5.6	19.5	29,500	21,200
9	As 8, with 4 of the highest points set as internal prescribed heads	10 /10 / 1 and areas of 1 / 1 / 0.1	0.01 / 0.01 / 0.001 over palaeochannel areas, otherwise 10/10/1	10 /10 / 1	14.6	45.2	10.6	16.4	39,700	25,500

## 5.5 RESULTS

### 5.5.1 The flow regime

The model results show that the basement topography has a big influence on the flow regime. The speed of groundwater flow increases in the palaeochannels as the groundwater is funnelled into the deep narrow incisions close to the coastline (**Figure 5-5**). The modelled groundwater flow replicates the major features of the observed groundwater flow. The higher water levels in the southeast are replicated, and flow from the southeast occurs towards the Elandsfontein aquifer system and northwest into the LRAS.

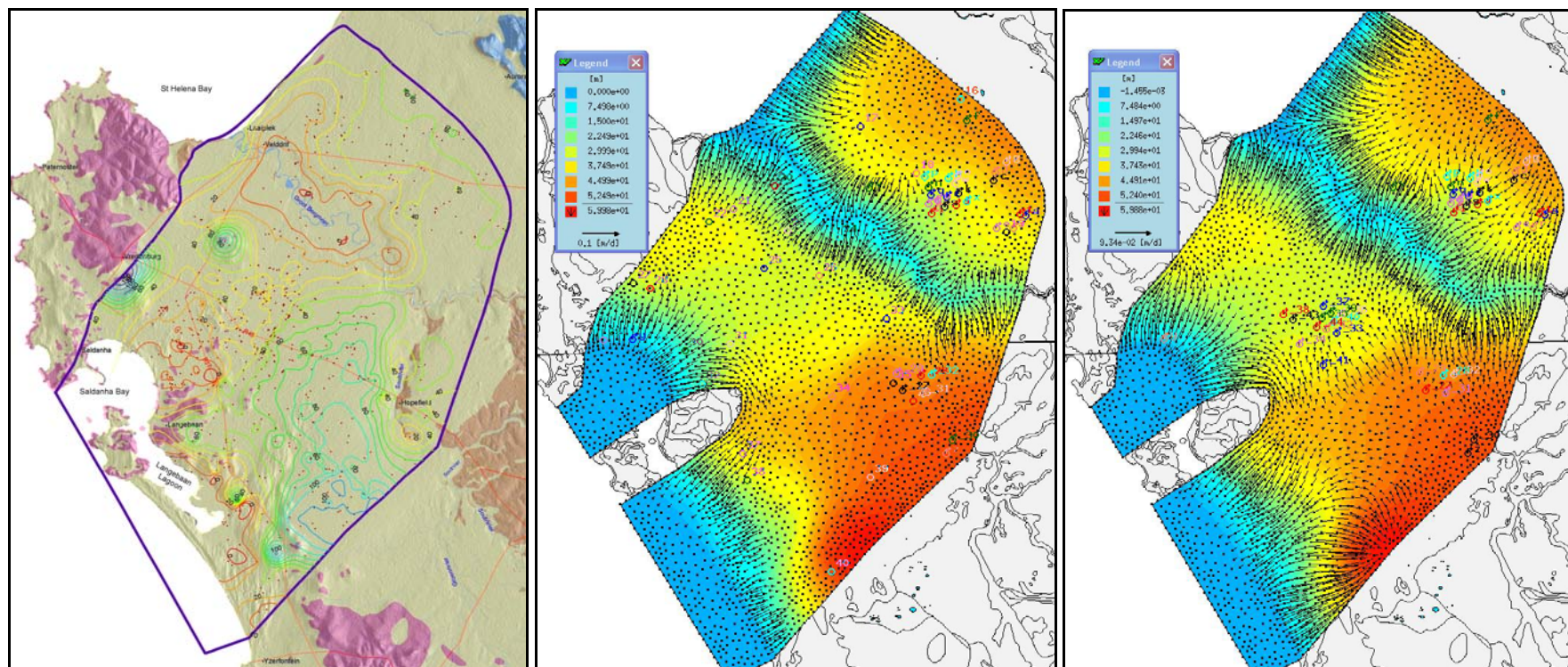
As flow occurs towards the LRAS the flux increases as the groundwater flows across areas where the basal layers thins between the two palaeochannels. In the same way that the observed water level plot is a combined representation of the two aquifers, the modelled water levels also appear to have combined the behaviour of the two aquifers; the flow regime is identical in each layer, just at different speeds due to the thicknesses of the layers (**Figure 5-5**).

The effect of the Berg River is clear as the groundwater speeds up closer to the transfer nodes (**Figure 5-5**). In these steady-state simulations the effect of the low K layer is to reduce the speed of groundwater flow within the layer. Because it is a steady-state simulation the model system has infinite time to reach equilibrium. Pressure is therefore transmitted through the confining bed and the effect of the Berg River is also “seen” in the lower aquifer. The modelled flow in the upper and lower aquifer is the same direction, the only the speed of flow is variable. In reality the confining bed may act to separate the flow directions.

The model allows the lower Aquifer to discharge to the Berg River because it allows transmission of pressure through layers that in reality wouldn't happen. This is because the model runs to steady-state whereas in reality the time factor means the water transmits through the clay slowly. An aquifer-specific model has been set up: the different water tables in the aquifers is traceable and their different responses to pumping for example are clear, however the modelled fluxes are lumped in the model.

The degree of confinement varies across the model, due to the variable extent of the low K layer. 4km inland from Saldanha Bay, within the centre of the Langebaan Road System palaeochannel, water levels in the basal aquifer are 1.3 m higher than the upper aquifer. At the head of the Elandsfontein Aquifer System palaeochannel, in the southeast of the model, the confining layer is present but the water levels in the upper aquifer are 0.3 m above the lower aquifer, indicating downward flow. This is intuitive as this is an area of higher recharge and higher water levels and therefore downward flow (recharge to the LAU) is expected.

This indicates that even though the difference in hydraulic conductivity is 3 orders of magnitude (0.01 m/d to 10 m/d), the effect at the regional scale, for a steady-state simulation, is a low degree of confinement.

**Observed:****Modelled Layer 1 (UAU):****Modelled Layer 5 (LAU):**

**Figure 5-5** Observed and modelled groundwater surface, upper and lower aquifer

## 5.5.2 Discussion

### 5.5.3 Parameter calibration summary

The final model scenario has a relatively low average point data error, however the range of the point data errors is high. The scatter plot in **Figure 5-6** shows the deviance from the 1:1 line, shown for this scenario and others with a similarly low average point-data error. Typically, modelled groundwater levels are of a shallower gradient than observed, with modelled levels higher than observed at low values, and lower than observed at high values.

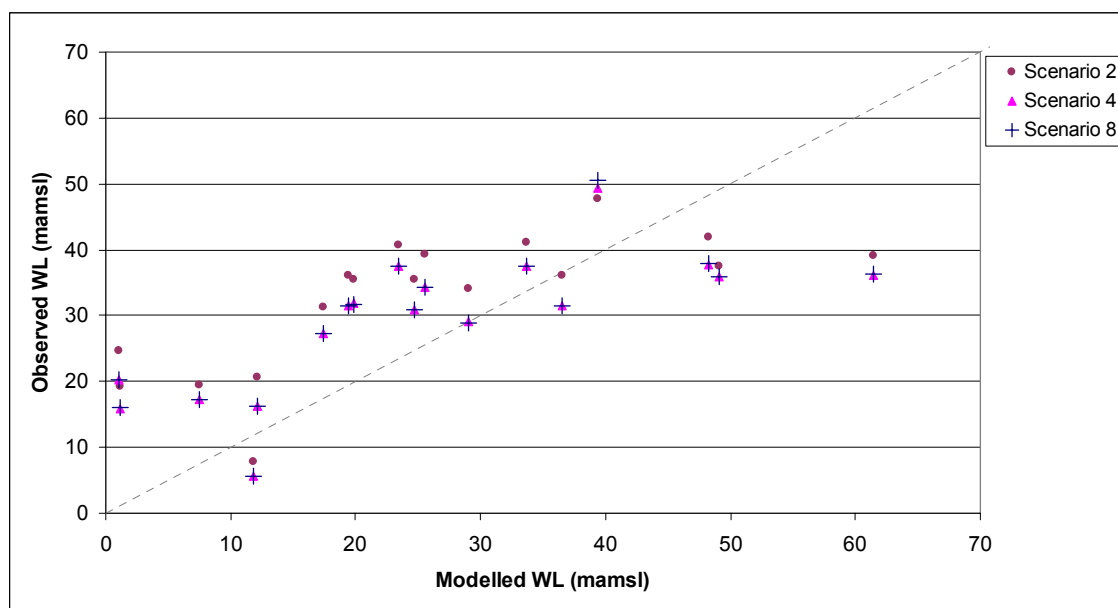


Figure 5-6 Scatter plot of modelled verses observed groundwater levels: Upper Aquifer

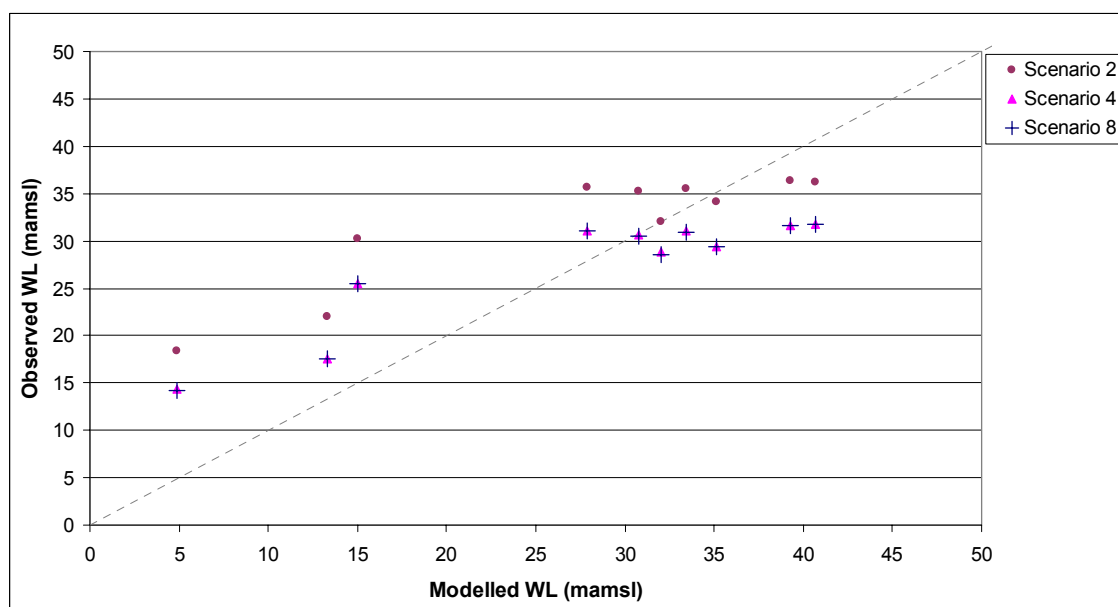


Figure 5-7 Scatter plot of Modelled verses Observed groundwater levels: Lower Aquifer

---

## 5.6 SURFACE WATER- GROUNDWATER INTERACTIONS

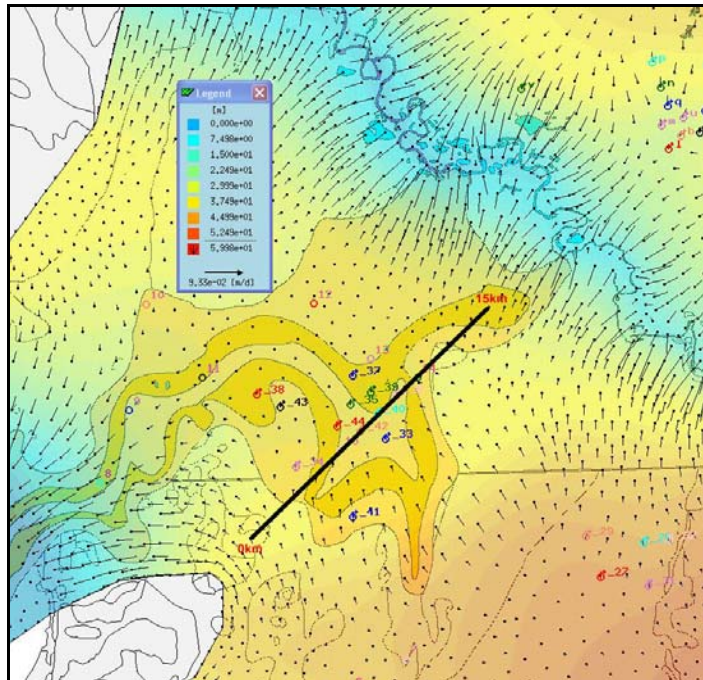
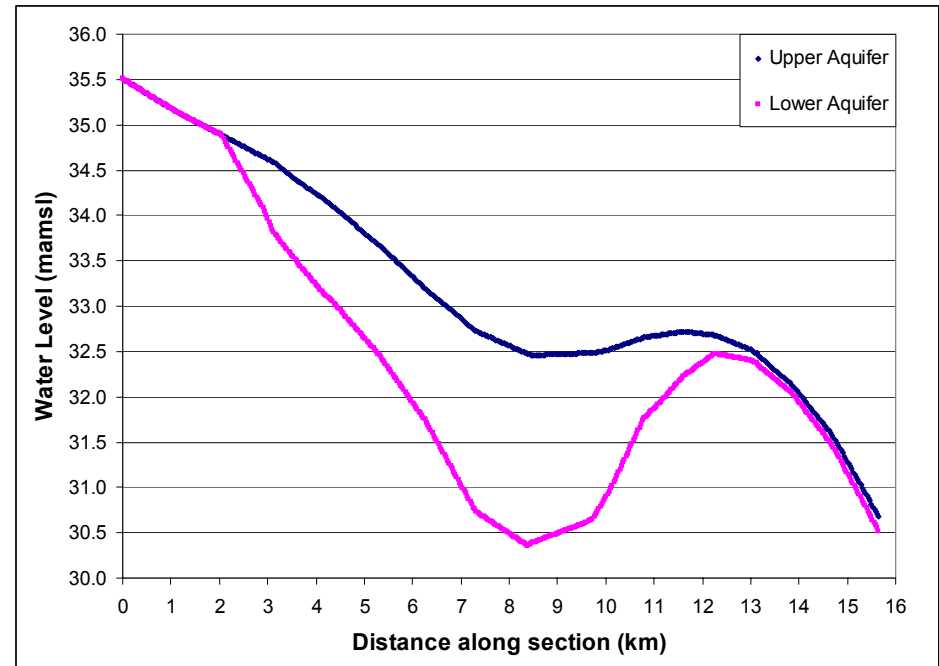
The fluxes of water to the ocean and to the modelled river is shown in **Table 5-2** above. The Berg River is the only river modelled (for this model domain) and therefore these fluxes represent the daily flux along the modelled length of the Berg. **Table 5-2** above also shows that for the majority of hydraulic conductivity scenarios, the flux to the Berg River is similar. This suggests that it is only moderately sensitive to the hydraulic conductivity and provides confidence in a value of  $\sim 21,000 \text{ m}^3/\text{day}$  ( $0.02 \text{ M m}^3/\text{day}$ ) discharged to the river from groundwater.

Over the steady-state simulation the Berg River acts as a sink to the aquifer. Whether the Berg recharges the aquifer during flood events is investigated in the transient modelling (section 6 and 7).

## 5.7 THE IMPACT OF CURRENT ABSTRACTION

At the head of the palaeochannel, near the West Coast Wellfield, the confining gradient is reversed due to the pumping in the lower aquifer, and the upper aquifer has a higher head than the lower by  $\sim 1\text{m}$ , indicating a downward flow component. Observations show that water levels are in decline in the lower aquifer and the upper aquifer is relatively unaffected by the pumping (Woodford et al, 2003). The real system has therefore not reached equilibrium yet. A steady-state model simulates a status of equilibrium. The modelled results show that the pressure is transmitted through the low K layer and groundwater levels decline in the upper aquifer, though to a lesser degree than the lower aquifer. A cross section of water levels through the wellfield area is shown in **Figure 5-8** below. The modelled cone of depression extends for a radius of  $\sim 3\text{-}4 \text{ km}$  from its centre. It should be noted that this is a representation of the system in steady-state, and although it is the state that the aquifer will reach under this abstraction regime if factors remained constant, due to the time lag for drawdown through clays, it is not possible to accurately say when the system will reach this state.



**Section line position****Modelled heads along section****Figure 5-8 The effect of abstraction at the West Coast Wellfield on water levels**

The modelled water level surface is used to show the position of the section line is shown over. The surface is shown as a transparent colour field so that an image of the basement topography is visible behind the modelled groundwater levels. The image is included for orientation, however it is not an accurate representation of the basement contours input to the model. The West Coast Wellfield is sited at the head of the palaeochannel.



Running the calibrated model without any abstraction generated the water-table map shown in **Figure 5-9**. Assuming that the abstraction activities have not affected the regional hydraulic conductivity of the system (reasonable), this is the potential water level surface if there were no abstraction. The effect of the current abstraction on the regional water table is clear if this is compared with **Figure 5-5**. The high water levels in the southwest of the model extend much further to the northwest in the case of no abstraction. The effect of the current abstraction on the mass balance of the model is shown in **Table 5-3**.

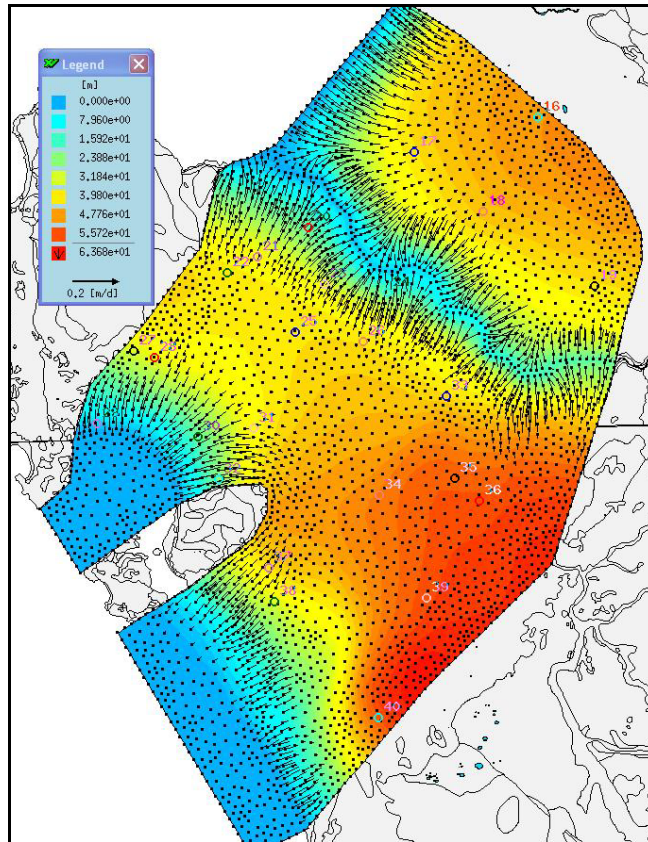


**Figure 5-9 Modelled water level surface with no abstraction (shown for Upper Aquifer)**

**Table 5-3 The Effect of current abstraction on modelled fluxes**

	Flux into model (m ³ /d)		Flux out of model (m ³ /d)			Balance error (m ³ /d)
	Recharge	Rivers	Ocean	Rivers	Abstraction	
abstraction (i.e. standard model case)	59 800	0	-29 500	-21 200	-10 100	-1000
Zero Abstraction	59 800	0	-32 800	-27100	0	-100
Difference caused by abstraction	-	-	Decrease of 10%	Decrease of 22%	-	Increase of 900%

---

## 5.8 MODEL CONFIDENCE

In order to calibrate the model to a greater degree of confidence it would be necessary to obtain actual river stage information. Here river stages have been assumed based on 1:50 000 scale topography sheets and the interpolated observed groundwater level map. The potential error in this is unknown.

The modelled groundwater contours are not as steep as observed. This may be a function of the fact that it is a regional model, however the data used in calibration is “local data”. The data pertains to local features. Smoothing the observed water level surface until the influence of individual measurements is lost could generate a regional calibration surface. Individual points could be abstracted from that surface for use as quantitative calibration data.

This model gives insights into the regional groundwater flow pattern. To detail the aquifer specific groundwater interaction with the Berg River, and further detail the affect of the abstraction at the wellfield, smaller-scale models would be required. Further testing of the lateral K values in the confining layers would be of interest in establishing whether or not the lower aquifer can actually discharge to the Berg River or not.

The overall mass balance is acceptable. There is a model error of 10% of the smallest modelled flux, which is the abstraction. Further mesh discretization in selected areas would reduce this. A model process experiment using smoothed data at selected nodes to calibrate against will contribute to model confidence.

## **6. TRANSIENT MODEL**

### **6.1 TRANSIENT MODEL ASSUMPTIONS**

In addition to the assumptions that underlie the steady-state model, the transient model assumes:

- The magnitude of the monthly variation in river stages is the same along the modelled length of the Berg River. This assumption is necessary as there is no data available to support any other representation of the river stages.
- The specific storativity (Ss) is  $1\text{E}^{-5}$
- The magnitude of the monthly variation in rainfall does not vary throughout the model domain. The steady-state rainfall average in each rainfall zone is varied by this fixed amount resulting in a heterogeneous recharge distribution.
- Recharge varies monthly with rainfall.
- The BRBS method for recharge calculation also applies to monthly data.
- Rain during the driest 6-month period (October to March inclusive) does not enter the aquifer as recharge. It is lost to evaporation / evapotranspiration. There is no evapotranspiration during the winter months.
- Major abstraction for irrigation purposes occurs in the dry summer months only. Irrigation is the dominant water user in the WARMS dataset. Therefore the abstractions registered in WARMS are applied in the model during a 6-month period of October to March (inclusive). The same positions and number of wells described in section 4.8 above are used, and the pump rates are adjusted from those used in the steady-state model to represent the same total abstraction but over 6 months only. The West Coast Wellfield pumps continually, and this is represented in the model.

### **6.2 REQUIRED INPUT DATA**

The input data for the transient model is shown in the table below. The data source and whether the parameter is varied in transient modelling or fixed is noted. Input data different to that used in the steady-state model (described in chapter 4) is highlighted in bold, and described further below.

**Table 6-1 Transient model input parameters**

Model Input Parameter		Source	Type
Topography		100 m DEM	Fixed (same as steady-state)
Bedrock topography		Literature and NGDB	Fixed (same as steady-state)
Layering		Based on geology and numerical requirements	Fixed (same as steady-state)
Current CFA abstraction		WARMS	Fixed (same as steady-state)
Transfer rate		Steady-state calibrated values	Fixed
Hydraulic conductivity		Steady-state calibrated values	Fixed
River Stages		Observed monthly variation in stages applied to Steady-state calibrated values	Fixed
Recharge		BRBS method and Berg WAAS monthly rainfall.	Fixed for calibration, varied in scenario testing
Storage	Specific Yield Sy	1 st approx from typical literature values	Transient calibration
	Specific Storativity Ss	Assumption based on literature	Fixed
Porosity		Typical literature values	Dictated by storage therefore calibrated through storage calibration

### 6.3 RIVER STAGES

The river stages from the steady-state situation are assumed to be the annual average of the stage in that position. Monthly river stages for the gauging station at Janjiesfontein were supplied by DWAF for the period 1980 – 2007. These are not convertible to mamsl (see section 4.9.1). Instead of using the data directly, the mean, over the years recorded, for each month (m above unknown datum) was calculated. From this, an annual mean was calculated and each month's level was converted to a variation from this annual mean. The same variation from mean was applied to each river stage along the Berg River to generate varying stages. This does assume therefore that the magnitude of seasonal variation is the same along the length of the River. It is likely to be less towards the mouth, but for regional mass balance numbers and regional behaviour, this is deemed acceptable, and without any other data, a necessary simplification.

### 6.4 RECHARGE DATA

Recharge in the area has a highly heterogeneous distribution, with a clear recharge high in the southeast, and lower recharge to the northwest. In the steady-state model each element has a different value. To apply varying recharge to each element however would require individual files to be created and imported over each element, and would generate unnecessary

computational effort. To maintain the heterogeneous distribution in the transient model recharge zones were generated. Elements were grouped into recharge zones based on their annual recharge;  $0-0.1 \text{E}^{-4} \text{ m/d}$ ,  $0.1-0.2 \text{E}^{-4} \text{ m/d}$ ,  $0.2-0.3 \text{E}^{-4} \text{ m/d}$  and so on.

Monthly rainfall data is generated by re-calculation of modelled mean monthly values, as given by agrohydrology data sets (Schultz et al, 1997), to sum to the annual modelled rainfall (section 2.2, **Figure 2-3**). The monthly rainfall was averaged for the whole area and converted to recharge by applying the BRBS percentages of rainfall (see Volume 5 of this report, DWAF, 2007d). The monthly departure in recharge from the annual average recharge was calculated. Applying this monthly departure, to the average for each zone, generated the monthly variation in each zone. The heterogeneous distribution is therefore retained.

The modified BRBS recharge calculation procedure above, generates recharge values in the summer months (**Figure 6-1**). However, it is unlikely that summer rainfall enters the aquifer as recharge, due to loss from the surface to evaporation and evapotranspiration. The recharge suggested over the summer months by the BRBS method was summed and distributed over the wet months, in order that the total recharge volume in the transient model would still equate to that used in the steady-state model.

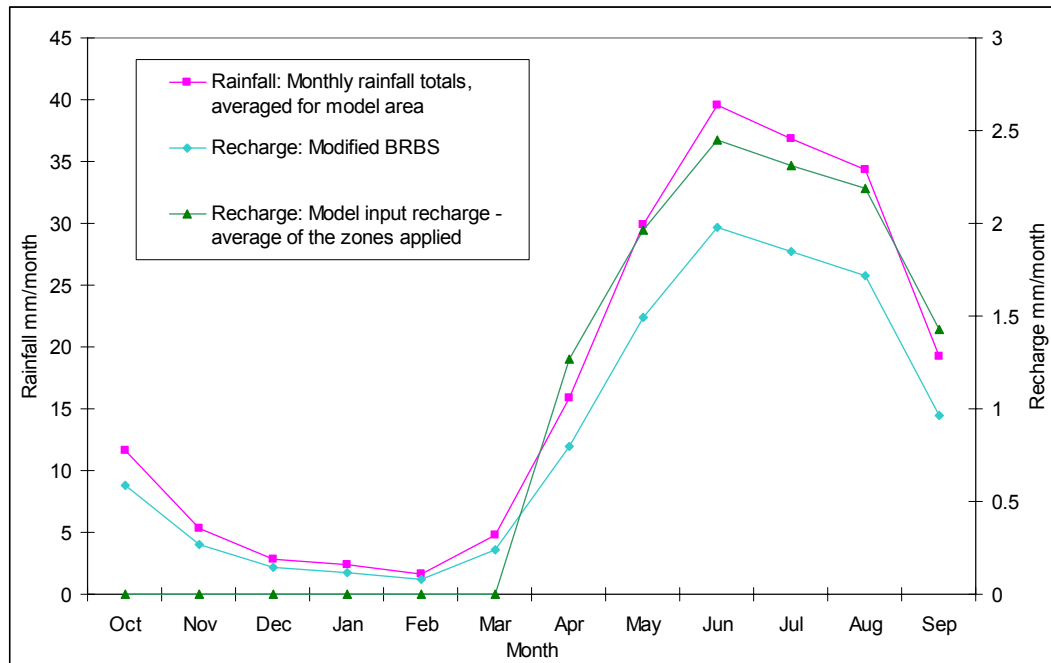


**Figure 6-1 Monthly rainfall and recharge**

## 6.5 STORAGE DATA

The storage parameters are the main calibration parameters in transient simulations. It is assumed that the specific storage ( $S_s$ ) is  $1\text{E}^{-5}$  and it is not varied. The specific yield ( $S_y$ ) will be varied in calibration and the values in **Table 6-2** used as a guide to test the reality of the result.

**Table 6-2 Typical values for specific yield (Driscoll, 1986)**

Lithology	Specific Yield [-]
Sand	0.1 – 0.3
Gravel	0.15 – 0.3
Limestone	0.005 – 0.05
Clay	0.01 – 0.1

## 6.6 CALIBRATION DATA AND STANDARD

A handful of the NGDB boreholes had good records of long, detailed, time-series data (monthly data extending >10 years), and these were included in the steady-state calibration data set. Out of the 89 boreholes selected for the steady-state calibration process, those without transient data or with short or sparse (<2 years) data sets were discarded. For those with time-series data, the water level at each borehole was analysed to ensure local pumping effects did not dominate the record and those with erratic records were discarded. 34 borehole records remained, 16 in the UAU and 18 in the LAU (**Table 6-3**).

The seasonal variability at each point was analysed. Clustered boreholes were grouped to one observation point and their variability's were averaged. The process generated 11 points for the UAU. Of these 11 points, 7 are individual and 4 are grouped. The distribution of the observation points is shown in **Figure 6-2** below. The process generated 8 points for the LAU. Of these, 2 points are individual and 7 are grouped. The distribution of the observation points is shown in **Figure 6-3**.

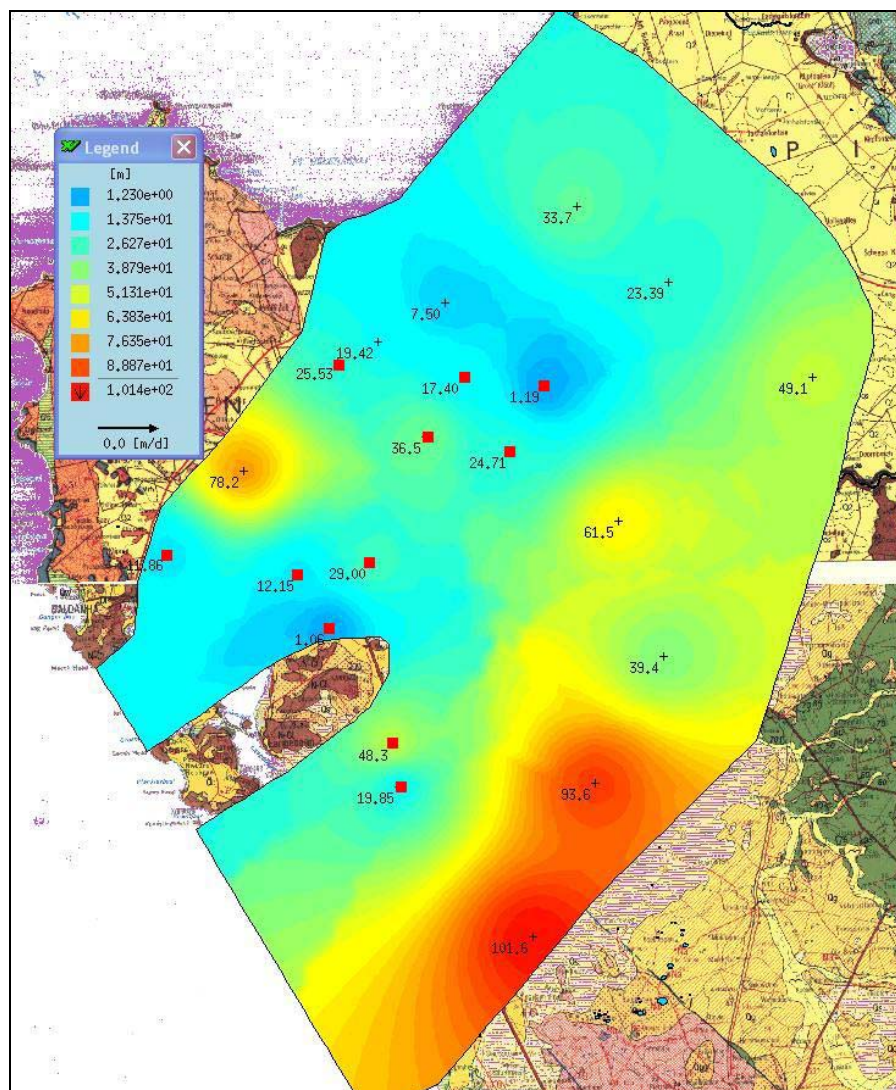


**Figure 6-2 UAU observation points.**

*The steady-state observation points which also act as transient observation points are highlighted in red squares. The figure shows the data points used in the calibration and a colour field of the water level surface interpolated from these points. This does not represent a true water level surface of the aquifer. It is based on these points only and simply included for display of the calibration data. The 1:250 000 geology map is used as the backdrop for orientation.*

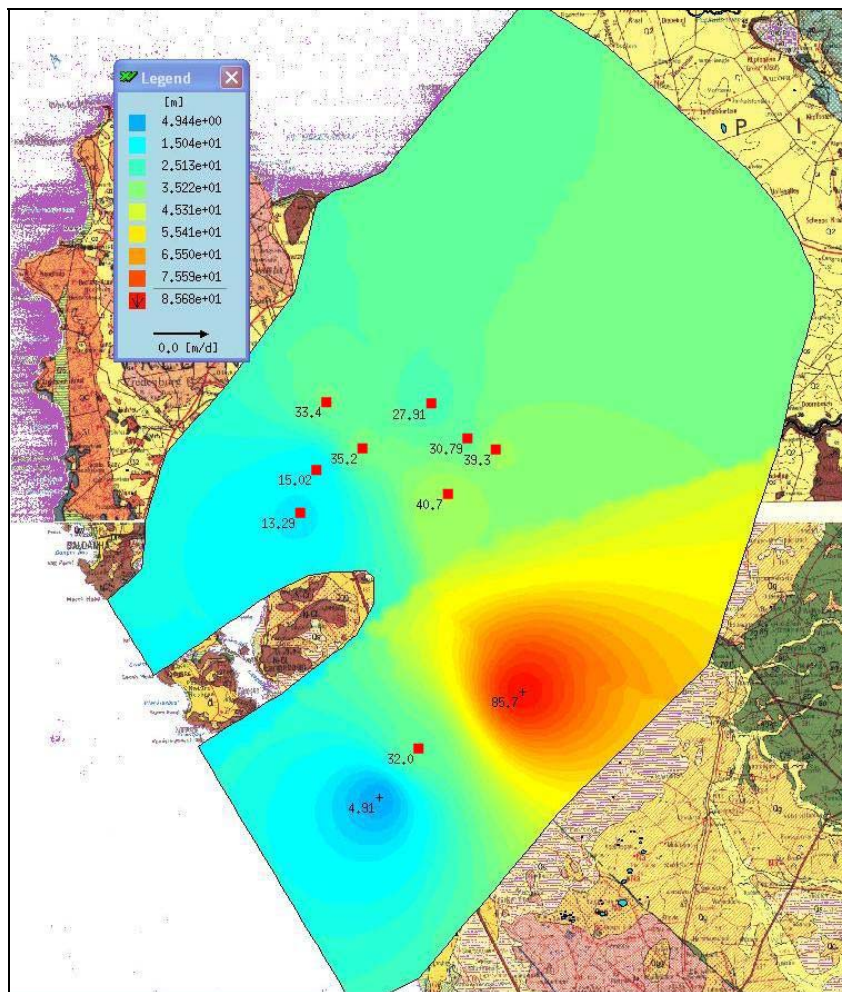


**Figure 6-3 LAU observation points.**

*The steady-state observation points which also act as transient observation points are highlighted in red squares. The figure shows the data points used in the calibration and a colour field of the water level surface interpolated from these points. This does not represent a true water level surface of the aquifer. It is based on these points only and simply included for display of the calibration data. The 1:250 000 geology map is used as the backdrop for orientation.*

The steady-state simulation is concerned with absolute water levels. The transient simulation is focussed on generating the observed variations in water level. Also, using averaged rainfall data it is not possible to recreate features in the observed water level data such as certain years of higher recharge in response to higher than average rainfall. Typical 1-year variations are of more relevance to calibration.

The water levels for each borehole record were analysed to manually determine a typical year's variation. A mean average annual variation was calculated from each year's annual rise in water levels. This mean is shown as lines in **Figure 6-4**. For transient observation points that are made up of more than one borehole record, an average was taken from each of the individual borehole averages.

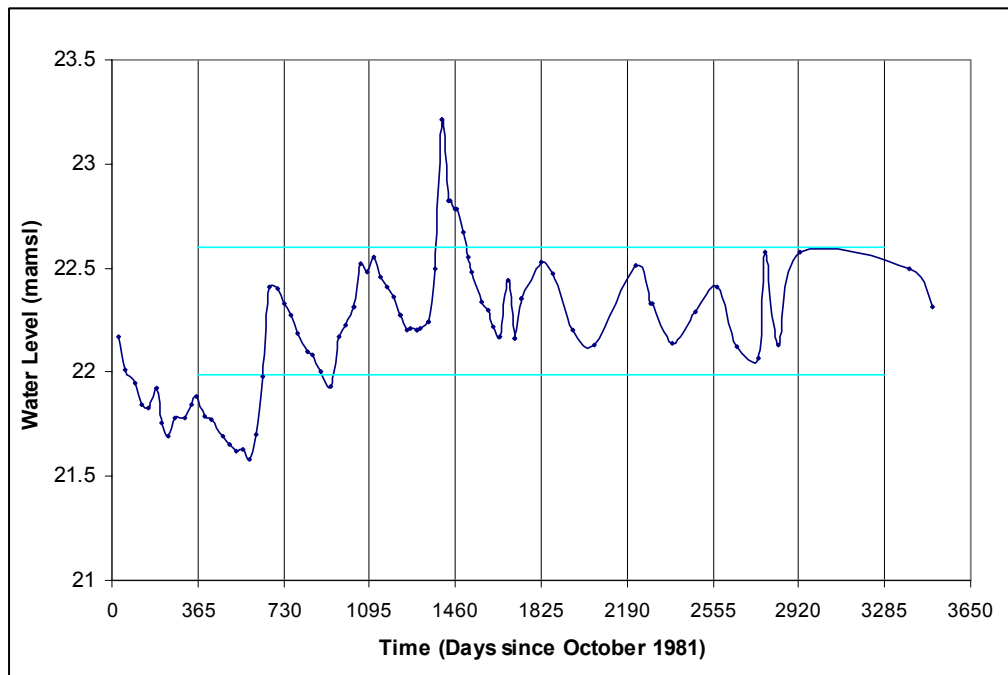


**Figure 6-4 Observed water level variations at borehole from observation point T1.8, in the UAU.**

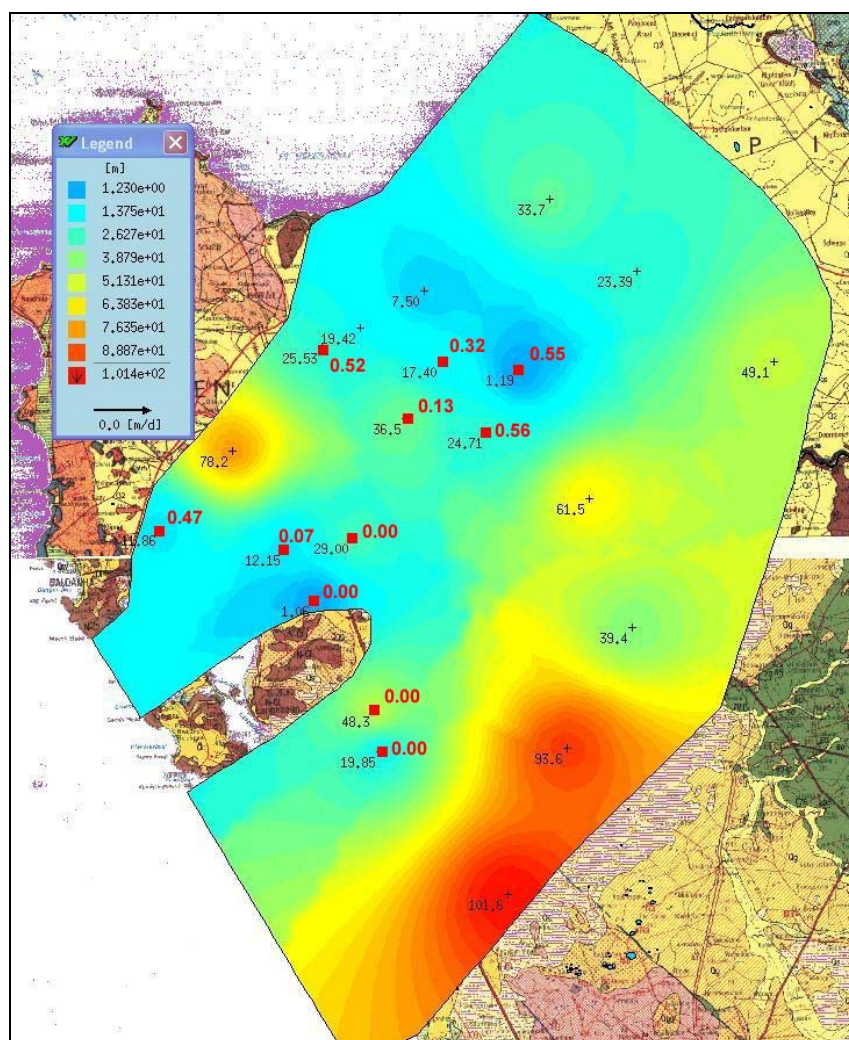
*Record exists for 1981 – 1990, and also 2001-2005. Years 1981-1989 are shown. Figure shows that water level peaks occur around October.*

A summary of the calibration-point data is shown in **Table 6-3** below. The observed data shows that typical annual variations average across the area to ~0.18 m in the LAU and slightly higher, 0.24 m, in the UAU. The range in observed variations is high; 0-0.56 m in the UAU, and 0-0.45 m in the LAU. The fluctuations are likely to be lower on average in the LAU due to the damping caused by the confining pressure. The data sets vary in their typical responses. Some records show clear annual fluctuations. Others, in both the LAU and UAU, appear to carry no imprint of the seasonality of the recharge and are either steadily decreasing over time (the majority of those which don't show fluctuation decrease) or are fairly constant in water levels, or a few even rise steadily. Different responses occur in the same years in different places suggesting a highly heterogeneous system. The majority of the later records for both aquifers (2000 onwards) show a gradual decrease in water levels either with or without the imprint of seasonality.

**Table 6-3 Observed annual water level variations at observation points**

Calibration point		Steady-state WL	Number of boreholes	Typical annual variation
Upper Aquifer	T1.1	1.06	1	0.00
	T1.2	1.19	1	0.55
	T1.3	11.86	2	0.47
	T1.4	12.15	2	0.07
	T1.5	17.40	2	0.32
	T1.6	19.85	1	0.00
	T1.7	24.71	1	0.56
	T1.8	25.53	3	0.52
	T1.9	29.00	1	0.00
	T1.10	36.51	1	0.13
	T1.11	48.30	1	0.00
			<b>Average</b>	<b>0.24</b>
Lower Aquifer	T2.1	13.29	2	0.00
	T2.2	15.02	1	0.21
	T2.3	27.91	3	0.09
	T2.4	30.79	1	0.44
	T2.5	32.00	3	0.00
	T2.6	33.42	1	0.42
	T2.7	35.16	1	0.00
	T2.8	39.27	5	0.00
	T2.9	40.69	1	0.45
			<b>Average</b>	<b>0.18</b>

There is a weak trend in the aerial distribution of the types of time-series response (**Figure 6-5** and **Figure 6-6**). In both aquifers, observation points closer to the Berg River tend to have a higher magnitude of average annual fluctuation. The annual fluctuations decrease towards Saldanha Bay and the lowest (zero fluctuation) are from observation points generally more SW than other points. This trend is weaker in the lower aquifer than the upper. This trend may reflect the seasonal influence of the Berg River, but could also be caused simply by points further to the SW having a higher volume of upgradient aquifer to them and thus their seasonal variations will be damped.



The steady-state observation points which also act as transient observation points are highlighted in red squares. The magnitude of the averaged annual variation in water level is shown in red text at each point. The colour field of the water level surface is interpolated from the steady-state water level at the points. This does not represent a true water level surface of the aquifer; it is based on these points only and simply included for display of the calibration data. The 1:250 000 geology map is used as the backdrop for orientation.

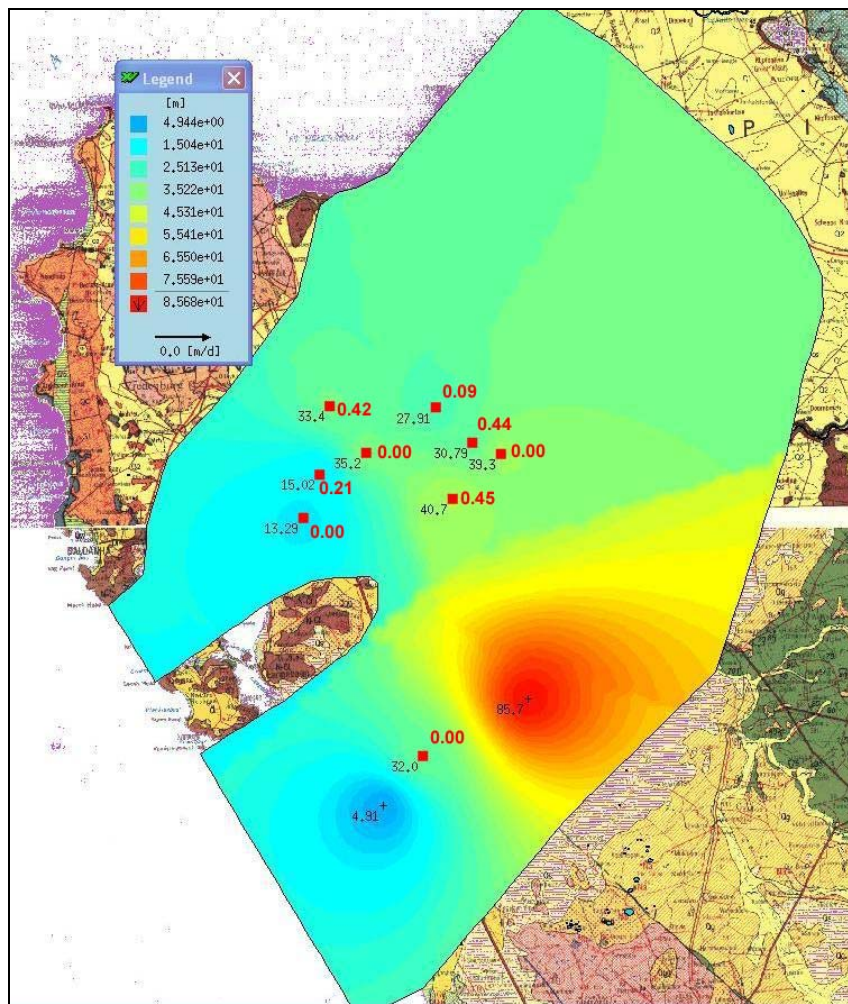


**Figure 6-6 Distribution of annual variation in water levels, LAU**

The steady-state observation points which also act as transient observation points are highlighted in red squares. The magnitude of the averaged annual variation in water level is shown in red text at each point. The colour field of the water level surface is interpolated from the steady-state water level at the points. This does not represent a true water level surface of the aquifer; it is based on these points only and simply included for display of the calibration data. The 1:250 000 geology map is used as the backdrop for orientation.

The majority of the NGDB water level records are monthly. Out of those records that do show the seasonal peaks, the timing of the recharge peak varies between July to December within some records and between. There is no notable delay in the peak in the LAU as compared to the UAU.

The transient model runs are calibrated to the average typical annual variation (bold in **Table 6-3**). The error reported for model runs is the observed typical variation minus the modelled variation (**Table 6-4**). The calibration standard set was to attain the observed variation to within 20% of its value:

- $(\text{Modelled variation} / \text{Observed typical variation}) \times 100 = 80\text{-}100\%$

This numerical approach allowed for a broad indication of how well the model run fitted the observed data. In addition, the distribution of the variations were taken into account and the distribution of the variations for each model run were analysed.

## 6.7 MODEL RESULTS

### 6.7.1 Parameter Calibration: Storage

The procedure for the calibration of the storage was to test the model response with the upper and lower bounds of the parameters shown in **Table 6-2** above, and from these results, narrow down the range of possible applicable values. The results of the calibration are shown in **Table 6-4** below (the table is presented in increasing order of Sy, not the order modelled).

**Table 6-4 Results for calibration of Sy**

*Error refers to (observed typical variation – modelled variation), averaged over the points. Range refers to the maximum – minimum error within the points.*

		Observed	Sy			
			0.2	<b>0.02</b>	0.01	0.002
UAU	Average 1 year fluctuation (m)	0.24	0.02	<b>0.22</b>	0.42	1.50
	Error (m)	N/A	0.22	<b>0.01</b>	-0.18	-1.26
	Range (m)	0 - 0.56	0.01-0.03	<b>0.17 - 0.36</b>	0.30 - 0.74	0.93 - 2.52
	Modelled variation as % observed	N/A	9	<b>94</b>	177	634
LAU	Average 1 year fluctuation (m)	0.18	0.06	<b>0.18</b>	0.30	0.70
	Error (m)	N/A	33.96	<b>103.43</b>	165.73	391.59
	Range (m)	0 - 0.45	0.01-0.16	<b>0.15 - 0.24</b>	0.25 - 0.41	0.60 - 0.95
	Modelled variation as % observed	N/A	34	<b>103</b>	166	392

A Specific Yield of 0.02 generates an averaged fluctuation that is well within the calibration standard. A Sy value of 0.02 replicates the averaged trend to within 2 cm in the UAU, and to within less than 1 cm in the LAU. The lower magnitude of variations in the LAU as compared variations with the UAU is replicated, but the range of the modelled variations is lower than the observed in both aquifers. The model does not reproduce those variations at the extreme (0 m or 0.5 m variation). A possible reason for the seasonal variations to be dampened in the model is that the real impact of the river is not replicated, because of the scale of the model versus the scale of the process, and because the nature of the seasonal flooding is not replicated on monthly time scales.

The distribution of the modelled variations loosely correlates to the observed: the highest variations are seen closer to the Berg River. **Figure 6-7** below shows a plot of the average fluctuations for modelled against observed, for the data set generated by the model run is Sy at 0.02. This shows that the points with the highest observed variations (which are generally closer to the Berg River) are also some of the higher modelled variations. This correlation exists for a few points – and more so in the LAU. The data is skewed by the observed points which show no variation, which has not been replicated. The reduced range of the modelled data is clear.

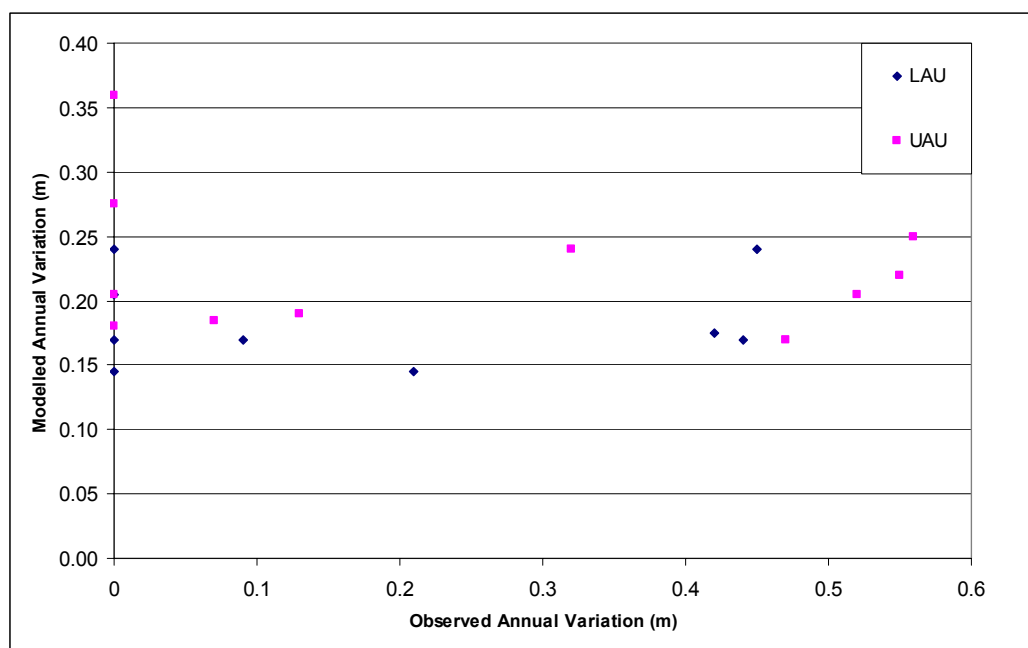


**Figure 6-7 Correlation between observed and modelled annual fluctuations specific yield (Sy is 0.02).**

The model is considered calibrated with a Sy of 0.02. This is low compared to typical Sy for sands and is closer to that of limestone or clay (**Table 6-2**). The modelled Sy represents an equivalent Sy and is reflecting the effect of the clay layers on the retention of water and the speed of release of water.

#### 6.7.2 Modelled water level variations

The specific yield Sy affects the magnitude of the variation. The lower the Sy the higher the variation in water levels (clear in **Table 6-4**). The timing of the *water level* peak and the steepness of the peak are controlled by the recharge curve. The modelled rise in water levels, and the modelled peak, occur at very similar times to the observed. This suggests that the recharge curve is an accurate representation of the real system, and that rainfall in the summer months does not contribute to recharge.

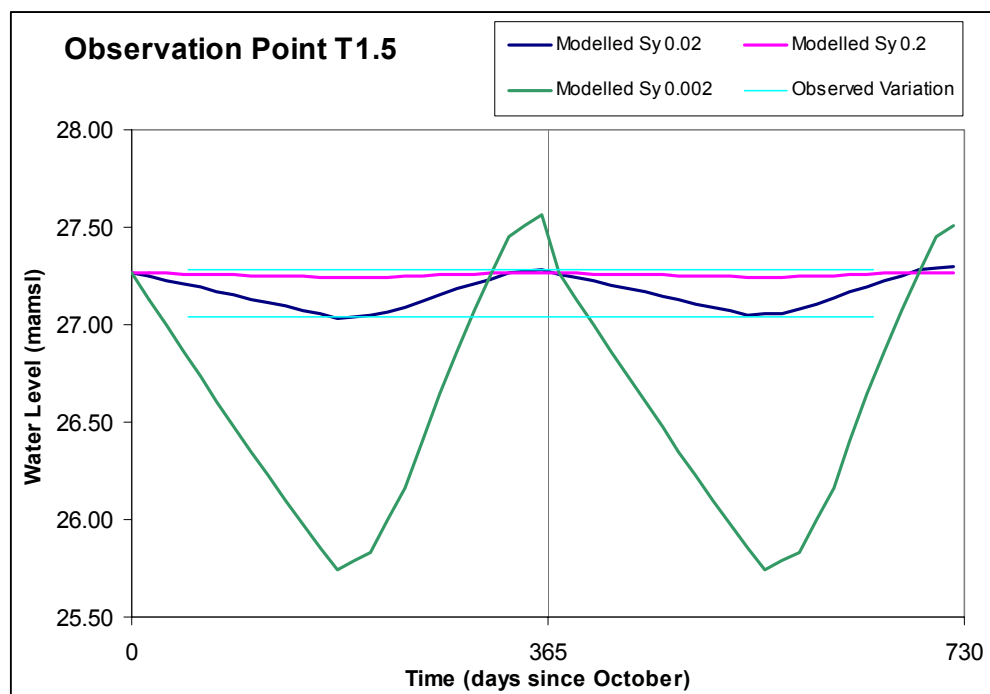


**Figure 6-8 Modelled water levels**

### 6.7.3 Mass balance

The modelled fluxes for monthly periods are shown in **Table 6-5** and **Figure 6-9**. The winter recharge flux is accommodated by an increase in flux to the ocean and an increase in the net flux to surface water (negative increase in **Figure 6-9**). As water levels rise in response to recharge, the difference between the head in the river and that in the aquifer increases, and so the flux to surface water increases. The balance shows the sum of the monthly fluxes. During winter more water enters the aquifer than discharges, generating a positive balance. During the summer months, more water discharges than enters the aquifer.

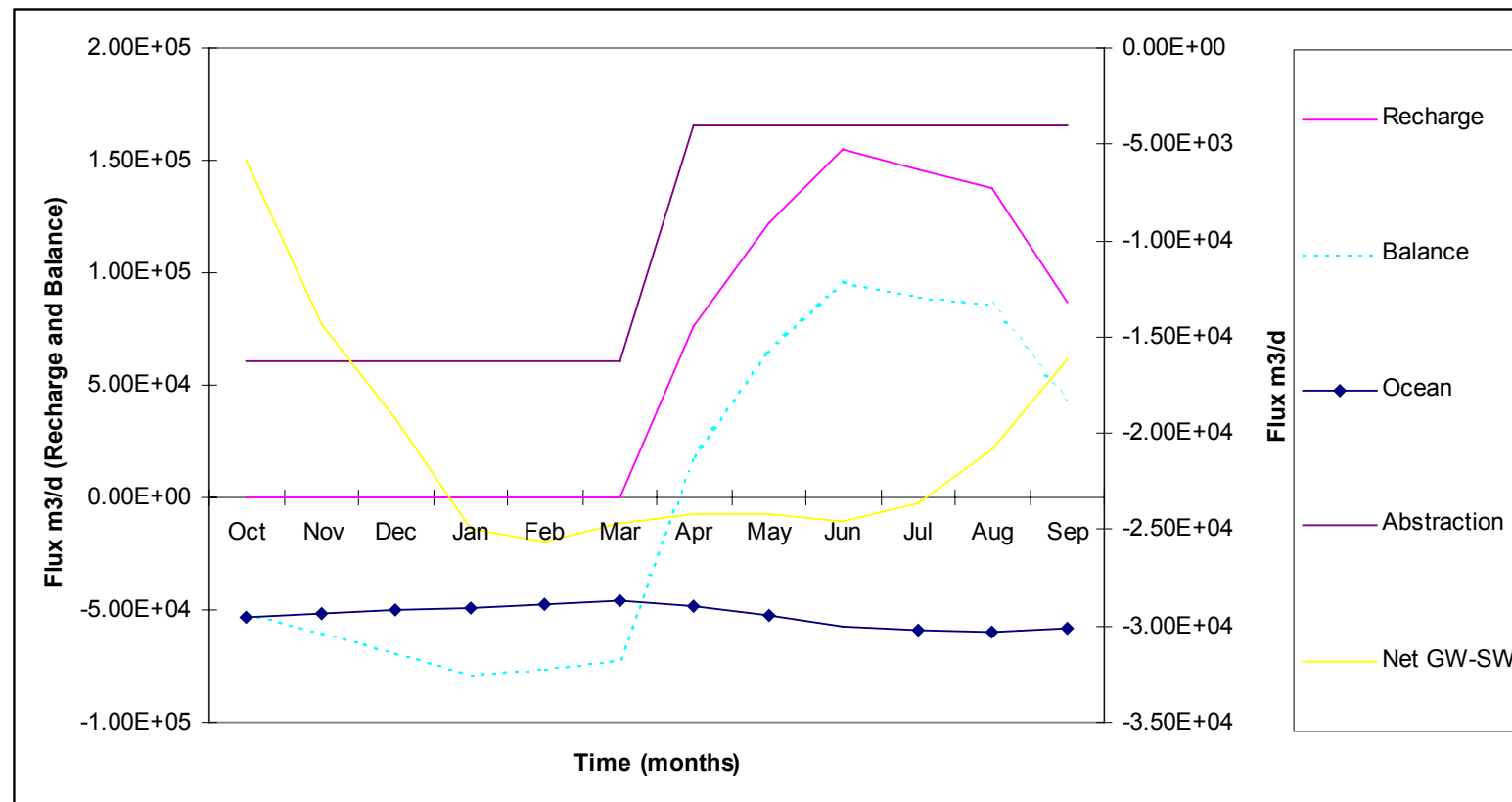
The balance shows an annual loss of water from the system (representing 1% of the total influx or outflux of the model). Although the abstraction is less than the recharge, the natural outflows to the ocean and Berg River dominate the discharge.

**Table 6-5 Monthly fluxes**

Month	Month	Influx m³/a		Discharge m³/a			Net GW- SW	Balance
		Recharge	SW to GW	Ocean	Abstraction	GW to SW		
1	October	0	0	-29639	-16212	-34357	-34357	-80208
2	November	0	0	-29362	-16212	-31266	-31266	-76840
3	December	0	0	-29150	-16212	-27417	-27417	-72778
4	January	0	0	-28977	-16212	-24591	-24591	-69779
5	February	0	0	-28825	-16212	-23194	-23194	-68230
6	March	0	0	-28686	-16212	-22923	-22923	-67821
7	April	75847	0	-28981	-4000	-20560	-20560	22306
8	May	122463	0	-29467	-4000	-15296	-15296	73700
9	June	154638	44	-29972	-4000	-8672	-8628	112038
10	July	145860	73	-30219	-4000	-6519	-6446	105196
11	August	137364	23	-30387	-4000	-15473	-15450	87528
12	September	86941	0	-30157	-4000	-24485	-24485	28299
Annual (Mm³/a)		21.69	0.004	-10.61	-3.64	-7.64	-7.64	-0.20
Total (Mm³/a)							N/A	
		Influx		Discharge				
		21.70		-21.90				
Contribution to total influx / discharge, as percentage		100	0	48	17	35	35	1

Positive fluxes are influxes to the aquifer, negative fluxes are aquifer discharges.

¹Given as percentage of total discharge

**Figure 6-9 Monthly fluxes**

---

#### **6.7.4 Groundwater – surface water interaction**

At the regional scale the aquifer discharges to the Berg River, which the model replicates (**Table 6-5**).

The river does not recharge the aquifer in the model because the regional gradient towards the river is too great. Surface- groundwater interactions is a multi-scale phenomena which this model does not replicate. The small amount of modelled influx from the Berg River occurs towards its mouth due to assumption that some seasonal variation exists long the length of the Berg River. Flooding events which can induce recharge to the aquifer, are not replicated here in the monthly averaged river stage variations.

## 7. SCENARIO TESTING

### 7.1 SCENARIO 1: SENSITIVITY TO RAINFALL

The recharge calculations for steady-state and transient models are based on a heterogeneous rainfall distribution; the modelled Berg WAAS rainfall (section 2.2 above, and Volume 2 of this series, DWAF, 2007a). This data is an averaged representation and has no dependence on time or reflection of variation from mean.

There is one rainfall station in the model area, near Hopefield, which has records from 1927 to 2003. The annual mean from this station is shown in **Figure 2-3**. The annual variation from the mean at this station is up to 40%: the year with the minimum annual rainfall is 36% less than the mean and the maximum year is 40% more than the mean.

This degree of variability from a typical rainfall mean was assumed applicable to the whole model area. To test the sensitivity to rainfall (and therefore recharge because there is a linear relationship in the model) the recharge was increased and decreased by 35% in all areas.

The resulting monthly mass balance, for one year's duration, with 35% increased recharge is shown in **Table 7-1** below. Comparing this to the mass balance for the "base case" (**Table 6-5**) shows that the additional recharge inflow causes the outflow to the ocean and surface water to increase. However over one year most of the additional water (an additional 7.55 Mm³/annum of recharge) is retained in the model as storage. This is shown in the balance column (**Table 7-1**). The influx exceeds the flux of the model by 6.8 Mm³/annum and this water is distributed as water- level rise. The travel time of water in the system is therefore largely in excess of 4 year.

With a decrease in recharge the system responds similarly (**Table 7-2**). The flux to the ocean and to surface water are more or less maintained by drawing from storage (compare **Table 7-2** and **Table 6-5**). The behaviour shown by these two runs suggests that the system is slow to respond to changes in recharge. The large decrease in the influx is not equilibrated by a decrease in the outflux. The flux remains the same and the effect being a reduced water level.

**Table 7-1 Mass balance for increased recharge**

Month	Month	Influx m³/a		Discharge m³/a			Net GW- SW	Balance
		Recharge	SW to GW	Ocean	Abstraction	GW to SW		
1	October	0	0	-30232	-16212	-35105	-35105	-81549
2	November	0	0	-29904	-16212	-31893	-31893	-78008
3	December	0	0	-29659	-16212	-27978	-27978	-73849
4	January	0	0	-29463	-16212	-25106	-25106	-70781
5	February	0	0	-29293	-16212	-23672	-23672	-69177
6	March	0	0	-29139	-16212	-23373	-23373	-68724
7	April	102117	0	-29551	-4000	-21157	-21157	47409
8	May	165075	0	-30217	-4000	-16130	-16130	114729
9	June	208530	41	-30920	-4000	-9728	-9687	163923
10	July	196675	72	-31287	-4000	-7642	-7571	153817
11	August	185201	11	-31545	-4000	-16691	-16680	132975
12	September	117100	0	-31281	-4000	-25800	-25800	56019
Annual (Mm³/a)		29.24	0.004	-10.87	-3.64	-7.93	-7.92	6.80
Total (Mm³/a)							N/A	
		Influx		Discharge				
		29.24		-22.44				
Contribution to total influx / discharge, as percentage		100	0	48	16	35	35	-30

**Table 7-2 Mass balance for decreased recharge**

Month	Month	Influx m³/a		Discharge m³/a			Net GW-SW	Balance
		Recharge	SW to GW	Ocean	Abstraction	GW to SW		
1	October	0	0	-29048	-16212	-33594	-33594	-78853
2	November	0	0	-28827	-16212	-30628	-30628	-75667
3	December	0	0	-28650	-16212	-26845	-26845	-71706
4	January	0	0	-28502	-16212	-24066	-24066	-68780
5	February	0	0	-28369	-16212	-22705	-22705	-67286
6	March	0	0	-28246	-16212	-22464	-22464	-66921
7	April	49168	0	-28396	-4000	-19953	-19953	-3182
8	May	79480	0	-28668	-4000	-14453	-14453	32360
9	June	100403	54	-28961	-4000	-7598	-7544	59898
10	July	94695	104	-29099	-4000	-5380	-5276	56321
11	August	89171	42	-29186	-4000	-14233	-14191	41794
12	September	56382	0	-29020	-4000	-23155	-23155	207
Annual (Mm³/a)		14.08	0.006	-10.35	-3.64	-7.35	-7.35	-7.25
Total (Mm³/a)							N/A	
		Influx		Discharge				
		14.08		-21.34				
Contribution to total influx / discharge, as percentage		100	0	48	17	34	34	34

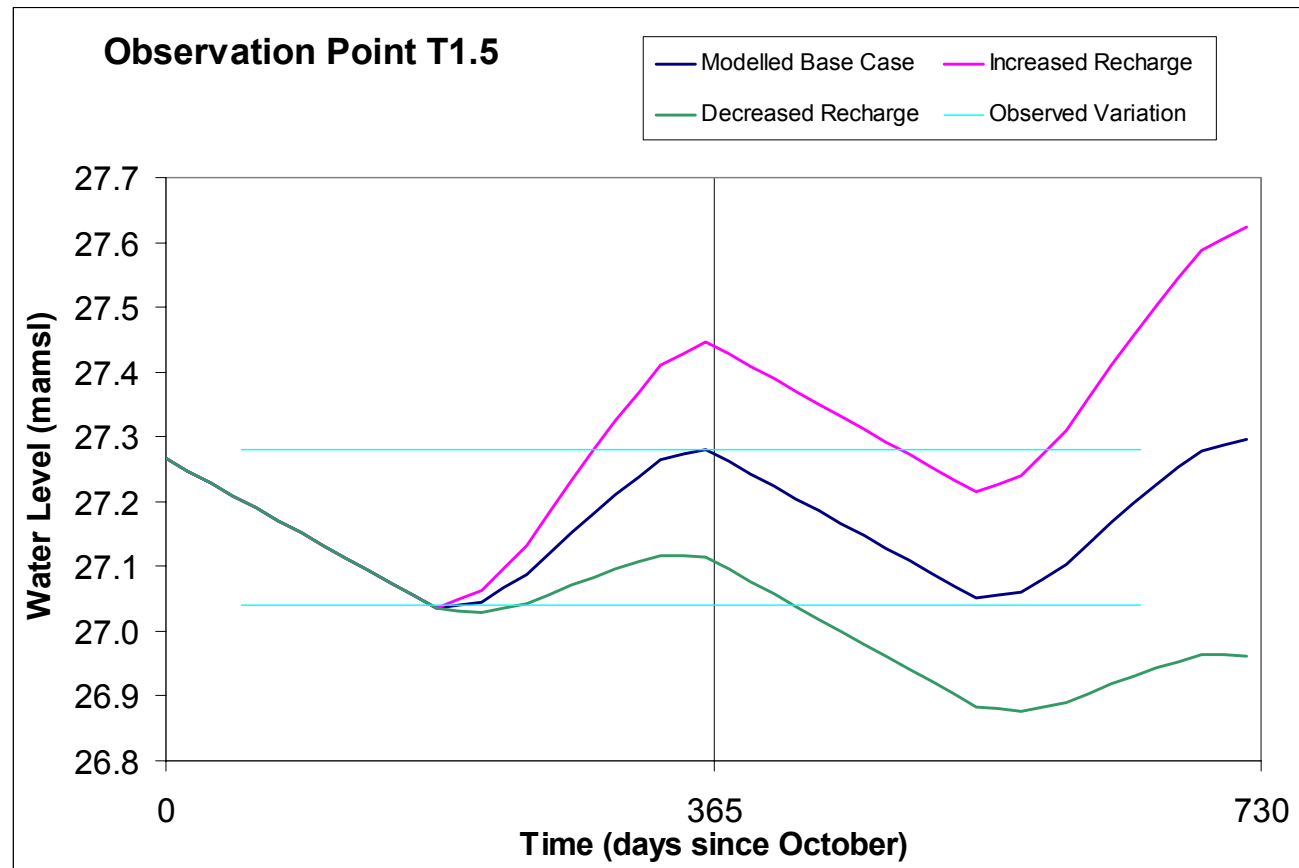


**Figure 7-1 Water level variation under increased and decreased recharge, at T1.5**

*The water level variation for the natural system ("base case") is shown for comparison.*

## 7.2 SCENARIO 2: UTILISATION OF THE LRAS/ EAS TO AUGMENT THE WATER SUPPLY TO THE WEST COAST MUNICIPALITY

### 7.2.1 Scenario 2.1 The West Coast Wellfield

The modelled effect of the West Coast District Municipality (WCDM) wellfield on regional water levels is shown in section 5.7 (**Figure 5-8, Figure 5-9, Table 5-3**). Woodford et al (2003) suggested that the sustainable yield from the LAU in the LRAS was 1.5 Mm³/annum, which is equivalent to the current abstraction at the WCDM wellfield. However decreasing water levels (which occur in the UAU and LAU) are observed and suggest that the current abstraction is potentially exceeding the sustainable yield of the aquifer, especially as the decrease is more common in records since 2000. Supporting this is the fact that there is also a loose spatial pattern in the distribution of those records that show a decrease and those which do not. Points on the periphery of the aquifer (ie close to the NW model boundary) do not show the decrease. Woodford et al (2003) report that water levels in two of the 4 abstraction boreholes have declined by 10 m since opening of the wellfield in ~2000.

Of the 8 observation points selected for the LAU in the LRAS, only 5 have observation data continuous after ~2000. Each of these 5 boreholes show a declining water level to varying degrees after this time, as shown in **Table 7-3**. Although the nearest point to the wellfield is T2.3, it is outside of the main palaeochannel. The point T2.7 is the nearest point within the palaeochannel and shows the largest decrease.

Prior to 2000 the observed water levels in some observation points showed large increases and decreases from the mean over time, responding to extended periods of lower or higher rainfall. For example one borehole at the point T2.8 rose by 1 m between 1988-1980. It is therefore difficult to be sure that all of the observed decreases in water levels are due to abstraction and not a natural fluctuation, however since the abstraction boreholes have shown a 10 m decline, it is clear abstraction is (was) having some effect within the wellfield domain.

The current data at the wellfield however apparently shows that the LAU water levels have been stable since 2003. Water levels in the UAU at the wellfield and beyond have shown a mixed trend since 2003, some stabilising, some rising due to high rainfall in the last 2 years, and some still declining (P. Seward pers comm., August 2008). The declining water levels in the UAU are not thought to be related to the WCDM wellfield (P. Seward pers comm., August 2008).

**Table 7-3 Observed water level decline in LAU since 2000**

(See **Figure 6-3** for orientation of the points. Two values are given for the observation point T2.1 because of the two boreholes making up this grouped point. Both had observation data post 2000 )

Observation Point	Observation Point SS Water Level (mamsl)	Observed fall in average water level since 2000 (m)
T2.8	39.3	1.0
T2.3	27.91	0.8
T2.7	35.16	2.5
T2.6	33.42	0.5
T2.2	15.02	1.5
T2.1	13.29	0.1 and 0.45

The observed decrease in water levels show clearly that the current abstraction is affecting the regional water table. Whether the current abstraction is above the sustainable yield however is a question of correct management of the aquifer at a wellfield scale. In the current situation the demand is being taken from storage, not from annual recharge. This practice is certainly sustainable if correctly managed over the natural cycle of the aquifer. During years of lower recharge, the storage is tapped into. During years of higher recharge, this recharge feeds the abstraction, and replenishes the deficit in the storage.

## 7.2.2 Scenario 2.2 Alternative Wellfield

The palaeochannel of the Elandsfontein Aquifer System is deeper than the LRAS and relatively under developed. The effects of a hypothetical wellfield in the EAS were tested. The mass balance results are shown in **Table 7-4** and the wellfield position in **Figure 7-2**.

The hypothetical wellfield abstracts  $0.7 \text{ Mm}^3/\text{annum}$  distributed between 4 boreholes. This is half of that abstracted at the WCDM wellfield. The mass balance shows that the increased abstraction causes the system to lose a greater quantity of water than the current situation (compare **Table 7-4** and **Table 6-5**). This indicates that the wellfield is supplied from storage. It is likely that a quasi steady-state could be reached where the affected water levels in the area decrease to an equilibrium that is simply a slightly lower water level than what it is currently. How much this water level is, would have to be tested in a local wellfield optimisation model.

The hypothetical wellfield has no effect on the fluxes of groundwater to the Berg River. The flux from groundwater to the river remains the same as it is for the base case. Many factors give this response, for example the low abstraction rate, but most significantly it is because the position of the wellfield is south of the flow divide on the crest of the recharge mound (**Figure 7-2**). The cross section of water levels shows that within ~5 km upstream (NE) of the hypothetical wellfield, the effect of the wellfield is negligible. The effect extends to only 2.5 km downstream of the wellfield, which is at least 7.5 km from the Langebaan Lagoon. The potential for saline intrusion under this regime is negligible due to the distance from the coast and the high water levels.

**Table 7-4 Scenario 2.2 Additional wellfield mass balance**

Month	Month	Influx m³/a		Discharge m³/a			Net GW-SW	Balance
		Recharge	SW to GW	Ocean	Abstraction	GW to SW		
1	October	0	0	-29639	-18212	-34357	-34357	-82207
2	November	0	0	-29362	-18212	-31266	-31266	-78839
3	December	0	0	-29149	-18212	-27417	-27417	-74777
4	January	0	0	-28976	-18212	-24591	-24591	-71779
5	February	0	0	-28824	-18212	-23194	-23194	-70229
6	March	0	0	-28684	-18212	-22923	-22923	-69820
7	April	75847	0	-28980	-6000	-20560	-20560	20308
8	May	122463	0	-29465	-6000	-15296	-15296	71702
9	June	154638	44	-29970	-6000	-8672	-8628	110040
10	July	145860	73	-30216	-6000	-6519	-6446	103199
11	August	137364	23	-30384	-6000	-15473	-15450	85530
12	September	86941	0	-30153	-6000	-24485	-24485	26302
Annual (Mm³/a)		21.69	0.004	-10.61	-4.36	-7.64	-7.64	-0.92
Total (Mm³/a)							N/A	
		Influx		Discharge				
		21.70		-22.61				
Contribution to total influx / discharge, as percentage		100	0	47	19	34	34	4

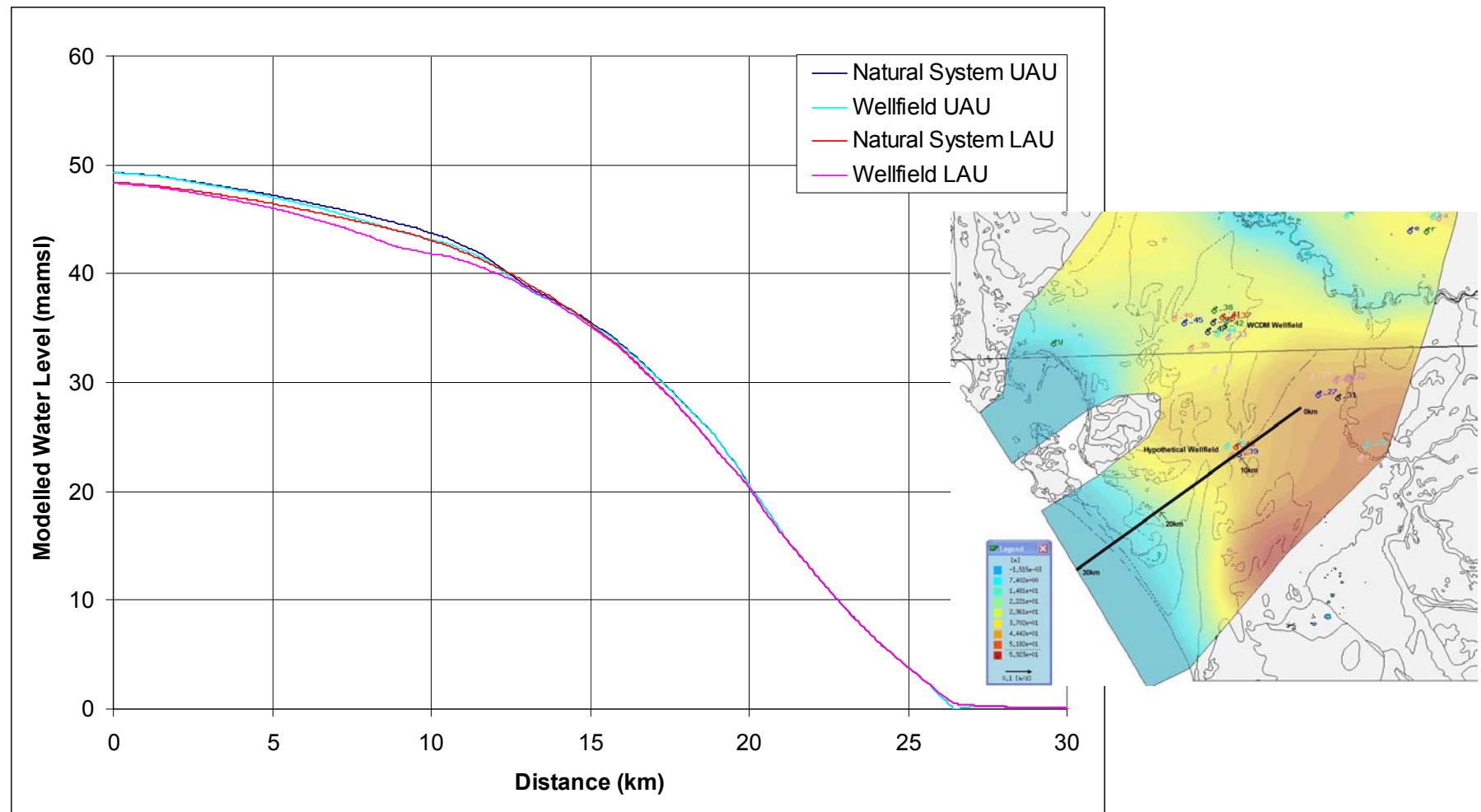


**Figure 7-2 Water levels under scenario 2.2 additional wellfield**  
(Graph plotted from NE to SW)

### 7.3 YIELD ESTIMATION

The modelled data and the observed data suggests that the WCDM wellfield currently affects regional water levels and requires careful management to ensure the depletion of storage is replenished, or its effects are minimised.

The steady-state calibrated recharge is 21.69 Mm³/a. Using the modelled recharge, the total available yield is:

Total yield = Recharge 21.69 Mm³/annum – current abstraction 3.64 Mm³/a = 18.05 Mm³/a.

The potential for an additional abstraction exists in the currently under exploited EAS palaeochannel. The scenario tested here (section 7.2.2 above) shows that abstraction of ~0.7Mm³/a from the LAU close to the head of the EAS has minimal effect on fluxes to surface water and to the ocean. A smaller scale wellfield model would be required to optimise the abstraction and predict the sustainable yield over the long-term.

### 7.4 SCENARIO 3 RIVER FLOOD EVENTS

Whether the Berg River gains from groundwater, or is a source to it, depends on the relative difference in heads of water between the river and surrounding groundwater. The river stages in the model are assigned based on the topography at the Berg River (from 1:50,000 topo sheets and 100 m scale DEM), and the modelled water table surface is calibrated to observed (within 10.3 m UAU and 5.6m LAU). It is interpreted that the true time-averaged hydraulic gradient between surface water and groundwater is replicated in the model (time averaged over one year because the rainfall and therefore recharge is based on an average precipitation, excluding high rainfall years for example). Under these averaged conditions the gradient towards the river is strong enough that the river is a permanent sink for the groundwater (in this model at this scale). The mass balance shows that a minimal amount of water enters the model cells from the river only in the months of June, July and August.

It is a common notion that the Berg River feeds the groundwater, especially during flood events. It may be difficult to see how this strong gradient would ever be reversed even if the river stages increased by metres. For example observed groundwater levels are ~36.5, 24.71 and 17.4 mamsl southwest of the Berg River (**Figure 5-1**), dropping to <5 mamsl at the river due NE of these points. However SW-GW interaction is a multi scale process. The regional gradient, as illustrated by this observation data, will be towards the Berg River (illustrated in the base case, section 6.3.3). During flood events the regional gradient will continue to be towards the Berg River, but locally the river stage may rise above the local groundwater levels, shifting the low point (or the sink) from the centre of the river to the land. Between this low point and the river, the flow direction is reversed from surfacewater to groundwater.

The effect of flood events was tested in the model. For the standard situation river stage fluctuation, the mean of the monthly river stages were used (section 6.3). To replicate a year with high river stages, the monthly data within the year with the maximum summed river stages over the data period was used. The records contain mean, maximum and minimum monthly data and showed a maximum river stage during June. This was entered as the mean for the whole of June to replicate an extended flood period, within a year of high levels. Again, the

---

numbers were converted to variations from a mean so as to be applied to the modelled river stages.

The results show much higher flux from surfacewater to groundwater extending from June to September (**Table 7-5**). During June the gradient is from surfacewater to groundwater along the total length of the Berg River. Water levels inland remain higher than the river stages and the regional flow directions are unchanged; the annual fluxes are similar to averaged years (in  $\text{Mm}^3/\text{annum}$  in **Table 6-5** and **Table 7-5**). The model is therefore replicating what is understood of the system in theory. Because the interaction is a multi-scale process however, additional small-scale modelling would be required to increase confidence in the numbers generated. In the same way that the model cannot predict water levels in the abstraction wells themselves, on the local scale of a few km from the river, the model cannot detect the small changes in water levels.

**Table 7-5 Mass balance under river flood event**

Month	Month	Influx m³/a		Discharge m³/a			Net GW- SW	Balance
		Recharge	SW to GW	Ocean	Abstraction	GW to SW		
1	October	0	0	-29646	-16212	-20876	-20876	-66733
2	November	0	0	-29407	-16212	-34105	-34105	-79724
3	December	0	0	-29168	-16212	-37121	-37121	-82501
4	January	0	0	-28989	-16212	-35724	-35724	-80925
5	February	0	0	-28834	-16212	-27917	-27917	-72964
6	March	0	0	-28694	-16212	-26081	-26081	-70986
7	April	75847	0	-28988	-4000	-23717	-23717	19142
8	May	122463	0	-29475	-4000	-25705	-25705	63283
9	June	154638	12295	-29967	-4000	0	12295	132966
10	July	145860	60	-30233	-4000	-9238	-9178	102450
11	August	137364	30	-30400	-4000	-18065	-18035	84929
12	September	86941	6	-30171	-4000	-19278	-19272	33497
Annual (Mm³/a)		21.69	0.372	-10.62	-3.64	-8.33	-7.96	-0.53
Total (Mm³/a)							N/A	
		Influx		Discharge				
		22.07		-22.59				
Contribution to total influx / discharge, as percentage		98	2	47	16	37	35	2



## 7.5 SCENARIO 4 AQUIFER STORAGE RECOVERY SCHEME

The Aquifer Storage and Recovery scenario suggested by Woodford et al (2003) was simulated in the model to understand the effect of injection on the regional water balance and flow regime. The proposed scheme involves the injection of  $1.2 \text{ m}^3$  excess Berg River water over a 4-month winter period.

It was suggested that the  $1.2 \text{ m}^3$  be injected to 3-4 injection boreholes. This would require very large boreholes with injection rates of  $\sim 10,000 \text{ m}^3/\text{day}$  per borehole. This model is unable to accurately model the actual water level at the borehole, and therefore the number of boreholes is not important, just the absolute injection. To improve numerical stability the required injection was distributed over 10 boreholes each injecting at  $\sim 1000 \text{ m}^3/\text{d}$ . The boreholes were centred on the WCDM wellfield, in the centre of the cone of depression shown in **Figure 5-8**. River stages are at their maximum between June and September and so these months were used as the 4-month injection period. The regime at the WCDM wellfield remained unchanged.

The effect of the ASR on the monthly mass balance is shown in **Table 7-6** below. The fluxes to the ocean and to surface water are almost unchanged from the base case. The additional water has swung from a negative to a positive; i.e. the region gains water and water levels rise. But as with scenario 7.4, it is likely a new quasi steady-state would be reached over time and the outflows adjust to balance the system.

The effect of ASR on the water levels is shown in **Figure 7-3** and **Figure 7-4** below. The figures are shown for the end of September and reflect the highest water levels generated at the end of an injection period (i.e. the maximum effect of the ASR wells). **Figure 7-3** shows that the maximum effect of the injection, regionally, is an increase in water levels of  $\sim 1.5 \text{ m}$ . Again, this is the regional print and it is possible that small-scale wellfield modelling would reveal a larger effect at a local scale.

Whether this  $1.5 \text{ m}$  increase is important regionally is illustrated in **Figure 7-4**, which shows the water levels with and without the ASR scheme, compared with topography and basement. The elevation of Slice 3 is also shown, which is approximately the level of the top of the confining clay bed. The figures show that

- the cone of depression is well above the clay layer,
- the effect of the ASR is to increase the water levels by  $\sim 1.5 \text{ m}$ ,
- the increase in water levels is limited to within the extent of the cone of depression.

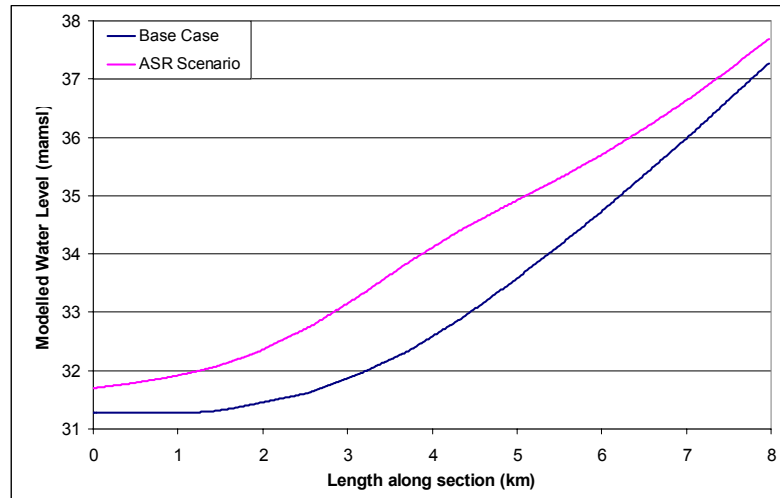
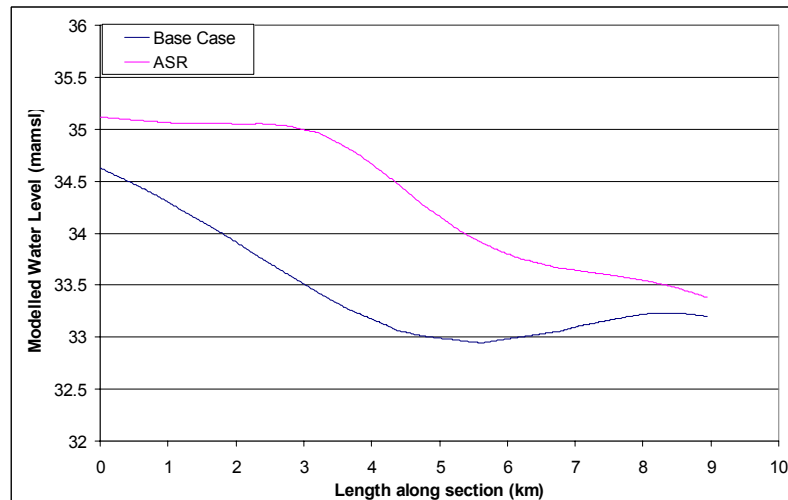
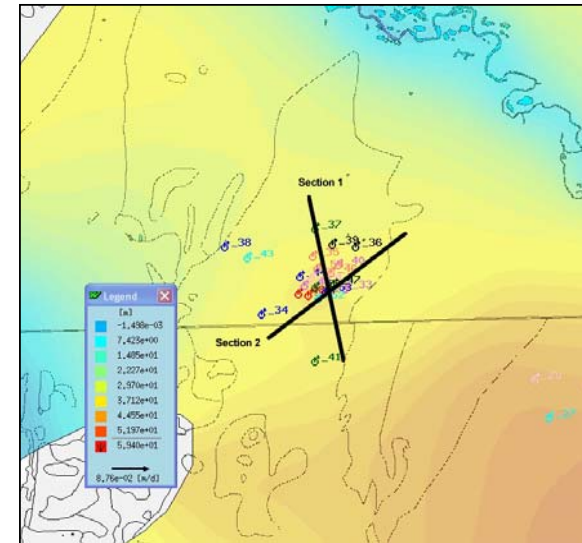
Cross section 1 in **Figure 7-4** shows that the topography dips beneath the modelled groundwater levels in the north. This is considered a function of the scale. At the regional scale aerially small changes in gradient contributed by a topographically-driven flow cannot be replicated.

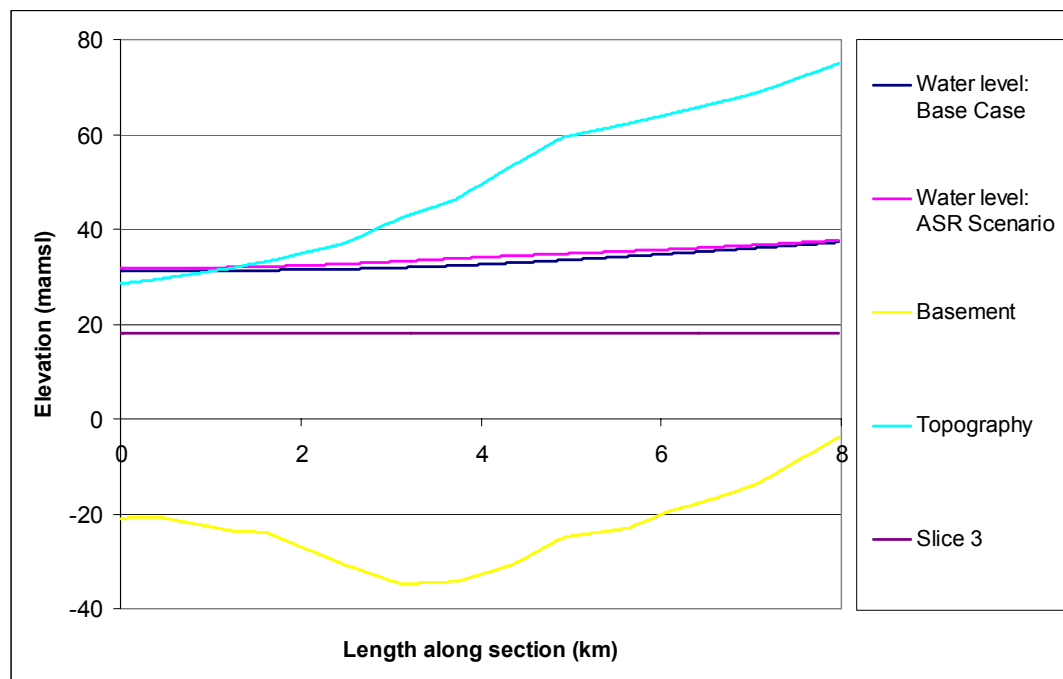
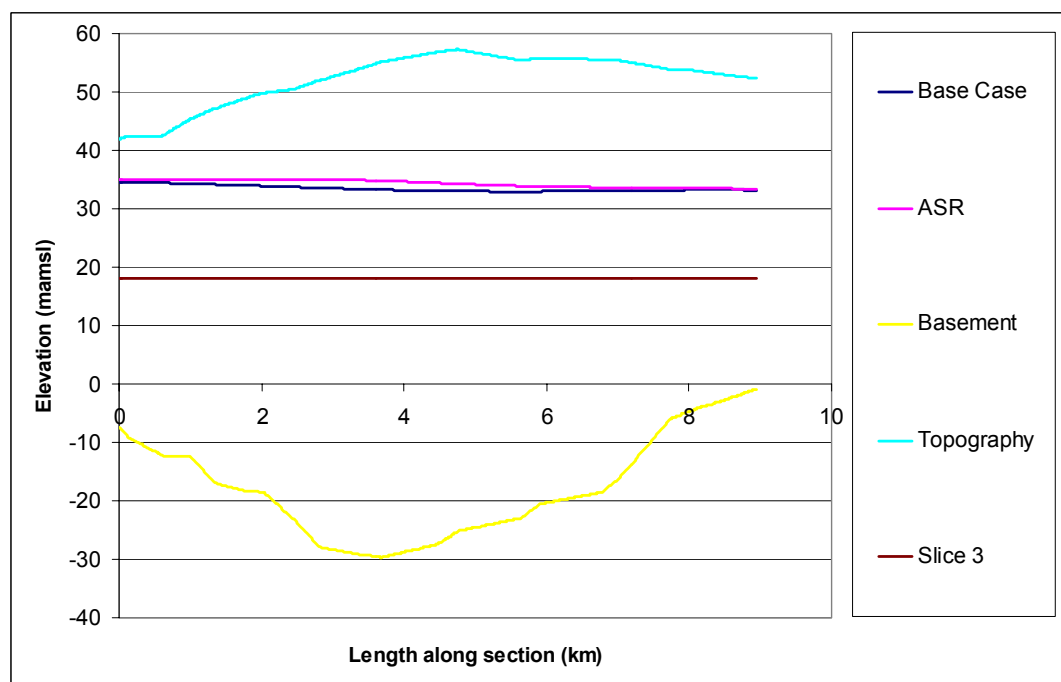
The simple model run conducted here suggests it is possible to inject large quantities of water with minimal regional effect.



**Table 7-6 Mass balance under Aquifer Storage and Recovery scheme**

Month	Month	Influx m³/a			Discharge m³/a			Net GW-SW	Balance
		Recharge	SW to GW	Injection	Ocean	Abstraction	GW to SW		
1	October	0	0	0	-29640	-16212	-34348	-34348	-80200
2	November	0	0	0	-29361	-16212	-31257	-31257	-76830
3	December	0	0	0	-29150	-16212	-27413	-27413	-72775
4	January	0	0	0	-28977	-16212	-24588	-24588	-69777
5	February	0	0	0	-28825	-16212	-23192	-23192	-68228
6	March	0	0	0	-28686	-16212	-22922	-22922	-67819
7	April	75847	0	0	-28982	-4000	-20558	-20558	22307
8	May	122463	0	0	-29467	-4000	-15295	-15295	73701
9	June	154638	44	9675	-29973	-4000	-8671	-8627	121714
10	July	145860	73	9675	-30219	-4000	-6453	-6379	114937
11	August	137364	24	9675	-30388	-4000	-15277	-15253	97398
12	September	86941	0	9675	-30158	-4000	-24463	-24463	37995
Annual (Mm³/a)		21.69	0.004	1.16	-10.61	-3.64	-7.63	-7.63	0.97
Total (Mm³/a)								N/A	
		Influx			Discharge				
		22.86			-21.89				
Contribution to total influx / discharge, as percentage		95	0	5	49	17	35	35	-4

**Water level cross section 1 (plotted from North to South)****Water level cross section 2 (plotted from SW to NE)****Position of wellfield cross-sections****Figure 7-3 Modelled water level for ASR scheme (small scale)**

**Water level cross section 1 (plotted from North to South)****Water level cross section 2 (plotted from SW to NE)****Figure 7-4 Modelled water level for ASR scheme (larger scale)**

## **8. CONCLUSIONS AND RECOMMENDATIONS**

### **8.1 SUMMARY OF INTERPRETATIONS**

The conceptual model developed here details a multi-layered aquifer system, extending over two separate palaeochannels. The southern palaeochannel system in the EAS, the northern is the LRAS. The lower gravel aquifer is disconnected between palaeochannel systems. The Lower Aquifer Unit (LAU) is overlain by a variable (0-20 m) thickness of clay that acts to (semi-) confine the aquifer. The Upper (unconfined) Aquifer Unit (UAU) is continuous across the area and therefore connects the LRAS and EAS. Recharge occurs to the upper aquifer through rainfall and through vertical leakage through the clay to the lower aquifer. Recharge is highest in the high ground to the south of the area.

The aquifer discharges to the ocean and to the Berg River. The major flow direction in the UAU is from high ground in the south of the area, flowing semi radially to the northeast, north and southwest. Flow in the LAU exploits the palaeochannel axis and is directed towards the southwest coastline.

The conceptual model was translated to a numerical model and the finite element groundwater software package Feflow was used to numerically model the aquifer. The landward borders of the model are no-flow boundaries, based on topographical highs or flow divides. The ocean was used as a constant head boundary in the northeast and southwest of the model. The Berg River is set as an internal transfer boundary. Calibration has achieved modelled groundwater levels that, on average, match the observation data to within 10% of the total head drop over the model, at ~10 m in the UAU and ~5 m in the LAU.

The basal model unit has a moderate hydraulic conductivity of ~10 m/d. The middle layer of the model has a low conductivity of 0.01 m/d. The upper model unit has a conductivity of 10 m/d in most areas, and an area with lower conductivity in the south, at 1m /d. The vertical hydraulic conductivity is an order of magnitude lower than horizontal. The seasonal variation of the aquifer was simulated in transient modelling. The averaged variation in water levels is matched in the UAU and LAU using a homogeneous isotropic specific yield of 2%. This is low for the sand units but its likely to represent the equivalent Sy of the system as a whole, including the clay beds.

Scenario testing on the transient model suggests there is a large storage volume available: significant variations in rainfall, increased abstraction, ASR scenarios all have little effect on the regional mass balance numbers, simply affecting the storage (causing a negative or a positive balance). There is a potentially under-exploited resource in the EAS and the wellfield scenario showed that water levels close to the Langebaan Lagoon wouldn't be affected by the abstraction. The potential for seawater intrusion is negligible.

In the following section recommendations to increase model reliability, and answer additional questions, are made.

## 8.2 GROUNDWATER LEVEL DATA

It is surprising that with the numerous records in the NGDB there are very few water level measurements usable for a modelling exercise. Out of all the records for the area only a small proportion have long and regular time-series water level data and a full geology with depth record. This affects the observation data and affects interpretations such as illustrated in analysing the effect of the current abstraction with a lack of time-series data available close to the WCDM wellfield.

With a larger data set the points that are affected by local features such as local pumping or abstraction, can be more confidently removed from the data set and a smooth water table, applicable at the regional scale can be generated.

*Summary Recommendation 1: Hydrocensus data to be collected across the Langebaan area: water levels and borehole use, accurate GPS of X,Y,Z coordinates*

## 8.3 SURFACE WATER DATA

There is a vast resource of reliable surface water data held within the DWAF flow gauging station records. These are continuously monitored, some even hourly. However, this data is of limited use to integrated water resource planning, as it is not measured from a universal datum. In order to really understand surface – groundwater interactions, data on both storage units (the surface water and the groundwater and water stores) is vital.

*Summary Recommendation 2: Make surface water data available to all disciplines by allowing it to be converted to a universal datum. All gauging stations are required to be surveyed at the point at which the measurements are taken.*

## 8.4 HYDRAULIC NATURE OF THE AQUIFER AND GROUNDWATER-SURFACE WATER INTERACTIONS

The conceptual model assumes that flow in the LAU is controlled by palaeotopography of old river courses, and flow in the UAU is more controlled by surface topography. This distinction in flow directions between the aquifers is not fully replicated in the model. Both units discharge into the Berg River for example, and so the water in the LAU flows against bedrock. To understand the hydraulic nature of the aquifer in greater detail a smaller-scale model is required, which would need to map the thickness of the clay more accurately and have a much finer scale.

Modelling at a smaller scale in the vicinity of the Berg River would also support quantification of surfacewater–groundwater interactions. During flood events of the Berg River, the river can recharge the aquifer. However the scale of this process is smaller than the regional scale modelled here. Understanding the recharge mechanisms for the LAU and UAU is crucial to understanding the aquifers and their potential yield. Smaller scale SW-GW modelling, which will require groundwater data close to the river and usable river stages, is recommended.

*Summary Recommendation 3: Additional modelling at a smaller scale in order to understand the hydraulic nature of the aquifers and replicate differing flow directions at different depths. In the vicinity of the Berg River this will generate a better understanding of the nature of the SW-GW interaction.*

## 8.5 MANAGEMENT OF CURRENT ABSTRACTION

It is clear that the West Coast District Municipality wellfield has at least contributed to falling water levels in the wellfield vicinity and possibly some way beyond. Even so, questions remain over whether the abstraction regime currently in place at the West Coast District Municipality wellfield (continuous abstraction) delivers the highest potential yield. The maximum (potentially unsustainable) capacity of the wellfield can be analysed in a model setting by testing how much (volume and time) pumping would be required in order for

- the cone of depression to extend beyond the aerial extent of palaeochannel,
- the water levels in the wells to drop beneath the level of the bottom of the clay.

A forward projection of the current reducing water levels could answer questions regarding when the current abstraction will cause dangerously low levels (i.e. below the top of the clay bed). Questions also remain over the effects of dramatically increasing the abstraction by, for example, an order of magnitude (Paul Seward, pers comm. 2008). However these questions cannot be addressed with the current regional model because the detail at the scale required for these wellfield management and optimisation queries is not fine enough. They also cannot be tackled accurately without correct modelling of the storage capability of the aquifer, and recognition of management over the natural cycle of the aquifer. A wellfield optimisation model is recommended which includes the management of the time lag for responses in the UAU to pumping in the LAU and for transmission through the clay layer.

*Summary Recommendation 4: Additional modelling at a smaller wellfield scale in order to manage the current situation of abstraction from storage.*

## 8.6 OPTIMISATION OF ADDITIONAL ABSTRACTION

It is known that the EAS is an under-exploited resource. The EAS wellfield scenario tested here shows that there is regionally no threat to the Langebaan Lagoon ecosystem, or of seawater intrusion with abstraction at the EAS. A regional-scale model such as this one, could be used as a basis for construction of a smaller-scale model centred on the EAS palaeochannel. These would be required for optimisation of the position of additional abstractions, with respect to yield and also proximity to surface water and other existing users.

*Summary Recommendation 5: Smaller-scale model constructed for the purpose of optimisation of abstraction volume and rate, and positions, for additional potential wellfields.*

## 8.7 OPTIMISATION OF ASR SCHEME

It is shown here that the regional affect of the ASR scheme is small. A regional-scale model such as this one could be used as a basis for construction of a smaller-scale model centred on the West Coast District Municipality wellfield. These would be required for optimisation of the position of injection boreholes and volume injected. A small-scale model is also required in order to accurately predict the effect of injection at the local scale.

*Summary Recommendation 6: Smaller-scale model constructed for the purpose of optimisation of ASR injection volume and rate, and borehole positions.*

## 9. REFERENCES

- Anderson, M. P. and Woessner W. W., (1992). *Applied Groundwater Modelling*. Academic Press. 373pp
- Calver, A. (2001). *Riverbed Permeabilities: Information from pooled data*. Groundwater, 39(4), 546-553.
- De La Cruz, M A. (1978). *Marine Geophysical and Geological Investigations in Saldanha Bay*. Joint Geol. Surv./Univ. Cape Town Mar. Geosci. Group, Bull No. 9, 115 pp.
- Department of Water Affairs and Forestry (2002) *Groundwater Assessment*. Prepared by G Papini of Groundwater Consulting Services as part of the Breede River Basin Study. DWAF Report No. P H 000/00/....
- Department of Water Affairs and Forestry, (2005). *The Assessment of Water Availability in the Berg Catchment (WMA 19) by means of Water Resource Related Models*: Inception Report, Final draft, September 2005 submitted by Ninham Shand in association with Umvoto Africa, Project No. W8147/04.
- Department of Water Affairs and Forestry (2007a). *The Assessment of Water Availability in the Berg Catchment (WMA 19) by Means of Water Resource Related Models : Groundwater Model Report Volume 2 – Data Availability and Evaluation*. Prepared by Umvoto Africa (Pty) Ltd in association with Ninham Shand (Pty) Ltd on behalf of the Directorate : National Water Resource Planning. DWAF Report No. P WMA 19/000/00/0407
- Department of Water Affairs and Forestry (2007b). *The Assessment of Water Availability in the Berg Catchment (WMA 19) by Means of Water Resource Related Models : Groundwater Model Report Volume 3 – Regional Conceptual Model*. Prepared by Umvoto Africa (Pty) Ltd in association with Ninham Shand (Pty) Ltd on behalf of the Directorate : National Water Resource Planning. DWAF Report No. P WMA 19/000/00/0407
- Department of Water Affairs and Forestry (2007c). *The Assessment of Water Availability in the Berg Catchment (WMA 19) by Means of Water Resource Related Models : Groundwater Model Report Volume 4 – Regional Water Balance Model*. Prepared by Umvoto Africa (Pty) Ltd in association with Ninham Shand (Pty) Ltd on behalf of the Directorate : National Water Resource Planning. DWAF Report No. P WMA 19/000/00/0407
- Department of Water Affairs and Forestry (2007d). *The Assessment of Water Availability in the Berg Catchment (WMA 19) by Means of Water Resource Related Models : Groundwater Model Report Volume 5 – Cape Flats Aquifer Model*. Prepared by Umvoto Africa (Pty) Ltd in association with Ninham Shand (Pty) Ltd on behalf of the Directorate : National Water Resource Planning. DWAF Report No. P WMA 19/000/00/0407
- Diersch, H.J.G., (2006). *Finite Element Subsurface Flow and Transport Simulation System*. User's Manual. WASY SOFTWARE Feflow 5.3.
- Driscoll, F. G. (1986) *Groundwater and Wells*. Reynolds Guyar Designs. 1089pp
- Freeze, R.A. and Cherry J.A. (1979) *Groundwater*. Prentice Hall. pp 604.
- Hay, E R and Hartnady, C J H (1995). *Geohydrogeological Assessment of Groundwater Reports Related to the Proposed Development of the Saldanha Steel Plant*. Umvoto Report No. UMW020 10 pp.
- Hiscock, K. (2005). *Hydrogeology Principles and Practice*. Blackwell Publishing UK pp389
- Johnson M. R, Anhaeusser C.R Thomas R.J. (2006). *The Geology of South Africa*. Council for Geoscience 691 pp
- Kleef, H.V. (DWAF) Personal Communication. August 2007
- Midgley D.C., Pitman W.V., and Middleton B.J., (1994). *Surface Water Resources of South Africa 1990: Book of Maps*. Vol IV, First Edition. Water Research Commission. WRC Report No 298/4.2/94.

- Midgley, D.C., Pitman, W.V. and Middleton, B.J., (1994). *Surface Water Resources of South Africa 1990 Volume IV Appendices*. Water Research Commission Report No. 298/4.1/94
- Mouski, F. (DWAF) Personal Communication, November 2007.
- NLC2000 (CSIR Environmentek, ARC, 2000) *Landuse mapping with Landsat satellite image classification and field verification*.
- Rogers, J. (1980). *First Report on the Cenozoic Sediments between Cape Town and Elands Bay*. Geological Survey of South Africa Open File Report No. 165.
- Rogers, J. (2006) *Sedimentology of Late Cenozoic Sediments, Including the Pliocene Duynfontyn Member of the Varwater Formation, Koeberg Nuclear Power Station, Melkbosstrand, Cape Town*. Unpublished Draft.
- Rushton, K.R. and Tomlinson, L.M. (1979). *Possible Mechanisms for Leakage between Aquifers and Rivers*. Journal Hydrology 40, 49-65
- Schulze R. E. Maharaj, M., Lynch, S.D, Howe, B.J., and. Melvil-Thomson, B. (1997). *South African Atlas of Agrohydrology and Climatology*.
- Stettler E. H., Smit J. P and Zadoroshnaya V. (2007) *Characterization of the Langebaan Weg aquifer with gravity and time domain EM techniques*. DWAF report in prep..
- Timmerman, L. R. A. (1988). *Regional Hydrogeological Study of the Lower Berg River Area, Cape Province - South Africa*. Unpublished PhD thesis, State University Ghent, 236 pp. (3 Vols.)
- Timmerman, L. R. A. (1985a). *Preliminary report on the Geohydrology of the Cenozoic Sediments of part of the Coastal Plain between the Berg River and Elands Bay (southern section)*. Department of Environment Affairs, Directorate of Water Affairs, Techn Rep. Gh3370.
- Timmerman, L. R. A. (1985b). *Possibilities for the development of groundwater from the Cenozoic sediments in the Lower Berg River region*. Department of Environment Affairs, Directorate of Water Affairs, Techn Rep. Gh3374, 51pp
- Timmerman, L. R. A. (1985c). *Preliminary report on the Geohydrology of the Langebaan Road and Enaldsfontein Aquifer Units in the Lower Berg River Region*. Department of Environment Affairs, Directorate of Water Affairs, Techn Rep. Gh3373, 51pp.
- Umvoto, (1995). *Preliminary Geohydrological assessment of groundwater reports relevant to the proposed development of the Saldanha Steel Plant*.
- Winter T. C., Harvey J. W. , Franke O. L. , Alley W. M. (1998). *Groundwater and Surface Water A single Resource*. U.S. Geological Survey circular: 1139.
- Woodford, A.C. and Fortuin, M., (2003): *Assessment of the Development Potential of Groundwater Resources for the West Coast District Municipality*, specialist geohydrological report for Kwezi-V3 Consulting Engineers, as part of the project: 'Pre-Feasibility Study of Potential Water Sources for the Area served by the West Coast District Municipality', SRK Consulting Engineers and Scientists, October 2003, Report No. 318611, Bellville, Cape Town, 94p.